ORIENTATION OF RIGID BODIES FREEFALLING IN NEWTONIAN AND NON-NEWTONIAN LIQUIDS

by

Ashwin Vaidya

B.Phil., University of Pittsburgh, Honors College, 1995

M.S., University of Pittsburgh, 1998

M.S., University of Pittsburgh, 1999

Submitted to the Graduate Faculty of

School of Engineering in partial fulfillment

of the requirements for the degree of

Doctor of Philosophy

University of Pittsburgh

2004

UNIVERSITY OF PITTSBURGH

SCHOOL OF ENGINEERING

This dissertation was presented

by

Ashwin Vaidya

It was defended on

April 2, 2004

and approved by

Peyman Givi, Professor, Department of Mechanical Engineering, University of Pittsburgh

Walter Goldburg, Professor, Department of Physics and Astronomy, University of Pittsburgh

Anne M. Robertson, Associate Professor, Department of Mechanical Engineering, University of Pittsburgh

Dissertation Director: Giovanni P. Galdi, Professor, Department of Mechanical Engineering, University of Pittsburgh

ABSTRACT

ORIENTATION OF RIGID BODIES FREEFALLING IN NEWTONIAN AND NON-NEWTONIAN LIQUIDS

Ashwin Vaidya, Ph.D.

University of Pittsburgh, 2004

This thesis deals with the subject of terminal orientations of rigid bodies, sedimenting in Newtonian and non-Newtonian liquids. It is a well established fact that homogeneous bodies of revolution around an axis (a) with fore-aft symmetry will orient themselves with respect to the direction of gravity (g) depending upon their shape and upon the nature of the fluid in which they are immersed. If, for instance, we are considering an ellipsoidal object falling in a Newtonian fluid such as water, then the body falls with a eventually becoming perpendicular to the direction of g. However, if the same body falls in a viscoelastic fluid where the inertial effects can be disregarded, then a will eventually become parallel to g. It has also been noted that long bodies falling in fluids with certain polymeric concentrations can take on angles between the horizontal and vertical orientations. These intermediate angles are referred to as *tilt angles*. The objective of this thesis is the explanation of this orientation phenomenon in different liquids.

Our approach to the problem has been three-fold, experimental, mathematical and also numerical. We perform several experiments on sedimentation of particles in a variety of viscoelastic and Newtonian liquids to verify and fill gaps in the previous observations. A

second set of experiments that we perform involves a modified flow chamber setup where the particle is fixed at the center of the chamber while water flows past it. We are able to replicate previous experiments at low and intermediate Re, with both these experiments.

The equations to describe the problem of freefall of a rigid body of arbitrary shape, in a liquid, are obtained from a frame attached to the body and is formulated for any general fluid model. In addition, we also obtain the equations for the body, since the problem we are dealing with is one of fluid-structure interaction. We establish well-posedness of the equations by showing the exitence and uniqueness of steady solutions to the problem of sedimentation in a Second order fluid, with $\mathrm{Re} = 0$ and arbitrary $\alpha_1+\alpha_2$ using the Banach fixed point theorem.

In order to explain the terminal orientation assumed by the body, we consider the effect of torques imposed by different components of the liquid such as inertia, viscoelasticity and shear-thinning. The equilibrium resulting from the competition of the different torques should reveal the terminal angle. Guided by the fact that the orientation phenomenon is observed at very small Re and We, we formulate the torque equations at first order in these material parameters. The calculation is performed for four different liquid models, Newtownian, Power-law, Second order fluid and a modified Second order model which we introduce here for the first time. The different orientation observations seen in experiments is well explained by these models. Finally, a simple quasi-steady stability argument is used to establish stability of the equilibrium states. For this final argument, we numerically evaluate the torque imposed by the individual components of the liquid upon a sedimenting prolate ellipsoid in an unbounded three dimensional fluid domain surrounding the body.

TABLE OF CONTENTS

LIST OF TABLES

LIST OF FIGURES

ACKNOWLEDGMENTS

This thesis would not be possible primarily without the help, guidance and constant encouragement of my dear advisor, Professor Giovanni Galdi. He is a great source of inspiration for me. Without a doubt, he has taught me all I know of mathematics. He has been much more than my advisor; he has been a parent to me during my study at the department. I will always fondly remember my conversations, long scientific discussions with him and more especially, his pasta dishes. From a professional standpoint, I am most thankful to him for imparting his scientific philosophy to me that 'All mathematics is created alike. The problem under investigation dictates what tools are appropriate and not vice versa.' This piece of essential wisdom has surely helped me become comfortable with all of mathematics. I look forward to several years of collaboration with him.

I wish to thank my committee members, Dr. Peyman Givi, Dr. Walter Goldburg and Dr. Anne Robertson for consenting to serve on my committee and for coming to my aid several times with suggestions and valuable advice.

I convey special thanks to Professor Donald Plazek. He has served as my surrogate advisor and taught me much. Much of experimental work has been performed under his guidance. I have learnt so much about the experimental techniques in polymer science from him. I would also like to thank him for his generosity with his time and resources in refurbishing our lab with much needed equipment which has been crucial for much of my experimental work.

Thanks to my friends and colleagues, Ana, Chung, David, Doni, Fernando, Hasballah, Khaled, Raffaella and Steve for their help suggestions during several phases of my work, for some stimulating conversations and in general for being wonderful friends. Also, I acknowledge Professor Daniel Joseph for his valuable suggestions on various occasions and to his

coworkers R.Bai and Jimmy Wang for their help. I would like to thank Professor Adelia Sequeira and IST for the support during the summer of 2001. Thanks also to the Swanson Research Center, the School of Engineering machine shop and the ME1043 course and all the undergradute students involved in the senior projects, through this course, for helping out with several aspects of the experimental work. Part of this work was funded by the NSF grant DMS-0103970.

These years of study have been among the best of my life and I shall remember them fondly. I acknowledge my family and friends for their moral support and encouragement which always uplifted my spirit. To Poochee, for helping me do my best and always helping me find the positive side of life and to my parents for always believing that I could do anything.

Dedicated to my Parents

1.0 MOTIVATION

The motion of bodies in fluids constitutes one of the oldest problems in fluid dynamics. This thesis falls under the general subject of sedimentation theory, which involves the mechanics and combined transport of solids and liquids. In studying sedimentation of a body into a fluid, one tends to look at the behavior of suspensions in a liquid, the rheology of the suspension and also the shape, size and interaction of the suspended particles. Also of interest is the behavior of individual particles such as their terminal speeds and orientation. In fact, the central theme of this thesis is the analysis of orientation of rigid bodies in fluids, in their steady state.

1.1 Historical Preview

A detailed account of the history of fluid mechanics and fluid-structure interaction is outside the scope of this thesis. In fact, one could perhaps devote several volumes to this subject. However, we must acknowledge the contributions of those whose shoulder we stand upon; at least the ones we are aware of. This section is also not meant to recount the details of any contributions but simply mention achievements which are in some way relevant to this thesis. We especially wish to bring to attention some of the important results in the subject which date back to at least a couple of centuries ago. The more modern contributions, especially from the past century, though innumerable are well recorded and will be discussed in the following introductory chapter. But it fascinates us to learn that the subject dates back to thousands of years ago, which to a scientist is sufficient motivation to pursue any problem.

Though it would be impossible to identify the earliest work done on the subject, we know from the records of ancient Egyptians[9] that they were familiar with the physics of sedimentation from their experience in digging and washing gold. In this respect it is well documented that several ancient civilizations were well versed with the practical aspects of sedimentation.[2,84] Perhaps the greatest acknowledged scientist in the history of mankind,

Aristotle (384 B.C.-324 B.C.), has contributed directly to the subject of fluid mechanics upon which are based several fundamental principles. In his book, *On the Heavens*[3], he claims that the every body seeks to find its *natural place* in the universe based on its 'heaviness'.[76] From this statement he inferred that bodies moving in water or the atmosphere would seek the bottom layers which are denser or *heavier* than the upper layers. This observation is definitely recognized to be true today and of fundamental importance to fluid mechanics. Also of much interest are the contributions of Leonardo da Vinci (1425-1519), whose study of fluids can alone can cover several books. Leanordo is acknowledged to have formalized the concept of continuity of a liquid, upon which is based our entire subject of *Continuum mechanics*. Leonardo's observations in fluid mechanics ranged from the study of eddies, motion of water in rivers and canals for irrigation purposes, the motion of waves in oceans to the flow of blood in the human body. His work in the subject of fluid particle interaction pertained to problems of navigation and the efficient design of boats for reducing drag. Leonardo also wrote proficiently on the theory of flight and made significant contributions to the subject of aerodynamics. Unlike Aristotle, most of Leonardo's scientific claims are acknowledged as being correct. His countryman Michel Angelo (1475-1564) is attributed with the discovery of the concept of friction in fluids. As a hydraulic engineer involved in several flow related projects, he recognized that the speed of flow at the center of the channel is higher than at the edges.[76,78] Isaac Newton (1642-1727) also made several interesting contributions to the subject of motion of rigid bodies in liquids in his more general attempt to understand the resistance of any medium to motion which takes up several pages of the second volume of the *Principia Mathematica*.[58] His formulation of the laws of motion are the foundation of any mathematical analysis of fluid flow.

After Newton formulated his laws of motion and Leibniz formulated his version of the calculus, the subject of mechanics found a natural language of expression. This gave rise to several significant contributions to mathematics and physics which were to have a significant

impact upon the subject at hand. These advancements were made to different aspects of viscous fluid mechanics. Among the modern stalwarts was Claude L.M.H. Navier (1785-1836) who formulated the now famous Navier-Stokes equations. Simeon Denis Poisson (1781-1840) and Pierre Simon Laplace (1749-1827) discovered the second order partial differential equations that bear their name and can be used to describe the very slow motion of extremely viscous liquids. George G. Stokes (1819-1903) contributed to several aspects of hydrodynamics his most famous being the work on the linearization of the equations of a viscous incompressible fluid.[36] This gave rise to the equations that describe the creeping flow motion of a viscous liquid, also known as the *Stokes equations*. The work of H.A. Oberbeck on the creeping flow solutions of for steady translational motion of an ellipsoid in a viscous liquid, is particularly pertinent to certain parts of our research. Osborne Reynolds (1842-1912) must be credited with the discovery of the role of viscosity on the stability of a flow based on a series of famous experiments resulting in the recognition of the significant parameter, Re, which is now universally used to classify flows. We refer the readers to[36] for an account of the more recent contributions to the specific subject of particle motion in fluids from the past century and to[76] for a thorough account of the history of fluid mechanics, both ancient and modern.

The work of Thomson and Tait[75] and Kirchoff[47] deserves special mention since much of this work can be thought of as an afterthought to their theories. In his voluminous book *Hydrodynamics*,[50] Lamb, discusses the motion of solid bodies through a liquid, in detail, based upon the previous work of Thomson, Tait and Kirchoff. In particular, in Chapter 6 of this book, which is devoted to the motion of solids through a liquid, he provides the solution to the problem of steady motion of a prolate spheroid thorugh an unbounded ideal fluid. Lamb argues analytically and heuristically that the stable orientation for a long body such as a cylinder or ellipsoid in an ideal fluid is with its broadside along the direction of motion. The attached Figure 1.1 [50, Page 86] outlines his argument based on the turning

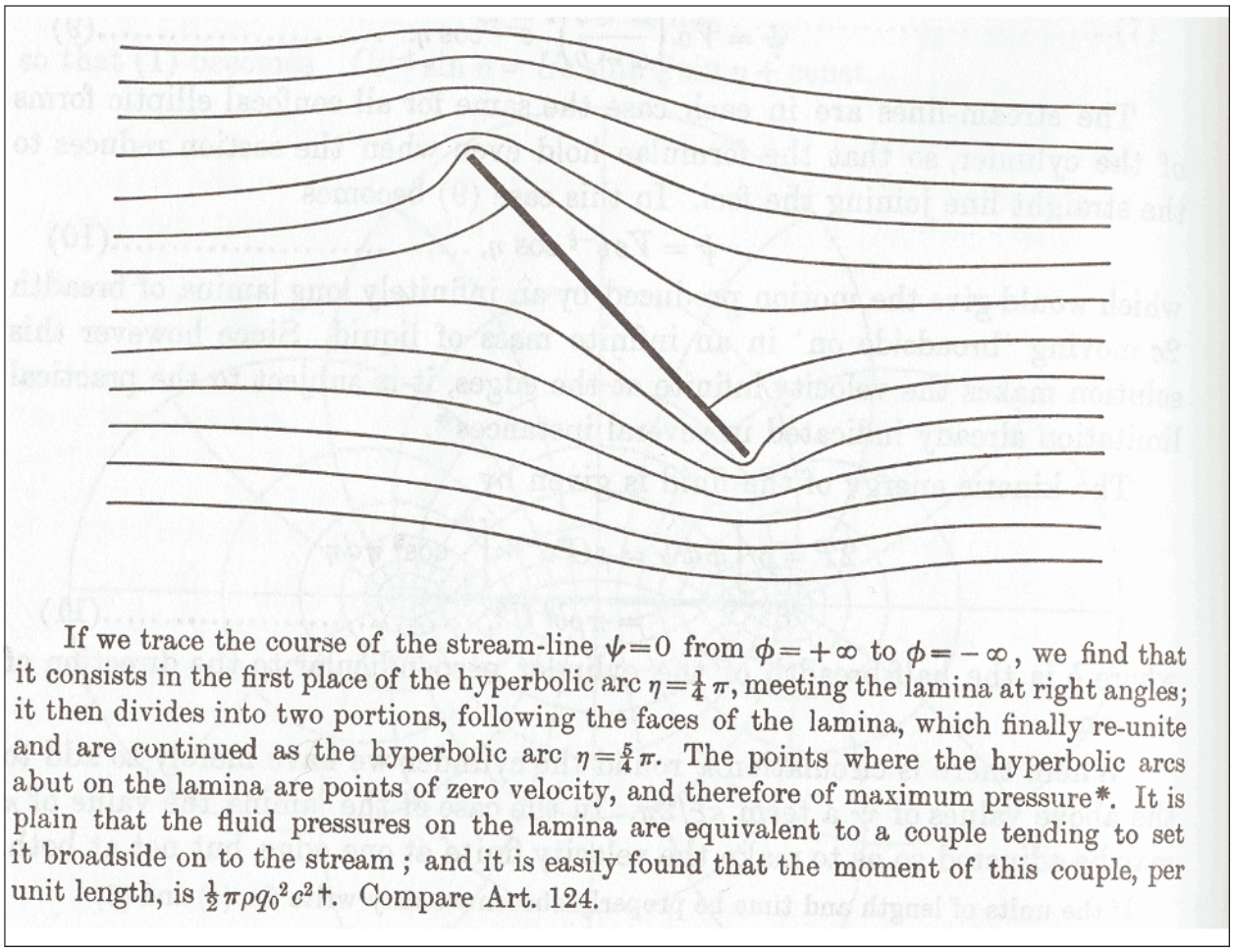

If we trace the course of the stream-line $\psi=0$ from $\phi=+\infty$ to $\phi=-\infty$, we find that it consists in the first place of the hyperbolic arc $\eta=\frac{1}{4}\pi$, meeting the lamina at right angles; it then divides into two portions, following the faces of the lamina, which finally re-unite and are continued as the hyperbolic arc $\eta=\frac{5}{4}\pi$. The points where the hyperbolic arcs abut on the lamina are points of zero velocity, and therefore of maximum pressure*. It is plain that the fluid pressures on the lamina are equivalent to a couple tending to set it broadside on to the stream; and it is easily found that the moment of this couple, per unit length, is $\frac{1}{2}\pi\rho q_0^2 c^2$†. Compare Art. 124.

Figure 1.1. Lambs argument for the steady stable orientation of a cylinder in an Ideal fluid[50] (Reprinted with permission).

couples on a cylindrical body, due to the fluid. In the absence of friction, he identifies inertial torques acting through the stagnation points on a submerged body as the cause for the steady orientation. Our thesis continues where Lamb left the subject to discuss the steady state orientation of particles in a variety of other liquids based on a very similar physical idea.

The subject of fluid-particle interaction has taken a more interesting turn with the discovery and characterization of viscoelastic fluids which unlike Newtonian fluids, like water, also possess elastic properties. Of particular interest, in several disciplines, is the difference in the interaction of solid bodies with these two kinds of fluids. In this thesis, we shall focus

our attention upon one such phenomenon which is described in detail below. Recent experiments made on elongated bodies falling in different fluids have indicated that the terminal behaviors of bodies in fluids can change with the kind of fluid medium. Using the ideas of Lamb and the modern theory of viscoelastic liquids, we investigate the problem of terminal motion in general, of a rigid body of arbitrary shape, in Newtonian and viscoelastic fluids, mathematically, numerically and experimentally.

1.2 Applications

In this section, we refer to a few applications of our subject. A preliminary task in the process of oil-drilling is the removal of debris from pipelines. It is observed that when one uses a Newtonian liquid such as water for the debris removal the waste particles and sediments in the pipelines have a tendency to align across the flow, thus leading to a potential clogging problem (see Figure 1.2). However if the water is infused with a certain amount of polymeric content, then the alignment behavior of the debris changes and the sediments align along the direction of the flow which is a desirable state (see Figure 1.3).

A second example comes from the field of human biology and physiology. An interesting question in these areas is the issue of orientation of cells in shear flows. The Figure 1.4 shows a numerical simulation of lipid membrane in the presence of a shear-flow.[48] Also of tremendous interest is the orientation of blood cells undergoing shear in plasma. The cartoon at the bottom of Figure 1.5 shows the aggregation and orientation behavior of cells at different shear-rate regimes.

However, the immediate motivation for this problem comes from the experimental work of D.D. Joseph[38,40–42,54] on flow-induced microstructures. Joseph and is coworkers have

Figure 1.2. Motion of debris across the flow in a Newtonian liquid.

Figure 1.3. Motion of debris along the flow in a polymeric liquid.

reported that mutiple speheres falling simultaneously in a liquid are seen to settle with curious steady, stable configurations (see Figure 1.6). In the case of two falling spheres in a Newtonian liquid, it is seen that the one dropped second catches up with the first (drafting), the two spheres touch (kissing) and since the contact configuration is not stable, they separate and fall side by side (tumbling). In a viscoelastic liquid, we see drafting and kissing but the in-contact configuration is now stable. Therefore, the spheres fall together, one on top of the other. The key to understanding the phenomenon of drafting, kissing, and tumbling and the symmetries adopted by the interaction of spheres in non-Newtonian fluids lies in the orientations of long bodies in different liquids, which is our central pursuit. Since, temporarily upon contact, the spheres replicate the behavior of a single long body, we take

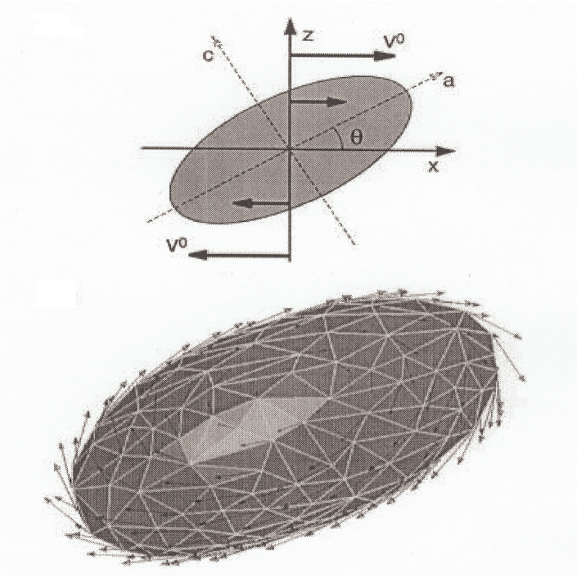

Figure 1.4. Orientation of lipid cells in shear flow[48] (Reprinted with permission).

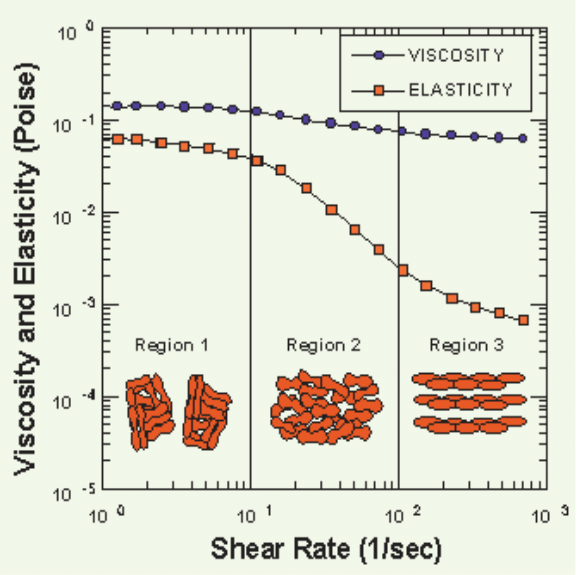

Figure 1.5. Alignment and orientation behavior of red blood cells at different shear rates[86].

up the study of the motion of a single long body, such as a cylinder or a prolate ellipsoid in Newtonian and Non-Newtonian liquids. As we shall see in the upcoming chapters, the problem of sedimentation of a single body can be extremely complex in itself.

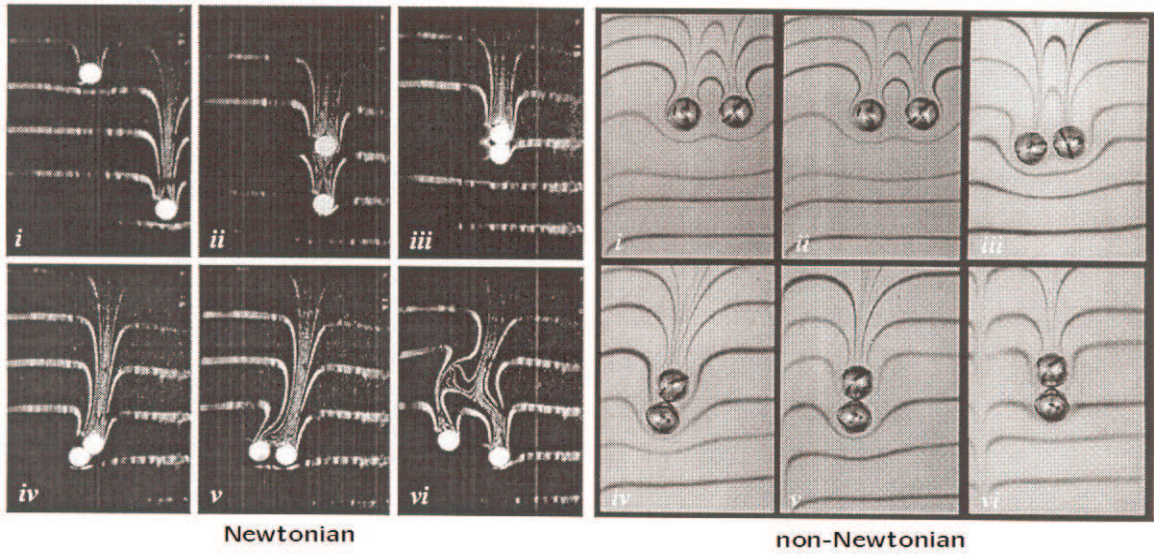

Figure 1.6. Flow induced micro-structures in Newtonian and Viscoelastic liquids (Courtesy of D.D. Joseph).

There is tremendous interest in the motion and behavior of particles in (i) quiescent liquids, (ii) laminar flow, (iii) shear flow, (iv) Poiseulle flow and even (v) turbulent flow. In this thesis, we restrict ourselves to case (i). Firstly, this is the appropriate physical setting for the phenomenon we wish to describe and also, a thorough analytical study of the behavior of rigid bodies in any other kind of flow would be highly complex, if at all possible.

Happel and Brenner, in their book, *Low Reynolds Number Flow*,[36] provide an impressive list of applications in science and technology, for their subject. We may stake claim to a large subset of their applications. In our thesis, we have studied the motion of a single particle in different liquids. However, this is a preliminary step to understanding the motion of multi-particle systems. Therefore, we believe that our work has impact in Chemical Engineering

where the motion of particles in liquids and gases is commonly seen. Our analysis and its extensions can find use in separation of dust particles and suspensions from liquids and gases (see[36] for detailed example). Mining industries need processes to separate minerals or to remove extraneous sediments. Hence the knowledge of behavior of suspended particles in liquids can be extremely useful. This work also has applications in fields such as biomechanics where the process of separation of biomolecules via electrophoresis involves sedimentation of particles through organic media[35] and in Material Science, where orientation of short fiber like particles in a polymer network is important for enhancing the mechanical properties of composite materials (see[53]).

2.0 INTRODUCTION

Experimental observations show that bodies freely falling in fluids eventually acquire a constant translational and angular velocity of descent, referred to as the *terminal velocity* of the body.[13,14,17,38,40,41,51] We use the term *terminal state* to collectively signify properties such as velocity and orientation of the sedimenting body as time, $t \to \infty$, i.e. in its steady state. Our specific objective, in this thesis, is to study the rather interesting phenomenon regarding the terminal orientation of symmetric rigid bodies falling in Newtonian and Non-Newtonian (viscoelastic) fluids.

2.1 Experimental Work

It is a well established fact that homogeneous bodies of revolution around an axis (call it a) with fore-aft symmetry will orient themselves with respect to the direction of gravity ($\mathbf{g}$) depending upon their shape and upon the nature of the fluid in which they are immersed. If, for instance, we are considering an ellipsoidal object falling in a Newtonian fluid such as water, then the body falls with a eventually becoming perpendicular to the direction of $\mathbf{g}$ (see Figures 2.1,2.2). However if the same body falls in a viscoelastic fluid where the inertial effects can be disregarded then a will eventually become parallel to $\mathbf{g}$.

It is to be noted that in these observations the Reynolds number, Re, is very small [1]. Qualitatively, Re can be said to be the ratio of inertia of the fluid to its viscosity. Therefore, for a fluid of given viscosity, a small Re would imply a small inertia for the fluid under consideration. However if the same body falls in a viscoelastic fluid where the inertial effects can be disregarded then a will eventually become parallel to $\mathbf{g}$. Similar to the Reynolds number, the parameter which characterizes the viscoelastic nature of the fluid is called the

[1] The Reynolds number is defined by $Re = \rho U d/\nu$ where U is the velocity of the object, d is its characteristic length and ν is the viscosity of the fluid. Hence a small Re corresponds to either small objects or very small velocities compared to the viscosity. In these experiments Re is varied by varying the material of the particle used and the viscosity of the fluid and We is varied by changing the polymeric concentration of the solution.

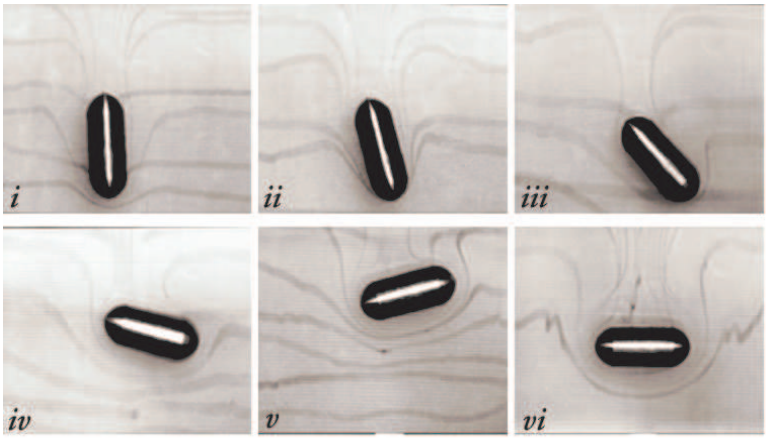

Figure 2.1. Terminal orientation of the body in a Newtonian Fluid (Courtesy of D.D. Joseph) .

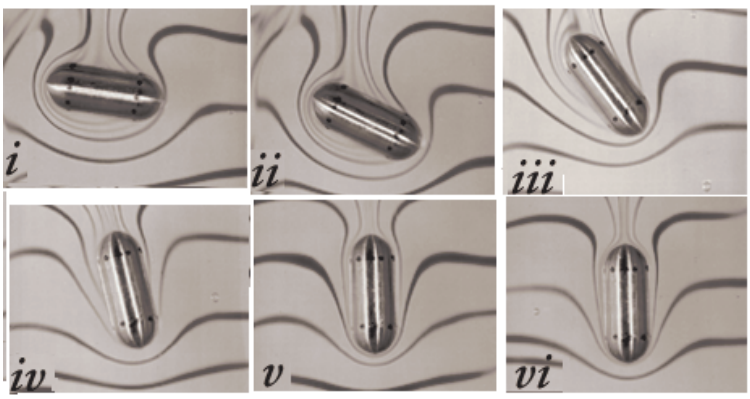

Figure 2.2. Terminal orientation of the body in a viscoelastic liquid (Courtesy of D.D. Joseph) .

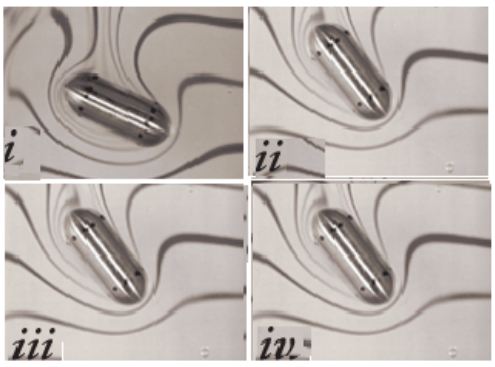

Figure 2.3. The tilt-angle phenomenon (Courtesy of D.D. Joseph).

Weissenberg number, denoted *We*, and qualitatively represents the ratio of elasticity of the fluid to its viscosity. Furthermore, it has also been observed that elongated bodies falling in fluids with certain polymeric concentrations can take on angles between the horizontal and vertical orientations. These intermediate angles are referred to in the literature as *tilt angles*[2]. Numerous experiments to this end have been performed in the last two decades by Prof. D.D. Joseph and his collaborators,[38,54] Chiba, Song & Horikawa,[14] Cho & Cho[13] and Leal[51] where the *tilt angle* is observed (see Figure 2.3). Furthermore, it is seen that this tilt angle changes continuously with the polymeric concentration.[13]

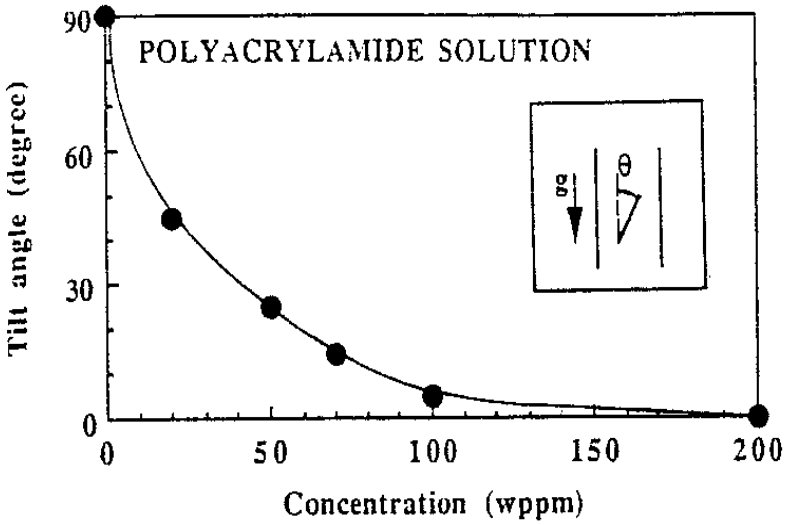

Figure 2.4. Variation of tilt angle with concentration[13].

Additionally, it has also been noticed[38,81] in the particular case of cubes or rectangular parallelopides, that when falling in a viscoelastic body, they tend to fall with their longest axis parallel to gravity. This usually means that the cube or the parallelepiped will fall with two of its diagonal vertices aligned (see Figure 2.5). This phenomenon has been referred to as *shape tilting* and may be indicative of some more expansive behavior in non-Newtonian fluids.

[2]mathematically, the *tilt angle*, θ, can be defined as the angle made by the axis of revolution, a of the body, with the horizontal.

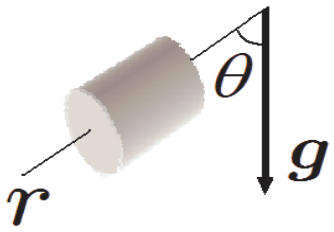

Figure 2.5. Shape tilting.

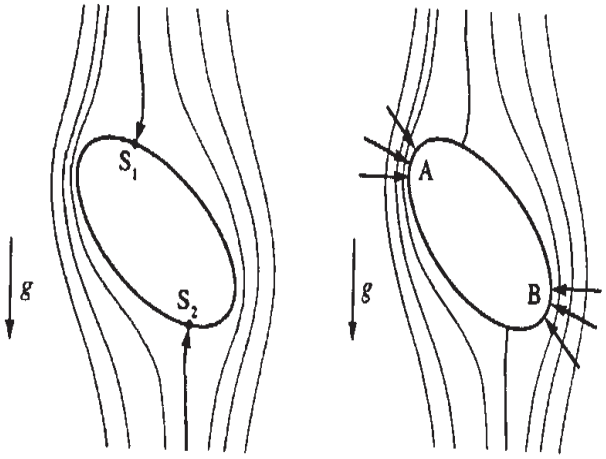

Figure 2.6. The first figure shows the nature of the inertial torque acting on the particle. S_1 and S_2 are the two stagnation points on the particle where the pressure is maximum and acts towards rotating the particle. The second figure shows the nature of viscoelastic torque on the particle. Strong shear forces give rise to normal forces at the points A and B.

Our work derives its primary motivation from the experiments of D.D. Joseph and his collaborators since they provide overwhelming evidence and sufficiently large data for this phenomenon. Their experiments[38,54] have been performed by dropping small cylindrical bodies of different materials (such as teflon, plastic, aluminum, tin, brass and steel) with lengths ranging from 30mm-1.7 cm in polymeric solutions (Non-Newtonian) of concentrations varying between $0.5\% - 2\%$. In these experiments Liu & Joseph have observed that

the *tilt angle*, θ varies continuously between 0^o and 90^o depending upon the weight, length and shape of the particle and upon the viscosity and polymeric concentration of the fluid.

The only explanation for this phenomenon is a heuristic one and outlined in the paper by Joseph & Feng.[39] The orientations of particles are described to be a direct result of the competition of the inertial versus viscoelastic torques on the particle. Figure 2.6 provides the qualitative explanation given for the competing effects of inertia and viscoelasticity as explained in.[39] Inertial torques acting at the stagnation points on the body, where the pressure is a maximum, is counteracted by the normal stresses generated by the viscoelasticity. Note that in the above experiments relatively heavy particles were used. So inertial effects become significant and cannot be ignored. Therefore, the victor in the competition between inertia and normal stress will determine the appropriate terminal orientation.

2.2 Mathematical Work

In the true spirit of scientific pursuit and for sake of mathematical rigor, it behooves us to first establish the mathematical setting of the problem in firm footing by showing existence of terminal motions for the different fluid models considered. Mathematically, the problem amounts to verifying that the set of steady state solutions to the freefall equations is non-empty. Existence and uniqueness of terminal states in the Stokes approximation of the Navier-Stokes equations has been solved almost in its entirety by Brenner.[36] The case of the unsteady Stokes problem has also been studied by Galdi,[23] for homogeneous bodies with fore-aft symmetry. Weinberger[82,83] and Serre[68] have treated the case of freefall in the Navier-Stokes fluid and the latter has proved existence of terminal states for bodies of arbitrary shape. We note that the mathematical literature on sedimentation of rigid bodies in Newtonian and viscoelastic liquids, to a large extent, is restricted to bodies of specific

geometries such as spheres or those with fore-aft symmetry like prolate or oblate spheroids. Also, the existing literature on existence of steady motions in Second order fluids is either restricted to motion in bounded domains[16]3, or with the assumption that the body undergoes no motion[60] or simply translations.[30,59,60] Furthermore, most previous work on Second order fluid models proceed under the thermodynamically implied restriction $\alpha_1 + \alpha_2 = 0$, where α_1 and α_2 are material parameters which depend upon the normal stress coefficients, even though experiments show that the sum of the two parameters is not zero for several real viscoelastic liquids. It must be stated however that showing existence and uniqueness for the simplest of fluid models is still a very complicated task. Therefore, with this in mind we have attempted to fill certain gaps in the previous literature, to the extent possible. Our contribution to the mathematical study of steady freefalling bodies in Second order fluids accounts for three significant factors, (i) bodies are of arbitrary shape, (ii) the body undergoes translation and rotation and (iii) the sum of the material parameters for the Second order fluid model, $\alpha_1 + \alpha_2$, can be arbitrary.

Previous mathematical explanations of the terminal orientation phenomenon are either qualitative[39,51] or numerical.[37] There has been very little done in terms of a rigorous mathematical analysis of the subject other than those by Galdi and his collaborators (see[23,24,26–28]).

2.3 Numerical Work

There is not very much in the literature in terms of numerical work done in this area. Among the few papers in this field are those by Huang, Hu and Joseph[37](also see[42] for more information on this subject). The work by Huang et.al. uses Direct Numerical Simulation to study the orientation of elliptical particles in a non-Newtonian liquid modeled by an

[3]The problem begin proposed for this thesis requires an unbounded, exterior domain, denoted $\Omega = \mathbf{R}^3\mathcal{B}$.

Oldroyd-B fluid in two dimensions. They correctly predict the terminal orientations in case of dominating inertial and normal stress effects and also observe that the tilt angle can be effectively predicted if a shear-thinning fluid model is considered(i.e. when the viscosity decreases with increasing shear rate). More recently, R. Glowinski and his collaborators have performed a direct numerical simulation of a single ellipsoid sedimenting in a Newtonian fluid in three dimensions.[44,61] The method employs a combination of the Domain embedding method and Operator Splitting methods to mimic the motion of an ellipsoid. The results of the code correctly show that in its steady state, the ellipsoids settles with its major axis perpendicular to the direction of gravity (see figure below). Other than these two results, the field remains open for exploration and there remain several unanswered questions that need to be resolved.

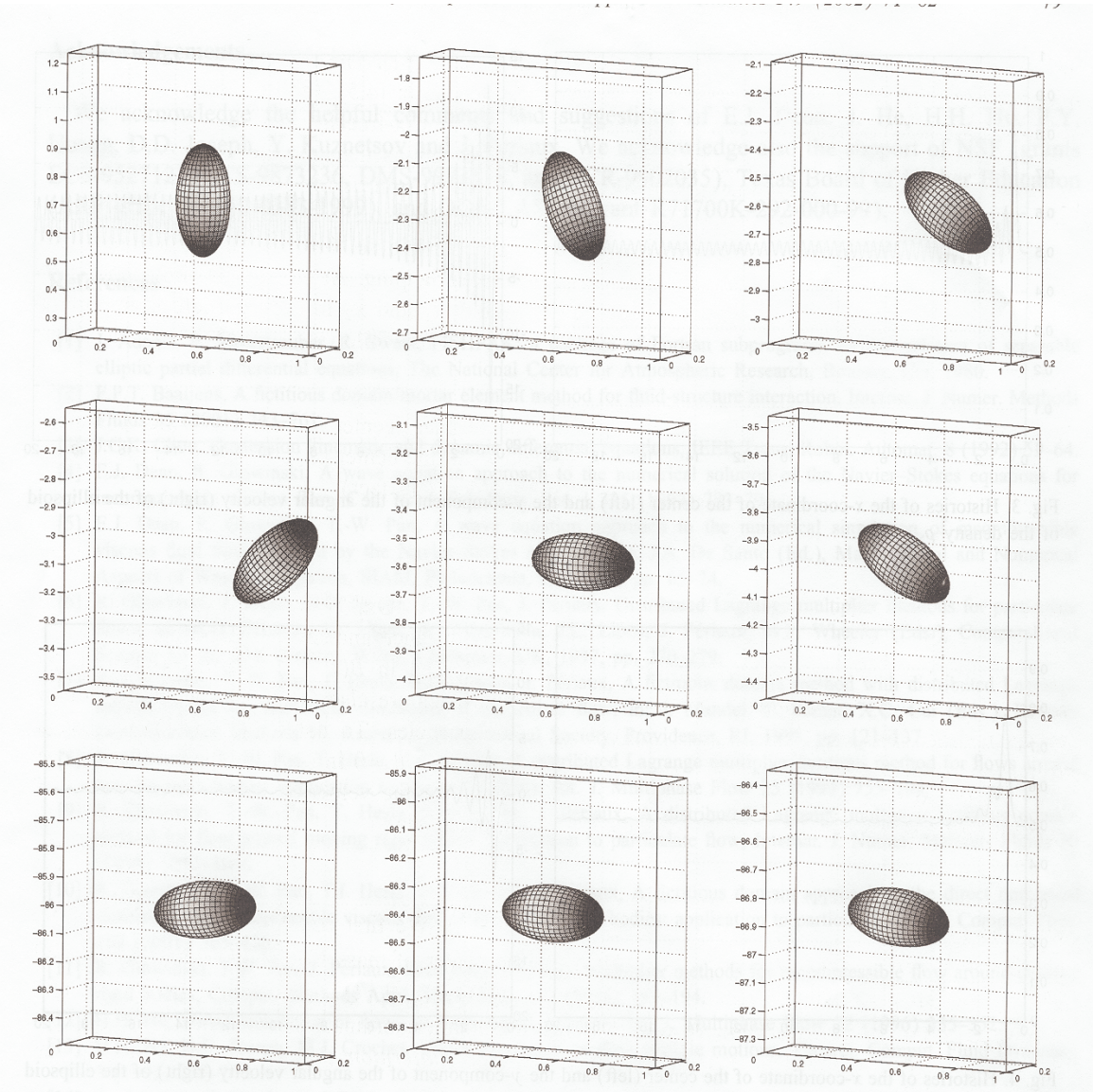

Figure 2.7. DNS simulation of ellipsoid settling in a Newtonian fluid[61].

2.4 Outline of Thesis

The objective of this thesis is the comprehensive understanding of the orientation phenomenon. As is apparent from our discussion above, the experiments performed in this area are elaborate, however, they are not systematic. Furthermore, there is no rigorous theory to explain the phenomenon. Hence, our objective is to fill the gaps in the literature. Specifically, we have the following aims:

1. A rigorous mathematical formulation of the problem. The governing equations of the problem must be carefully formulated in order to keep the problem tractable. This work comes under the general area of fluid-structure interaction. Therefore the governing equations must contain relevant equations for the fluid as well as for the sedimenting rigid body in a coupled system. We formulate the coupled system of equations in Chapter 7.

2. A study of the well-posedness of the governing equations. Our central task is a mathematical analysis of the orientation of bodies in Newtonian and non-Newtonian liquids. However, in the spirit of true scientific rigor, we must verify if the model of the fluid-structure problem that we are investigating is mathematically correct. Therefore, we will discuss the existence and uniqueness of solutions to our equations. We use tools from nonlinear functional analysis and partial differential equations to study the problem. Chapter 8 focuses on the existence and uniqueness of solutions to the steady freefall problem, for arbitrary values of the parameters $\alpha_1 + \alpha_2$.

3. A third aspect of the thesis is the analysis of the orientation phenomenon in different fluid models, Newtonian and non-Newtonian. We wish to replicate the results of experiments using different fluid models. For this purpose, we have chosen to work with models which characterize different effects that are significant to the terminal orientation phenomenon. We

have isolated three important relevant features that must be considered in our analysis. In Newtonian liquids, we see the effect of inertia, in generalized Newtonian fluid models such as the Power-law model, we have pure shear-thinning effects i.e. viscosity as a function of the shear-rate, in viscoelastic models such as the Second-order liquid, the significant effects are those of inertia and viscoelasticity and finally in the modified Second order fluid, we have the interplay of inertia, viscoelasticity and shear-thinning. With these different models we are able to analyze the independent and coupled effects of the three factors upon the orientation of the rigid body. Our argument in Chapter 9 is therefore systematic and complete in this regard.

4. To genuinely understand the problem under investigation, it is important that we fill the gaps in previous experiments by making our study systematic. For this reason, we have also pursued the problem via experiments, which are discussed in detail in Chapter 6. Two sets of experiments have been designed and conducted, the first is a sedimentation experiment where the particle is dropped in a quiescent liquid, like in previous studies, whereas the second experiment is a flow chamber study, where the particle is held fixed at the center of a flow chamber wile the liquid moves past it. We have managed to replicate the results of the previous experiments while at the same time make some significant changes which can provide more information. The experiments have been conducted with three different types of liquids, (a) Newtonian and (b) Shear-thinning viscoelastic polymers. Previous studies have been conducted upon the first two kinds of liquids. Once again, the objective behind our choice of these liquids is in order to understand the effect that inertia, viscoelasticity and shear-thinning play on our phenomenon. The liquids that we choose possess these effects in different combinations allowing for a comparison with our analytical studies.

5. In addition to an analytic and experimental approach, we also perform a numerical investigation of the torques imposed upon rigid bodies with fore-aft symmetry in exterior

domains. In fact, we make this calculation for the Navier-Stokes, Second order and Oldroyd-B fluid models. Besides, we have also conducted a preliminary investigation of the torque on a prolate spheroid due to the modified Second order fluid. In addition to the physical significance of the torque, this calculation, also has implications upon the stability of the terminal orientation of the sedimenting body.

3.0 MATHEMATICAL PRELIMINARIES

3.1 Notation and Definitions

By $\mathbf{R}^3$, we denoted the three dimensional Euclidean space and $\Omega \subset \mathbf{R}^3$ represents an exterior domain, i.e. an open and connected set, exterior to the body $\mathcal{B}$, which is a compact, connected subset of $\mathbf{R}^3$. By Σ we refer to the boundary of Ω and n is the outer unit normal to Σ. The term B_R is defined by the set $\{y \in \mathbf{R} : |x - y| < R\}$ and ∂B_R denotes the boundary of this set.

For $\gamma_i \geq 0$ $(i = 1, 2, 3)$, with $|\gamma| = \sum_i \gamma_i$, we define

$$\text{grad }^k u = \partial_{i_1} \partial_{i_2} ... \partial_{i_k} u_m$$

and also

$$D^\gamma u = \frac{\partial^{|\gamma|} u}{\partial {x_1}^{\gamma_1} \partial {x_2}^{\gamma_2} \partial {x_3}^{\gamma_3}}$$

Throughout the thesis, we employ the Einstein summation convention and the standard convention for the saturation of second order tensors. Therefore, if A and B represent two second order tensors, their saturation is represented by the Gibbs notation, namely $A : B = A_{ij} B_{ij}$.

Definition 3.1.1 *The symbol, $\mathcal{C}^k$ with integer $k \geq 0$, represents the Banach space of continuously differentiable functions upto the boundary in Ω with norm*

$$||u||_{\mathcal{C}^k(\hat{\Omega})} = \ max_{0 \leq |\gamma| \leq k} sup |D^\gamma u|.$$

Definition 3.1.2 (Sobolev Space) *By $W^{m,q}$, $m \geq 0$, $1 \leq q \leq \infty$, we denote the usual*

Sobolev space with norm

$$||u||_{m,q} = \left(\sum_{k=0}^{m} \int_{\Omega} |D^k u|^q \right)^{1/q}$$

and

$$||u||_{m,\infty} = max_{0 \leq |k| \leq m} esssup |D^k u|.$$

When $m = 0$, $||u||_{W^{0,q}} = ||u||_q$.

Definition 3.1.3 (Homogeneous Sobolev Space) *The space* $D^{m,q}(\Omega)$ *denotes a homogeneous Sobolev Space, defined as*

$$D^{m,q}(\Omega) = \{u \in L^1_{loc}(\Omega) : D^l u \in L^q(\Omega), |l| = m\}.$$

with the seminorm

$$||u||_{D^{m,q}} = |u|_{m,q} = \left(\sum_{|l|=m} \int_{\Omega} |D^l u|^q \right)^{1/q}.$$

Definition 3.1.4 *We define the Banach space* X *in which our existence results will be established as the space*

$$\tilde{D}^{2,t}(\Omega) \cap [\cap_{m=0}^{k} D^{m+2,q}(\Omega)] \times D^{1,t}(\Omega) \cap [\cap_{m=0}^{k} D^{m+1,q}(\Omega)]$$

with the norm

$$\begin{aligned} ||u||_X + ||\pi||_X &= ||u||_{\frac{3t}{3-2t}} + |u|_{1,\frac{3t}{3-t}} + |u|_{2,t} + ||\pi||_{\frac{3t}{3-t}} + |\pi|_{1,t} \\ &+ \sum_{n=0}^{k+1} (|u|_{n+2,q} + |\pi|_{n+1,q}) \end{aligned}$$

where $1 < t < 3/2$ *and* $q > 3$.

Definition 3.1.5 *Let* K *be an operator from Banach spaces, mapping* B *to* $\hat{B}$. *Then for the sequence,* $\{Ku_k\} \subset \hat{B}$ *is said to be* precompact *in* $\hat{B}$, *implies that there exists a* $\{u_k\} \subset B$ *such that* $\{Ku_k\}$ *converges in* $\hat{B}$.

Definition 3.1.6 *The operator K as defined above is said to be* compact *if for each bounded $\{u_k\} \subset B$, the sequence $\{Ku_k\}$ is precompact in $\hat{B}$.*

Definition 3.1.7 *If $B \subset \hat{B}$, then we say that B is* compactly embedded *in $\hat{B}$, provided (a) $||u||_{\hat{B}} \leq c||u||_B$ for some constant c and (b) every bounded sequence in B is precompact in $\hat{B}$.*

Definition 3.1.8 (Eigenvalues & Eigenvectors) *If an operator A satisfies*

$$A \cdot u_i = \lambda_i u_i$$

for $i = 1, 2, .., n$ and where u is a vector field and λ is a scalar, then we refer to the pair (u_i, λ_i) as the eigenvector and eigenvalue corresponding to u of the operator A, respectively. If A satisfies

$$A \cdot u_i = \lambda u_i$$

for all $i = 1, 2, ..., n$, then we have that λ has multiplicity *n. In the particular case when the multiplicity of λ is one, we say that λ is a* simple eigenvalue.

Definition 3.1.9 (Frechet Derivative) *Let F be a bounded linear operator which maps $\Omega \subset B \to \hat{B}$ where $B, \hat{B}$ are Banach spaces, then*

$$\lim_{x \to 0} ||\frac{F(x+a) - F(a)}{|x|}||$$

for $x, a \in \Omega$ is called the Frechet derivative of F.

3.2 Basic Inequalities

In this section, we present some useful, though basic inequalities. The proof of these results are not presented here since most of the results are well known. For proof, we

refer the readers to elementary text books in Partial Differential Equations or Functional Analysis.[1,19,49,71,85]

Theorem 3.2.1 (Cauchy-Schwarz Inequality) *Let $a, b \in \mathbf{R}^+$, then*

$$ab < \epsilon a^2 + \frac{b^2}{\epsilon}$$

where $\epsilon > 0$.

Theorem 3.2.2 (Minkowski's Inequality) *Let u,v $\in L^p(\Omega)$ with $1 \leq p \leq \infty$. Then*

$$||u + v||_p \leq ||u||_p + ||v||_p.$$

Theorem 3.2.3 (Holder's Inequality) *Let $p \geq 1$ and $q < \infty$ be such that $\frac{1}{p} + \frac{1}{q} = 1$. Then for $u \in L^p(\Omega)$ and $v \in L^q(\Omega)$, the following inequality holds,*

$$\int_\Omega |uv| \leq ||u||_p ||v||_q.$$

Theorem 3.2.4 (Interpolation Inequality) *Let $u \in L^s(\Omega) \Cup L^t(\Omega)$ with $1 \leq s, t \leq \infty$. Also let us assume that $u \in L^r(\Omega)$, where $1 \leq r \leq \infty$. Then the following inequality holds.*

$$||u||_r \leq ||u||_s^\theta ||u||_t^{1-\theta}.$$

The next inequality is extremely useful for our purposes and is termed the *Sobolev inequality*. For a more detailed discussion, refer to.[1,25]

Theorem 3.2.5 (Sobolev Inequality) *Let $1 < q < n$ and $r = nq/(n-q)$. Then for all $u \in C_0^\infty(\Omega)$, we have*

$$||u||_r \leq \frac{q(n-1)}{2\sqrt{n}(n-q)} ||grad\ u||_q.$$

3.3 Essential Theorems

Theorem 3.3.1 (Gauss' Theorem) *Let Ω be a volume with boundary denoted Σ. Also, let n be the unit outward normal to Σ. Then,*

$$\int_{\Omega} div\, v\, d\Omega = \int_{\Sigma} y \cdot n\, d\Sigma.$$

Theorem 3.3.2 (Banach Fixed Point Theorem) *Let $A : B \to B$ be a nonlinear mapping. Let us also assume that*

$$||A[u_1] - A[u_2]|| \leq \alpha ||u_1 - u_2||$$

where $u_1, u_2 \in B$ and $\alpha < 1$. Then the mapping A has a unique fixed point.

Proof:

The proof of this theorem see[19,49,66] or any other elementary text books in Functional Analysis. □

Theorem 3.3.3 (Implicit Function Theorem) *Let $F : \mathbf{R}^{n+1} \to \mathbf{R}^n$ be a C^∞ map. Take $x \in \mathbf{R}^n$ and $z \in \mathbf{R}$ and assume that the pair (x_0, z_0) satisfies*

$$F(x_0, z_0) = 0,\ \frac{\partial F}{\partial z}(x_0, z_0) \neq 0.$$

Then there is an open ball, $U \subset \mathbf{R}^n$ containing x_0 and an internal $V \subset \mathbf{R}$ containing z_0, such that there is unique function $z = g(x)$ which satisfies $F(x, g(x)) = 0$.

Proof:

See[19,85] for proof. □

Theorem 3.3.4 (Fredholm Alternative) *Let $A : H \to H$ be a compact linear operator. Also, suppose $N(A)$ and $R(A)$ refer to the null space and the range of A, respectively, then*

1. *$N(I - A)$ is finite dimensional*
2. *$R(I - A)$ is closed*
3. *$R(I - A) = N(I - A^*)^{\perp}$*
4. *$N(I - A) = \{0\}$ iff $R(I - A) = H$*
5. *$dim N(I - K) = dim R(I - A^*)$.*

Proof:

See[19, 85] for proof of this theorem. □

Lemma 3.3.1 *Let A be a positive-definite and symmetric operator. Then all the eigenvalues of A, denoted λ_i, for $i = 1, 2, ..., n$ are positive and real.*

Proof:

See[73] for proof. □

3.4 The Stokes Equations

The Stokes equations are obtained from the Navier-Stokes equations in the limit $Re \to 0$. Physically this amounts to cases when either the characteristic velocity of the flow is very slow or if the fluid is very viscous. The governing equations for the flow of an incompressible Newtonian liquid in the *Stokes regime* of can be written in dimensional form as

$$\left.\begin{aligned} -\eta \Delta u + \text{grad } \pi = 0 \\ \text{div } u = 0 \end{aligned}\right\} \tag{3.1}$$

where η represents the viscosity of the fluid and (u, π) represent the velocity and pressure fields, respectively, corresponding to the flow.

The primary feature of the Stokes equations is its inherent symmetry which helps simplify several of our calculations. The Figure 3.1 shows the symmetry of the flow past an ellipse where the lines are indicative of the streamlines of flow. It is easily seen that the equation is linear, hence allowing for closed form solutions to several problems which are otherwise not solvable in the case of higher Re. Since the equations are linear, it is easily verified that (u, p) and $(-u, -p)$ are both solutions to the equation (3.1). This final observation in fact, informs us that physical quantities such as the drag, stress remain unchanged by the change of direction of flow.

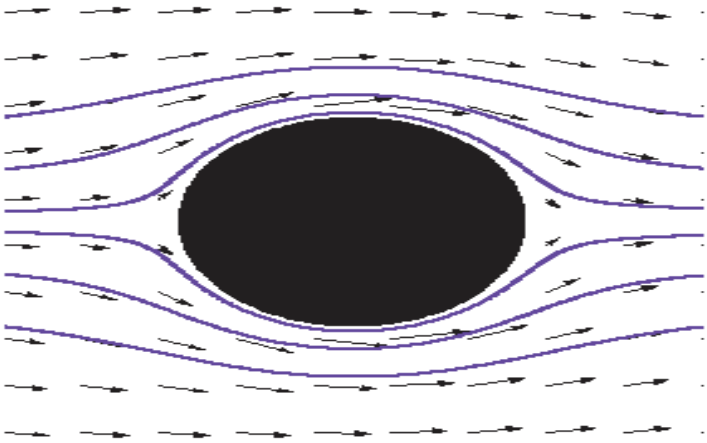

Figure 3.1. Streamlines for Stokes flow. .

In this section we introduce some fundamental results on the Stokes system concerning the existence and uniqueness of solutions in exterior domains. Let us consider the equations for Stokes flow around a body $\mathcal{B}$ in an exterior domain i.e. in the unbounded region surrounding $\mathcal{B}$. In such domains, one typically requires that the velocity field at large distances approaches some prescribed value v_*. Hence,

$$\left.\begin{array}{rcl} -\Delta v + \text{grad } \pi & = & f \\ \text{div } v & = & 0 \\ v & = & 0 \text{ on } \partial\Omega \\ \lim_{|x|\to\infty}[v(x) + v_*] & = & 0. \end{array}\right\} \tag{3.2}$$

Theorem 3.4.1 *Let Ω be an exterior domain of class $C^{k+2}(\Omega)$, $k \geq 0$. Let us also consider $\psi \in W^{k+1,q}$, $u_* \in W^{k+2-1/q,q}(\partial\Omega)$, div $\psi \in L^t(\Omega)$ and $u_* \in W^{2-1/t,t}(\partial\Omega)$ for $1 < t < 3/2$ and $3 < q < \infty$. Then, there exists a unique solution, (u, π) to the Stokes problem (8.53) such that*

$$u \in \tilde{D}^{2,t}(\Omega) \cap [\cap_{m=0}^{k} D^{m+2,q}(\Omega)]$$

$$\pi \in D^{1,t}(\Omega) \cap [\cap_{m=0}^{k} D^{m+1,q}(\Omega)].$$

Also, (u, π) satisfies the estimate

$$\begin{array}{rcl} ||grad\ u||_{C^k} + ||u||_s & + & |u|_{1,r} + |u|_{2,t} + ||\pi||_r + |\pi|_{1,t} \\ + \sum_{m=0}^{k} (|u|_{m+2,q} + |\pi|_{m+1,q}) & \leq & c(||div\ \psi||_t + ||\psi||_{k+1,q} + |\xi| + |\omega|) \end{array}$$

with $r = \frac{3t}{3-t}$, $s = \frac{3t}{3-2t}$, $v = u + v_*$ and $c = c(q, t, k)$.

Proof:

See [25, Theorem V.4.3]. □

We introduce a new of fields which we shall term the *auxiliary fields* and denoted $(h^{(i)}, p^{(i)})$ and $(H^{(i)}, P^{(i)})$ for $i = 1, 23$ in three dimensions. These auxiliary fields serve as a basis field for the Stokes velocity and pressure. Hence, they satisfy the Stokes equations. The full set of equations for these fields are given below.

$$\left.\begin{array}{rcl} \Delta h^{(i)} & = & \text{grad } p^{(i)} \\ \text{div } h^{(i)} & = & 0 \\ \lim_{|x|\to\infty} h^{(i)}(x) & = & 0 \\ h^{(i)}(y) & = & e_i, \quad y \in \Sigma \end{array}\right\} \tag{3.3}$$

and

$$\left.\begin{array}{rcl} \Delta H^{(i)} & = & \text{grad } P^{(i)} \\ \text{div } H^{(i)} & = & 0 \\ \lim_{|x|\to\infty} H^{(i)}(x) & = & 0 \\ H^{(i)}(y) & = & e_i \times y, \quad y \in \Sigma. \end{array}\right\} \tag{3.4}$$

The figures 3.2,3.3 and 3.4 should help clarify the physical meaning of these fields. The first set of the auxiliary fields, $h^{(i)}$, indicate the flow past the body if the body is translating in the e_i direction and the second set of auxiliary fields, $H^{(i)}$, indicates the flow past a body which is rotating about the respective e_i direction. Furthermore, we have the following estimates for the auxiliary fields.

Theorem 3.4.2 *For each $i = 1, 2, 3$ the problems (3.3) and (3.4) have unique solutions $(h^{(i)}, p^{(i)})$ and $(H^{(i)}, P^{(i)})$, such that $(h^{(i)}, p^{(i)})$, $(H^{(i)}$ and $P^{(i)}) \in C^\infty(\Omega)$,*

$$h^{(i)}, H^{(i)} \in L^s(\Omega) \Cap D^{1,r}(\Omega) \Cap D^{2,t}(\Omega)$$

$$p^{(i)}, P^{(i)} \in L^r(\Omega) \Cup D^{1,t}(\Omega)$$

for $3 < s \leq \infty$, $3/2 < r \leq \infty$ and $1 < t < \infty$. Furthermore the auxiliary fields also obey the

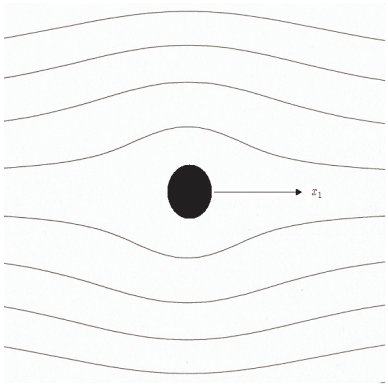

Figure 3.2. The field $h^{(1)}$ corresponding to translation of body along the x_1 direction .

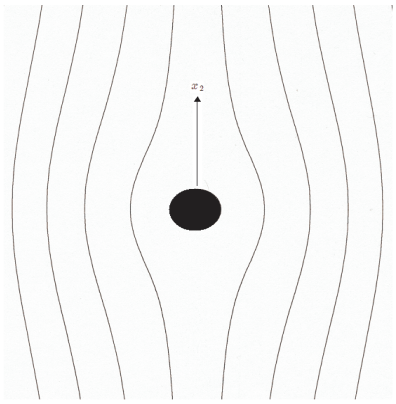

Figure 3.3. The field $h^{(2)}$ corresponding to translation of body along the x_2 direction .

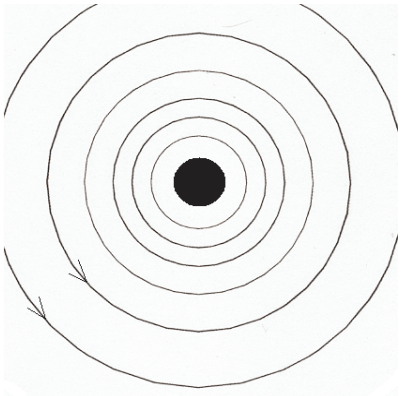

Figure 3.4. The field $H^{(3)}$ corresponding to rotation of body about the x_3 direction .

following estimates,

$$\begin{aligned} ||(1+|x|)\tilde{H}_i||_\infty &+ ||grad\ \tilde{H}_i||_\infty + ||\tilde{P}_i||_\infty + ||\tilde{H}_i||_s \\ &+ |\tilde{H}_i|_{1,r} + |\tilde{H}_i|_{2,t} + ||\tilde{P}_i||_r + |\tilde{P}_i||_{1,t} \leq C \end{aligned} \tag{3.5}$$

where C is a constant depending upon Σ and at most on s, r and t. Also, $(\tilde{H}_i, \tilde{P}_i) = (h^{(i)}, p^{(i)})$ for $i = 1, 2, 3$ and $(\tilde{H}_i, \tilde{P}_i) = (H^{(i)}, P^{(i)})$ for $i = 4, 5, 6$.

The estimates on the field $H^{(i)}$ can be further improved. This is presented in the Lemma below.

Lemma 3.4.1 *Let $(H^{(i)}, P^{(i)})$ be auxiliary fields that satisfy the equations (3.4). Then, for all $s > 3/2$ and $r > 1$, there is a positive constant $c = c(\mathcal{B}, s, r)$ such that*

$$||H^{(i)}||_s + |H^{(i)}|_r \leq c$$

for $i = 1, 2, 3$.

Proof:

For proof of this Lemma, see.[27,31] □

We now introduce certain definitions which helps in classifying the symmetries of the auxiliary fields.

Definition 3.4.1 (Rotational Symmetry)

We say that a body $\mathcal{B}$ has rotational symmetry about an axis, say x_1, if and only if :

$$(x_1, x_2, x_3) \in \Sigma \Rightarrow (x_1, -x_2, x_3), (x_1, x_2, -x_3) \in \Sigma.$$

Definition 3.4.2 (Symmetry Operators)

We define certain new symmetry classes next. We define the operators $\mathcal{P}_i$, $i = 1, 2, 3$ such that:

$$\begin{aligned}
\mathcal{P}_1 f(x_1, x_2, x_3) &:= f(-x_1, x_2, x_3) \\
\mathcal{P}_2 f(x_1, x_2, x_3) &:= f(x_1, -x_2, x_3) \\
\mathcal{P}_3 f(x_1, x_2, x_3) &:= f(x_1, x_2, -x_3) \\
\mathcal{P}_4 f(x_1, x_2, x_3) &:= f(-x_1, -x_2, x_3)
\end{aligned}$$

Definition 3.4.3 (Symmetry Class for Scalar Functions)

Suppose $\phi = \phi(x_1, x_2, x_3)$ is a scalar field. Then, we define the following symmetry classes:

$$\begin{aligned}
\mathcal{C}_1^s &:= \{\phi : \mathcal{P}_1\phi = \phi, \mathcal{P}_2\phi = -\phi, \mathcal{P}_3\phi = \phi\},\ \mathcal{C}_2^s := \{\phi : \mathcal{P}_1\phi = -\phi, \mathcal{P}_2\phi = \phi, \mathcal{P}_3\phi = \phi\} \\
\mathcal{C}_3^s &:= \{\phi : \mathcal{P}_1\phi = -\phi, \mathcal{P}_2\phi = -\phi, \mathcal{P}_3\phi = -\phi\},\ \mathcal{C}_4^s := \{\phi : \mathcal{P}_1\phi = \phi, \mathcal{P}_2\phi = \phi, \mathcal{P}_3\phi = -\phi\} \\
\mathcal{C}_5^s &:= \{\phi : \mathcal{P}_4\phi = \phi, \mathcal{P}_3\phi = \phi\},\ \mathcal{C}_6^s := \{\phi : \mathcal{P}_4\phi = -\phi, \mathcal{P}_3\phi = \phi\} \\
\mathcal{C}_7^s &:= \{\phi : \mathcal{P}_4\phi = \phi, \mathcal{P}_3\phi = -\phi\},\ \mathcal{C}_8^s := \{\phi : \mathcal{P}_1\phi = \phi, \mathcal{P}_2\phi = -\phi, \mathcal{P}_3\phi = -\phi\} \\
\mathcal{C}_9^s &:= \{\phi : \mathcal{P}_1\phi = -\phi, \mathcal{P}_2\phi = \phi, \mathcal{P}_3\phi = -\phi\},\ \mathcal{C}_{10}^s := \{\phi : \mathcal{P}_1\phi = -\phi, \mathcal{P}_2\phi = -\phi, \mathcal{P}_3\phi = \phi\}
\end{aligned}$$

Definition 3.4.4 (Symmetry Class for Vector Fields)

Suppose $w = (w_1, w_2, w_3)$ is a vector field, then we define the following classes (see[28]):

$$\begin{aligned}
\mathcal{C}_1^v &:= \{w : w_1 = \mathcal{P}_1 w_1 = \mathcal{P}_2 w_1 = \mathcal{P}_3 w_1, w_2 = -\mathcal{P}_1 w_2 = -\mathcal{P}_2 w_2 = \mathcal{P}_3 w_2, \\
w_3 &= -\mathcal{P}_1 w_3 = \mathcal{P}_2 w_3 = -\mathcal{P}_3 w_3\} \\
\mathcal{C}_2^v &:= \{w : w_1 = -\mathcal{P}_1 w_1 = \mathcal{P}_2 w_1 = \mathcal{P}_3 w_1, w_2 = -\mathcal{P}_1 w_2 = -\mathcal{P}_2 w_2 = \mathcal{P}_3 w_2, \\
w_3 &= \mathcal{P}_1 w_3 = -\mathcal{P}_3 w_3 = -\mathcal{P}_3 w_3\} \\
\mathcal{C}_3^v &:= \{w : w_1 = -\mathcal{P}_1 w_1 = -\mathcal{P}_2 w_1 = -\mathcal{P}_3 w_1, w_2 = \mathcal{P}_1 w_2 = \mathcal{P}_2 w_2 = -\mathcal{P}_3 w_2, \\
w_3 &= \mathcal{P}_1 w_3 = -\mathcal{P}_2 w_3 = \mathcal{P}_3 w_3\} \\
\mathcal{C}_4^v &:= \{w : w_1 = \mathcal{P}_1 w_1 = \mathcal{P}_2 w_1 = -\mathcal{P}_3 w_1, w_2 = -\mathcal{P}_1 w_2 = -\mathcal{P}_2 w_2 = -\mathcal{P}_3 w_2, \\
w_3 &= -\mathcal{P}_1 w_3 = \mathcal{P}_2 w_3 = \mathcal{P}_3 w_3\} \\
\mathcal{C}_5^v &:= \{w : w_1 = \mathcal{P}_1 w_1 = -\mathcal{P}_2 w_1 = \mathcal{P}_3 w_1, w_2 = -\mathcal{P}_1 w_2 = \mathcal{P}_2 w_2 = \mathcal{P}_3 w_2, \\
w_3 &= -\mathcal{P}_1 w_3 = -\mathcal{P}_2 w_3 = -\mathcal{P}_3 w_3\}.
\end{aligned}$$

Theorem 3.4.3 *Let $\mathcal{B}$ be a symmetric body with fore-aft symmetry. Then the auxiliary fields, $(h^(i), p^{(i)})$ and $(H^(i), P^{(i)})$ as defined in equations (3.3) and (3.4) have the following symmetry properties:*

$$\begin{aligned}
\mathbf{h}^{(1)} \in \mathcal{C}_1^v \quad &, \quad \mathbf{h}^{(2)} \in \mathcal{C}_2^v \\
\mathbf{H}^{(1)} \in \mathcal{C}_3^v \quad &, \quad \mathbf{H}^{(2)} \in \mathcal{C}_4^v, \quad \mathbf{H}^{(3)} \in \mathcal{C}_5^v.
\end{aligned} \tag{3.6}$$

Proof:

For proof of this theorem, refer to[24, 27, 28] □

.

The auxiliary fields also motivate more definitions. We define four tensor fields

$$K_{ij} = \int_{\Sigma} \left(T(h^{(i)}, p^{(i)}) \cdot n\right)_j \tag{3.7}$$

$$C_{ij} = \int_{\Sigma} \left(x \times T(h^{(i)}, p^{(i)}) \cdot n\right)_j \tag{3.8}$$

$$\Omega_{ij} = \int_{\Sigma} \left(x \times T(H^{(i)}, P^{(i)}) \cdot n\right)_j \tag{3.9}$$

$$S_{ij} = \int_{\Sigma} \left(x \times T(H^{(i)}, P^{(i)}) \cdot n\right)_j . \tag{3.10}$$

Remark 3.4.1 *K_{ij} represents the force on a body $\mathcal{B}$ which is only translating in the e_i direction, C_{ij} is the force on $\mathcal{B}$ due to translation of the body along the e_i axis, Ω_{ij} is the torque on $\mathcal{B}$ due to the rotation of the body about the e_i direction and S_{ij} is the torque on $\mathcal{B}$ due to the rotation of the body about the e_i axis. Note that the tensors depend only upon the geometry, shape and size of the body.*

We now list some useful properties of the above tensors. The proof of these results will not be provided below. We refer the readers to[36] for a detailed discussion regarding the proof.

Property 3.4.1 *The tensors K and Ω are positive definite and symmetric.*

Property 3.4.2 *$S = C^T$.*

Property 3.4.3 *The matrix*

$$\begin{pmatrix} K & C \\ C^T & \Omega \end{pmatrix}$$

is positive definite and symmetric.

4.0 REVIEW OF CONTINUUM MECHANICS

4.1 Fluid Mechanics

Continuum mechanics deals with the motion and deformation of bodies. A body $\mathcal{B}$ is defined as a set of points that occupy a certain region of the Euclidean space. In particular, fluid mechanics deals specifically with the motion and deformation of liquids and gases. To describe the former, we must begin with a choice of a suitable coordinate system, $\mathcal{S}$ and for the latter a reference configuration must be chosen. This reference configuration is the configuration of $\mathcal{B}$ at time $t = 0$. If X denotes the coordinates of the material points of $\mathcal{B}$ at $t = 0$ with respect to the coordinate system $\mathcal{S}$ and x represents the coordinates of the same material points at some later time t, then the motion of the material points may be described through the smooth mapping

$$x = \chi(X, t).$$

The *Principle of impenetrability of matter* requires that the above mapping have an inverse. Therefore,

$$X = \chi^{-1}(x, t).$$

In continuum mechanics we distinguish two different approaches. The first is the Lagrangian approach where we study the motion of a fluid particle, p between a certain time interval (t_1, t_2). The second approach, called the Eulerian approach is one where we study the motion of particles passing through a fixed point x in space. In fluid mechanics, it is conventional to take the second approach. The Eulerian velocity and Eulerian acceleration are defined as follows:

$$v(x, t) = \frac{d\chi}{dt}(x, t)$$

$$a(x, t) = \frac{dv}{dt}(x, t)$$

where the time derivative employed is the material derivative which is defined as

$$\frac{d\phi}{dt}(x,t) = \frac{\partial \phi}{\partial t}(x,t) + v(x,t) \cdot \nabla_x \phi(x,t).$$

We define the velocity gradient tensor, L, as

$$L(x,t) = \nabla_x v(x,t).$$

Also, related to the tensor L are its symmetric and skew-symmetric counterparts respectively, namely

$$D = \frac{1}{2}(L + L^T),\ W = \frac{1}{2}(L - L^T)$$

where L^T indicates the transpose of L.

We will now discuss the important conservation rules in continuum mechanics. However, prior to that we need to make some important definitions. Let $\rho = \rho(x,t)$ be the Eulerian density of $\mathcal{B}$ and $m(V)$ be the mass contained in a material volume, $V(t)$ at time t. Then,

$$m(V) = \int_{V(t)} \rho(x,t) dt.$$

The *Principle of conservation of mass* states that

$$\frac{d}{dt} \int_{V(t)} \rho(x,t) dt = 0, \tag{4.1}$$

that is, the mass contained in any arbitrary material volume is a constant, independent of time $t > 0$. The local or differential form of this conservation rule may be stated as

$$\frac{\partial \rho}{\partial t} + \text{div } (\rho v) = 0.$$

The second conservation law is the *Principle of conservation of linear momentum*, which states that

$$\frac{d}{dt}\int_{V(t)} \rho(x,t)v(x,t)dx = \int_{V(t)} \rho(x,t)b(x,t)dx + \int_{\partial V(t)} \hat{t}(s,t;n)ds \tag{4.2}$$

for all material volumes $V(t)$, with $t > 0$. Also, here $b(x,t)$ is the body force per unit mass and $\hat{t}(s,t)$ is the tractional force per unit area and n is the normal vector to the surface $\partial V(t)$. The conservation of linear momentum suggests that the total rate of change of linear momentum inside an arbitrary material volume $V(t)$ is equal to the net force acting upon this volume. In this context, it was shown by Cauchy that there exists a second order tensor, $T(x,t)$ which is independent of n such that

$$\hat{t}(x,t;n) = T(x,t)\cdot n.$$

This relation is also referred to as the *Cauchy Stress Principle.* Consequently, the local form of equation (4.2) is written as

$$\rho\frac{dv}{dt} = \rho b + \text{div } T. \tag{4.3}$$

Similarly, the *Principle of Conservation of Angular Momentum* states that the net rate of change of angular momentum with respect to some fixed point, x_0 and the total intrinsic angular momentum of a material volume is equal to the total torque acting upon this material volume. In integral form, this is represented by the equations

$$\begin{aligned}\frac{d}{dt}\int_{V(t)} \rho(x,t)[(x-x_0) \quad \times \quad v(x,t)+l(x,t)]dx &= \int_{V(t)} \rho(x,t)[(x-x_0)\times b(x,t)+c(x,t)]dx \\ + \quad \int_{\partial V(t)} &[(x-x_0)\times \hat{t}(s,t)+M(s,t)]ds. \end{aligned}\tag{4.4}$$

In case the body $\mathcal{B}$ is non-polar, i.e. it a body that cannot sustain local torques, then

$$l(x,t) = c(x,t) = M(x,t) = 0$$

and consequently, the local form of equation (4.4) becomes

$$T = T^T. \tag{4.5}$$

Hence, in conclusion, the motion of a non-polar body $\mathcal{B}$, under the action of an external body force, b, must satisfy the following equations:

$$\left.\begin{array}{rcl} \dfrac{\partial \rho}{\partial t} + \text{div } (\rho v) & = & 0 \\ \rho\left(\dfrac{\partial v}{\partial t} + v \cdot \nabla v\right) & = & \text{div } T + \rho b \\ T = T^T. & & \end{array}\right\} \tag{4.6}$$

Additional to these three equations, one also needs to specify the constitutive equation, which is the characteristic equation of the fluid and which accounts for the material properties of the fluid under consideration. In the next sections, we shall look at a few constitutive equations corresponding to Newtonian and certain Non-Newtonian liquid models.

4.2 Principle of Material Objectivity

A fundamental requirement for the stress tensor is that it satisfy the *principle of material objectivity* or *frame invariance* which essentially requires that the the dynamic processes and the stress tensor will remain the same for two different observers. Mathematically, this is satisfied by showing that the stress tensor remains invariant under an orthogonal transformation. That is,

$$T(u,p) = Q^T \cdot T(Q \cdot u, p) \cdot Q$$

where Q is an orthogonal transformation[1]. We will try to deal with this theme in some detail here. This will require some preliminary definitions and results.

Remark 4.2.1 *In general, we know that scalars transform according to the rule*

$$\hat{\phi}(\hat{x}, t) = \phi(x, t),$$

vectors according to the rule

$$\hat{u}(\hat{x}, t) = Q \cdot u(x, t)$$

and second order tensors according to

$$\hat{S}(\hat{x}, t) = Q \cdot S(x, t) \cdot Q^T$$

where Q is an orthogonal transformation.

Consider a change in reference frames $\mathcal{F} \to \hat{\mathcal{F}}$. The related orthogonal transformation is a function of time and will be denoted $Q(t)$ and are known to preserve distances. We will now recount some essential properties of such a transformation. These properties will prove useful in later discussion in this chapter.

Property 4.2.1 *Position vectors in the reference frames transform according to the rule*

$$\hat{x} = Q(t) \cdot x + c(t)$$

where $c(t)$ is a vector valued function of time.

At time $t = 0$, we have $Q(0) = I$ and $c(0) = 0$.

Property 4.2.2 *Velocity fields transform according to*

$$\hat{u} = \frac{dc(t)}{dt} + A \cdot Q \cdot x + Q \cdot u.$$

[1]An orthogonal transformation, Q must satisfy $QQ^T = I$.

Proof:

The transformation of the velocity vector in the two frames can then be computed from Property 4.2.1. Hence,

$$\begin{aligned} \hat{u} &= \frac{dc(t)}{dt} + \frac{dQ}{dt} \cdot x + Q \cdot \frac{dx}{dt} \\ &= \frac{dc(t)}{dt} + \frac{dQ}{dt} \cdot x + Q \cdot u. \end{aligned}$$

Let us define the tensor A as

$$A := \frac{dQ}{dt} \cdot Q^T.$$

Then it follows that

$$A^T = Q \cdot \frac{dQ^T}{dt}.$$

Therefore, combining the two relations, we have

$$A + A^T = 0$$

which implies that A is skew-symmetric. Therefore, in light of this property of A, we can write,

$$\hat{u} = \frac{dc(t)}{dt} + A \cdot Q \cdot x + Q \cdot u. \tag{4.7}$$

□

A third relation that we derive regards the transformation of the tensor $L = \text{grad } u$.

Property 4.2.3 *The tensor L transforms according to the rule*

$$\hat{L} = A + Q \cdot L \cdot Q^T.$$

Proof:

We write

$$\begin{aligned}\hat{L} &= \frac{\partial \hat{u}}{\partial \hat{x}} = \frac{\partial \hat{u}}{\partial x} \cdot \frac{\partial x}{\partial \hat{x}} \\ &= (A \cdot Q \cdot I + Q \cdot L)Q^T \\ &= (A \cdot Q + Q \cdot L)Q^T \\ &= A + Q \cdot L \cdot Q^T. \end{aligned} \tag{4.8}$$

□

4.3 Dimensionless Numbers

In continuum mechanics, we employ dimensionless numbers for scaling arguments and in order to identify significant factors which effect the flow of different fluids. In Newtonian liquids, the relevant parameter is the Reynolds number,[69] denoted Re which is defined as

$$Re = \frac{\rho U d}{\eta}$$

where ρ is the density of the liquid, U is the characteristic velocity of the flow, d is the characteristic length scale of the flow and η is the viscosity of the liquid. Loosely speaking, one may think of the Re $\approx \frac{inertial\, effects}{viscous\, effects}$, i.e. the Reynolds number describes a competition between the viscosity and the inertia of the fluid. When the viscosity of the liquid is very high or U is very small, then the fluid is said to be in the *creeping flow* or *Stokes* regime.

For viscoelastic liquids, there are two useful dimensionless parameters, that is relevant for us, the Weissenberg number (We) or the Deborah number (De). Let λ refer to the characteristic time scale or the liquid, also referred to as a relaxation parameter and κ be a

second charactersitic time scale based upon the strain rate. The Weissenberg number can then be defined as

$$We = \lambda\kappa.$$

A second way of defining We is directly in terms of the normal stress coefficients of the viscoelasic liquid. Let α_1 be a parameter which is related to the first and second normal stress coefficients. Then,

$$We = \frac{-\alpha_1 U}{d\eta}.$$

The second definition is pertinent in the case of the Second order fluid. The Deborah number is then similarly defined by[38]

$$De = \frac{\lambda U}{d}.$$

So, loosely speaking $We \approx \frac{elastic\,effect}{viscous\,effects}$ and $De \approx \frac{characteristic\,time\,of\,liquid}{characteristic\,time\,of\,flow}$. Another useful parameter that we use is the Elasticity number, E, which is defined as

$$E = We/Re.$$

So, $E > 1$ implies that elastic effects dominate, whereas $E < 1$ suggests that inertial effects of the liquid dominate.

4.4 Newtonian Fluids

The consitutive equation for a viscous fluid can in general be written as

$$T = -pI + \sigma$$

where p is the inviscid component depending only upon the pressure and σ is the extra-strss tensor depending upon the viscosity of the liquid. In general, $\sigma = \sigma(\rho, L(u))$, where ρ is the density of the liquid and $L(u)$ is the gradient of the velocity, as defined earlier. The

principle of material objectivity suggests that the tensor σ can depend not upon $L(u)$ but its symmetric part, $D(u)$ (see Property 4.2.3). Therefore

$$\sigma = \sigma(D(u)).$$

Specifically for a Newtonian fluid, the extra-stress tensor is of the form

$$\sigma = c_0 I + c_1 D(u)$$

where $c_0 = \lambda \text{div } u$ and $c_1 = 2\eta$. Hence the constitutive equation becomes

$$T(u,p) = T_N(u,p) = (-p + \lambda \text{div } u)I + 2\eta D(u).$$

Here, η and λ are the relevant material parameters which are termed the *first* and *second viscosity coefficients*, respectively. If we further assume that the fluid is incompressible then div $u = 0$ and hence

$$T_N(u,p) = -pI + 2\eta D(u). \tag{4.9}$$

Remark 4.4.1 *We can easily verify that the Newtonian stress tensor is frame invariant. We know that the identity, I is frame invariant, therefore it is sufficient that we verify that the symmetric part of L is invariant. This follows from the observation that*

$$\begin{aligned} \hat{D}(u) &= \frac{1}{2}(\hat{L} + \hat{L}^T) = \frac{1}{2}(A + Q \cdot L \cdot Q^T) + \frac{1}{2}(A + Q \cdot L \cdot Q^T)^T \\ &= \frac{1}{2}(A + A^T) + \frac{1}{2}(Q \cdot [L + L^T] \cdot Q^T) \\ &= Q \cdot D(u) \cdot Q^T. \end{aligned} \tag{4.10}$$

Putting equation (4.9) into the equation (4.3) and taking ρ to be a constant in the continuity equation, gives us the Navier-Stokes equations

$$\left.\begin{aligned} \rho\left(\frac{\partial v}{\partial t} + v \cdot \nabla v\right) &= -\text{grad } p + \eta \Delta u + \rho b \\ \text{div } u &= 0. \end{aligned}\right\} \tag{4.11}$$

In the Navier-Stokes model, the only material function of importance is the viscosity, η, which is a positive quantity.

4.5 Power-Law Fluids

A simple model for a Non-Newtonian fluid is the Generalized Newtonian Fluid Model (GNF). The primary difference between this model and the Newtonian fluid model is that in the case of the GNF, the viscosity is not a constant but depends upon the shear-rate, i.e. $\eta = \eta(\dot{\gamma})$. Therefore the stress tensor may be written as

$$T(u,p) = T_N(u,p) + T_E(u)$$

where T_E refers to the extra stress tensor and is given by

$$T_E(u) = \eta(\dot{\gamma}) D(u).$$

There are several models that specify the form of the viscosity function. The one that we are interested in, in particular, is the Power-Law model,[56,57] where

$$\eta(\dot{\gamma}) = \kappa \dot{\gamma}^{n-1}$$

so

$$T = -pI + \kappa |D(u)|^{n-1} D(u). \tag{4.12}$$

Here, the parameter κ is the *consistency index* and has units $Pa \cdot s^n$, while n is a dimensionless quantity which measures the viscoelastic nature of the liquid. The Power-Law model can describe three different kinds of liquids depending upon the value of n. If $n = 1$ then the model describes a Newtonian fluid, if $n > 1$ then the model describes a Shear-thickening fluid and if $n < 1$, then the model describes a Shear-thinning fluid.

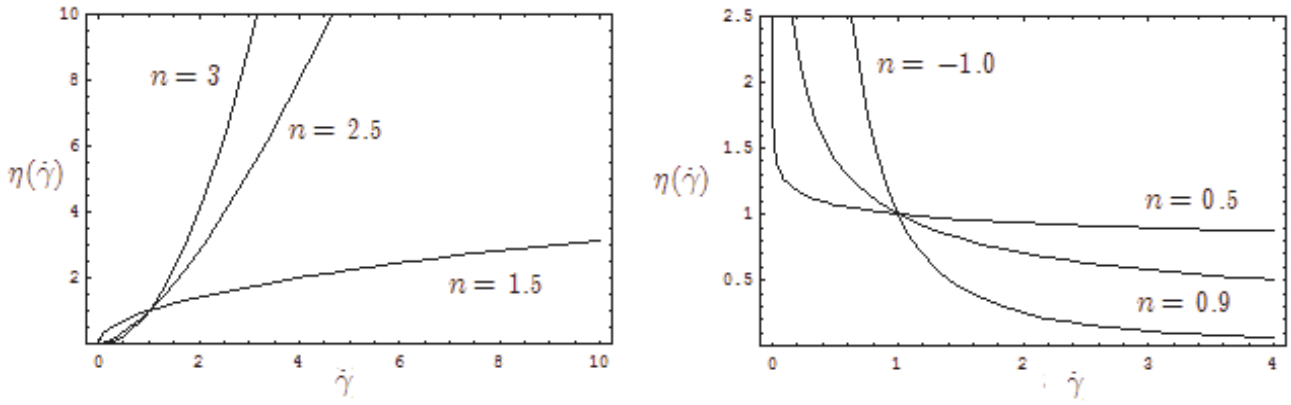

Figure 4.1. Some examples of viscosity as a function of shear rate for (a)shear thickening liquids and (b) shear thinning liquids .

Let us calculate the material functions, i.e. the viscosity, η and the first and second normal stress coefficients, Ψ_1 and Ψ_2 respectively, for the Power-Law fluid under shear flow. Consider the shear flow, defined by

$$u = (\dot{\gamma} x_2, 0, 0)$$

where $\dot{\gamma}$ is a constant. Then it follows that

$$D(u) = \frac{1}{2}(\text{grad } u + \text{grad }^T u) \tag{4.13}$$

$$= \frac{1}{2}\begin{pmatrix} 0 & \dot{\gamma} & 0 \\ \dot{\gamma} & 0 & 0 \\ 0 & 0 & 0 \end{pmatrix} \tag{4.14}$$

and hence,

$$T_E(u) = \frac{1}{2}\begin{pmatrix} 0 & \kappa|D(u)|^{n-1}D(u) & 0 \\ \kappa|D(u)|^{n-1}D(u) & 0 & 0 \\ 0 & 0 & 0 \end{pmatrix}. \tag{4.15}$$

Consequently, we have the three material functions, for the Power-Law fluid, namely

$$\eta = \frac{\tau_{21}}{\dot{\gamma}} = \frac{\kappa}{2}|D(u)|^{n-1},$$

$$\Psi_1 = \frac{(\tau_{11} - \tau_{22})}{\dot{\gamma}^2} = 0$$

and

$$\Psi_1 = \frac{(\tau_{22} - \tau_{33})}{\dot{\gamma}^2} = 0.$$

Therefore, the Power-Law fluid, in fact the GNF model does not exhibit any normal stress and therefore cannot account completely for the behavior of viscoelastic liquids. This is perhaps the primary disadvantage of the model. Also, the time dependent behavior of the polymer cannot be predicted from this sample since the relaxation time is not included as a parameter in this model. The advantage of the model comes primarily from its simplicity and capacity to make some simple predictions regarding the flow properties of viscoelastic liquids.

4.6 Second Order Fluids

The Second order fluid model is the simplest case of a viscoelastic fluid. The constitutive equation for this model can, in general be written as[77]

$$T = [-p+\frac{1}{2}\lambda tr(A_1)+\alpha_{10}tr(A_2)+\alpha_{20}tr(A_1^2)+\alpha_{30}(trA_1)^2]I+[\mu+\alpha_{11}tr(A_1)]A_1+\alpha_1 A_2+\alpha_2 A_1^2]$$

where

$$A_1 = 2D(u),\ A_2 = \frac{\partial A_1}{\partial t} + u \cdot \text{grad } A_1 + L^T A_1 + A_1 L,$$

and μ, λ, α_{10}, α_{20}, α_{30}, α_1 and α_2 are material constants. However, using the incompressibility condition, suggests that the extra-stress tensor must be of the form

$$\begin{aligned} T_E &= \alpha_1 A_2 + \alpha_2 A_1^2 \\ &= \alpha_1 \left(A_2 + \epsilon A_1^2\right) \end{aligned}$$

where $\epsilon = \frac{\alpha_2}{\alpha_1}$ and α_1 and α_2 are material parameters that depend upon the normal stress coefficients.

Lemma 4.6.1 *Let u be a solenoidal vector field. Then, the following identity holds:*

$$div\ (u \cdot \nabla A_1 + A_1 \nabla u) = u \cdot \Delta u + div\ A_1^2.$$

Proof:

For proof of this result, see.[43] □

In light of the above Lemma, we have a tractable form of the expression for div T, which may be written as

$$\text{div } T = -\text{grad } p + \mu\Delta u + \alpha_1 u \cdot \nabla\Delta u + \alpha_1 \text{div } [\text{grad }^T u A_1] + (\alpha_1 + \alpha_2)\text{div } A_1^2.$$

Remark 4.6.1 (Comments on the sign of α_1 and α_2) . *There is controversy regarding the value and sign of these coefficients. The Second order fluid model can be perceived in two different ways. The first school of thought is that this model is realistic. Therefore suitable application of thermodynamics and the Clausius-Duheim principle requires that* $\mu > 0$ *and* $\alpha_1 + \alpha_2 = 0$.[18] *Furthermore, if the above conditions are satisfied, then the model can be shown to be asymptotically stable, if* $\alpha_1 \geq 0$. *In fact rheological studies of viscoelastic liquids and polymers indicates that very often,* $\alpha_1 + \alpha_2 \neq 0$. *Based on this assumption, it has been shown*[32] *that the Second order fluid model has a rest state which is stable, provided* $\alpha_1 > 0$. *However, for the steady problem, the sign of* α_1 *is of no consequence. The second perception is that the Second order fluid model is not necessarily realistic but simply possesses all features of a viscoelastic liquid. Also, since the Second order fluid model is simply an approximation of the Simple fluid model, it can be argued that thermodynamic and stability conditions and must apply to the full Simple fluid model and not to each expansion of the full model. In any case, since we are concerned simply with the steady state equations, we make no assumptions upon the material functions.*

In order to evaluate the material functions η, α_1 and α_2, we analyze the Second order model in a shear flow $u = (\dot{\gamma} x_2, 0, 0)$. Then, using the same argument as in the earlier section, we have the three material functions, of the form[56]

$$\begin{aligned} \eta &= \mu \\ \Psi_1 &= (2\alpha_1 + \alpha_2) \\ \Psi_2 &= \alpha_2. \end{aligned}$$

Theorem 4.6.1 (Giesekus' Theorem[5,34]) *Given a velocity field* u *and a pressure,* P_N *that satisfy the equations for stokes flow for an incompressible Newtonian fluid, then the*

same velocity u and a pressure field P given by

$$P = P_N + \frac{\alpha_1}{\mu}(\frac{\partial P_N}{\partial t} + u \cdot grad\ P_N) + \frac{\alpha_1}{4}(\dot{\gamma} : \dot{\gamma})$$

satisfy the creeping flow of an incompressible Second order fluid with $\alpha_1 + \alpha_2 = 0$.

4.7 Rate-Type Models

In this section, we introduce a few nonlinear viscoelastic models. The higher order complexity in these models comes from the fact that these are designed to operate in the high strain regime. We shall refer to these models in general as the Maxwell models. The most general of these models has the extra stress tensor, $\sigma \equiv T_E$, of the form[56,57]

$$\begin{aligned} \sigma &= \sum_i^N \sigma^{(i)} \\ \sigma^{(i)} + \lambda_i \overset{\square}{\sigma}^{(i)} &= 2\eta_i D(u) \end{aligned} \tag{4.16}$$

where λ_i and η_i are material constants. Furthermore, the operator, $\square$ is defined as

$$\overset{\square}{A} = (1 - \frac{\zeta}{2})\overset{\triangle}{A} + \frac{\zeta}{2}\overset{\nabla}{A}$$

where

$$\overset{\nabla}{A} = \frac{\partial A}{\partial t} + u \cdot \text{grad } A + \text{grad } u \cdot A + A \cdot \text{grad }^T u$$

and

$$\overset{\triangle}{A} = \frac{\partial A}{\partial t} + u \cdot \text{grad } A - \text{grad } u \cdot A - A \cdot \text{grad }^T u.$$

When only two terms are given in equation (4.16), then we obtain the *Johnson-Segalman model*, namely

$$\begin{aligned} \sigma^{(1)} &= \eta_1 A_1 \\ \sigma^{(2)} + \lambda_1 \overset{\square}{\sigma}^{(2)} &= \eta_2 A_1 \\ \Rightarrow \sigma + \lambda_1 \overset{\square}{A}_1 &= \eta A_1 + \lambda_2 \overset{\square}{A}_1 \end{aligned} \tag{4.17}$$

where, in the final equation (4.17), we have

$$\sigma = \sigma^{(1)} + \sigma^{(2)},\ \lambda_1 = \lambda,\ \eta = \eta_1 + \eta_2,\ \lambda_2 = \eta_1 \lambda_1.$$

When $\zeta = 0$, then the Johnson-Segalman model reduces to the *Oldroyd-B model*. This in turn becomes the *Upper Convected model* as $\lambda_2 = 0$. Similarly, the Johnson-Segalman model reduces to the *Oldroyd-A model* as $\zeta = 2$ which becomes the *Lower Convected model* as $\lambda_2 = 0$. For $0 < \zeta < 2$, the Johnson-Segalman model is also referred to as the *Jeffreys model*. The material parameters λ_1 and λ_2 are referred to as the relaxation and retardation constants.

The viscometric functions for the Johnson-Segalman model in shear flow can be given by[56]

$$\mu = \frac{\eta_2}{1 + 2\zeta\lambda_1^2(1 - \zeta/2)\dot{\gamma}^2} + \eta_2 \tag{4.18}$$

$$\Psi_1 = \left(\frac{2\eta_2\lambda_1}{1 + 2\zeta\lambda_1^2(1 - \zeta/2)\dot{\gamma}^2} \right) \tag{4.19}$$

$$\Psi_2 = \left(\frac{\zeta\eta_2\lambda_1}{1 + 2\zeta\lambda_1^2(1 - \zeta/2)\dot{\gamma}^2} \right). \tag{4.20}$$

It is easily seen that the viscosity function is non-constant for the Jeffreys model but reduces to a constant for the Oldroyd-A and Oldroyd-B models. Similarly, the normal

stress coefficients for the Johnson-Segalman model scale as $1/\dot{\gamma}^2$, however, in the case of the Oldroyd A and B fluids, the coefficients become constants. Hence the Oldroyd-B model in which we are primarily interested does not exhibit shear thinning (or thickening) not do its normal stress coefficients display any variation with the shear-rate. The advantage of this model is that it is empirically derived and hence is used frequently in modeling Boger fluids (i.e. fluids that exhibit viscoelastic properties but no shear-thinning) and also those that exhibit non-zero constant normal stresses.

4.8 Equivalence of Models

In this section, we want to justify our choice of the Second order fluid equations as the primary model for studying viscoelastic liquids. We wish to show that in the creeping flow approximation as $u \to u_s$, the Stokes velocity field and for small viscoelastic effects, the Maxwell-type models become equivalent to the Second order model. In fact, by a similar argument to the one provided below, it is possible to verify that under the same conditions, several other models such as the *Giesekus model* and the *Phan-Thien Tanner model* reduce to the Second order fluid model. We shall provide the argument for the Johnson-Segalman fluid below.

Theorem 4.8.1 *Let u, u_s denote the velocity field and the Stokes velocity field respectively. Then, in the creeping flow limit, $u \to u_s$ and small viscoelastic parameters, i.e. $\lambda_i << 1$ for $i = 1, 2$, the extra stress tensor for the Johnson-Segalman model may be written in the form*

$$\sigma = \eta A_1(u_s) - \eta_2 \lambda_1 \left(\overset{\Delta}{A_1}\,(u_s) + \zeta A_1(u_s)^2 \right).$$

Proof:

Rewriting the equation (4.17), we have

$$\sigma = \eta A_1 + \lambda_2 \overset{\square}{A}_1 - \lambda_1 \overset{\square}{A} .$$

Then it is easily verified that in the limit $u \to u_s$ and $\lambda_1 \to 0$,

$$\sigma|_{u \to u_s, \lambda_1 \to 0} = \eta A_1(u_s).$$

Therefore for small λ_1, we may write

$$\sigma = \eta A_1(u_s) + (\lambda_2 - \lambda_1 \eta) \overset{\square}{A}_1 (u_s) = \eta A_1(u_s) - \eta_2 \lambda_1 \overset{\square}{A}_1 (u_s). \tag{4.21}$$

Using the fact that $\overset{\nabla}{A} = \overset{\Delta}{A} + 2A^2$, we have

$$\overset{\square}{A} = \overset{\Delta}{A} + \zeta A^2.$$

Hence, the extra stress tensor in equation(4.21) can be rewritten as

$$\sigma = \eta A_1(u_s) - \eta_2 \lambda_1 \left(\overset{\Delta}{A}_1 (u_s) + \zeta A_1(u_s)^2 \right)$$

which we recognize to be similar to the Second order fluid model, in the sense that it contains the same terms. □

Since we have shown this equivalence for the general Johnson-Segalman model, it follows that this equivalence is valid for the Oldroyd A and B models and for the Jeffreys models as well. In the creeping flow regime, therefore, the Maxwell models, as well as most other models it can be shown behave like the Second order fluid, and exhibit constant viscosity and normal stresses. Since our research work is performed in the creeping flow regime and for

small viscoelastic parameters, on account of Theorem 4.8.1, it is sufficient that we consider the Second order fluid model.

4.9 The Modified Second Order Fluid

We note that the viscoelastic models considered so far do not contain any shear-thinning or thickening properties. For reasons that will be apparent in later chapters, we wish to consider a model which contains inertial effects, normal stresses and shear-thinning properties. For sake of convenience, we consider a modification of the second order fluid model, where we force one of the material parameters, α_2 to be a function of the shear-rate.

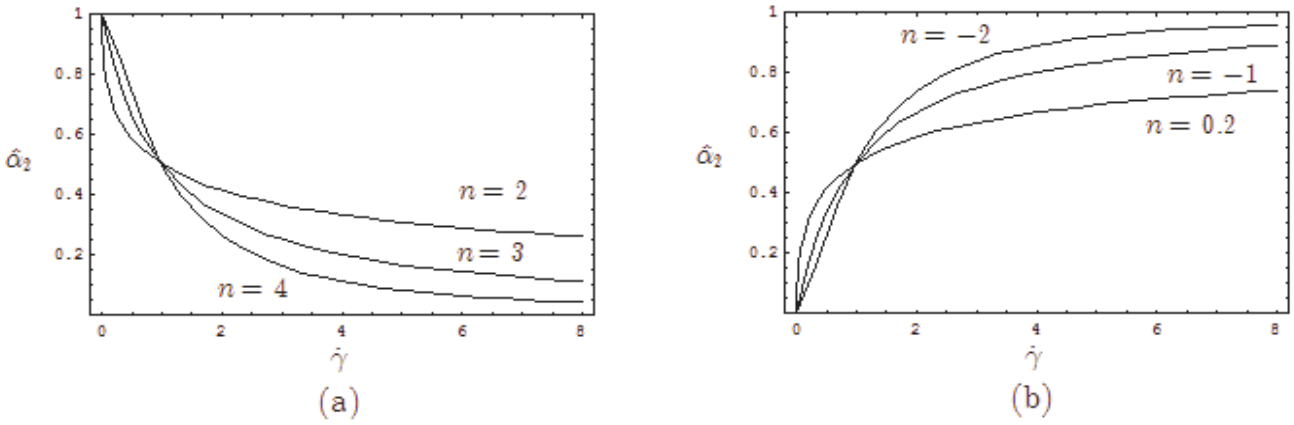

Figure 4.2. Some examples of the parameter, $\hat{\alpha}_2$ as a function of shear rate for (a)shear thickening liquids and (b) shear thinning liquids .

A realistic model such as the Johnson-Segalman model might be perhaps more appropriate in the future. As will be seen later, this is done primarily for sake of convenience in calculations. The chosen model is not realistic, however since it possesses all the relevant features that we need to make our case, it suffices for our purposes. The modified Second

order model is define by the stress tensor

$$\begin{aligned} T &= -pI + \mu A_1(u) + \alpha_1 A_2(u) + \hat{\alpha}_2(|A_1(u)|)A_1(u)^2 \\ \hat{\alpha}_2 &= \frac{1}{\frac{1}{\alpha_2} + k[A_1(u) : A_1(u)]^{\frac{n-1}{2}}} \end{aligned} \tag{4.22}$$

where the constant k is similar to the consistency index that was introduced in the Power-Law model. It is easy to see that as $k \to 0$, the Modified Second order fluid model reduces to the standard Second order fluid. It can be verified, that under shear stress, the material functions for this model can be given by

$$\begin{aligned} \eta &= \mu \\ \Psi_1 &= (2\alpha_1 + \hat{\alpha_2}) = 2\alpha_1 + \frac{\alpha_2}{1 + (\sqrt{2})^{n-1} k\dot{\gamma}^{n-1}} \\ \Psi_2 &= \hat{\alpha_2} = \frac{\alpha_2}{1 + (\sqrt{2})^{n-1} k\dot{\gamma}^{n-1}}. \end{aligned}$$

Therefore, the normal stress coefficients are certainly dependent upon the shear rate and hence the model is shear-thinning.

5.0 REVIEW OF RHEOLOGY

5.1 Basics

Rheology pertains to the study of the deformation and flow of matter. In particular, the subject of rheology is used in the study and characterization of Non-Newtonian liquids. Properties such as viscosity, viscoelasticity, shear-thinning and thickening can be understood and quantified using the techniques of rheology. In our study, as is discussed in later chapters of this thesis, we perform several sedimentation experiments upon polymeric liquids. The knowledge of specific molecular and rheological properties of these liquids is essential to the correct interpretation of our experimental observations. Therefore, in this chapter, we shall outline a few essential rheological tests that we perform upon our test liquids. These include, (a) Steady Shear Test, (b) Creep and Recovery Test and (b) Small Amplitude Oscillatory Test (see[56,57,72]).

Since Non-Newtonian liquids typically tend to show variation in their properties with changing shear-rates, it is essential that we make measurements upon them at varying shear-rates in order to completely understand their behavior. Perhaps the most convenient way of making these measurements is with the *Cone and Plate Rheometer*(see figure below). The instrument consists of a plane plate and a cone of radius r. The cone makes an angle, θ with the plate and rotates at angular velocity ω about the tip of the cone which just barely touches the plate. The gap between the cone and the plate is where the test liquid is placed.

The Cone and Plate Rheometer operates under the assumptions that, (a) the Reynolds number for the sample is low, (b) the wall temperature and the thermal conductivity are maintained constant, (c) the pressure is the same everywhere within the liquid, (d) centrifugal forces and gravitation forces can be ignored, (e) the effects at the free surface of the sample liquid can be ignored and (f) for small enough cone angle, θ, the shear-rate can be

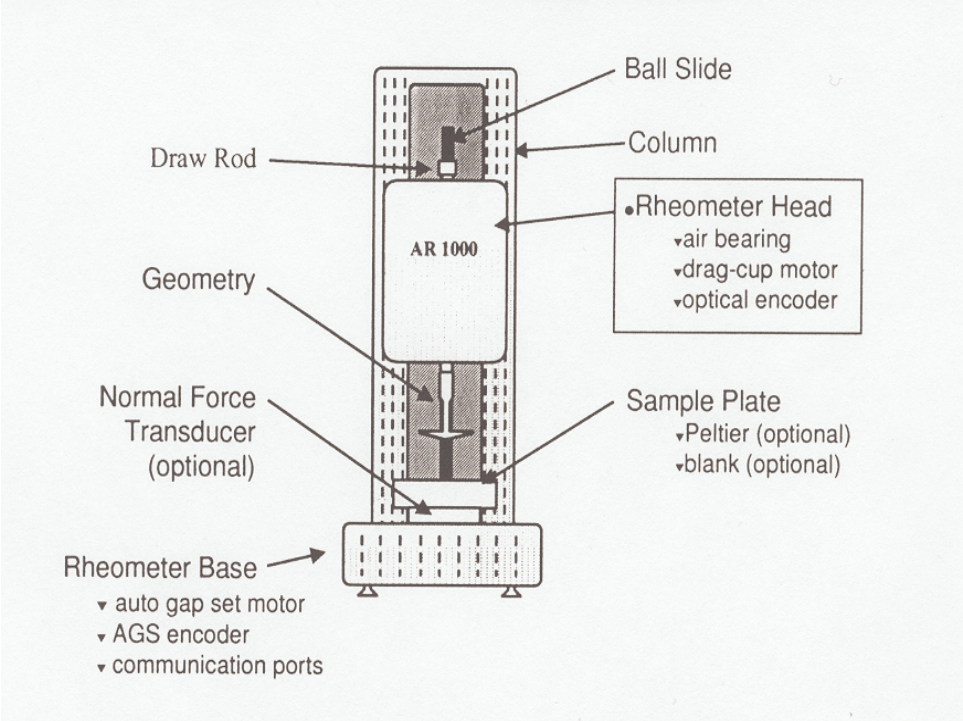

Figure 5.1. A schematic of the AR1000 rheometer manufactured by TA Instruments.

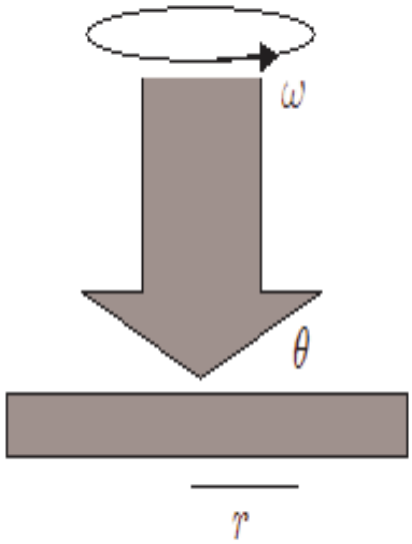

Figure 5.2. A sketch of the cone and plate rheometer.

considered to be independent of the radial direction. We will now briefly outline the three main rheological experiments that have been performed in the course of our experimental studies.

5.2 Steady Shear

In this experiment, the shear rate $\dot{\gamma}$, is held constant, so that the flow is steady. This is achieved in a cone and plate rheometer by rotating the cone at a constant angular velocity. Also, in this experiment, the stress tensor $\tau = \tau(\dot{\gamma})$ is a constant. Three stress quantities, τ_{11}, $\tau_{11} - \tau_{22}$ and $\tau_{22} - \tau_{33}$ are measured. Using these we evaluate the following material functions,

- The viscosity, $\eta = \frac{\tau_{21}}{\dot{\gamma}}$
- The first normal stress coefficient, $\Psi_1 = \frac{(\tau_{11}-\tau_{22})}{\dot{\gamma}^2}$
- The second normal stress coefficient, $\Psi_2 = \frac{(\tau_{22}-\tau_{33})}{\dot{\gamma}^2}$

5.3 Creep and Recovery

The shear creep experiment is intended to produce a shear flow at a constant stress τ_0. In a cone and plate rheometer, this is achieved by driving the cone with a constant torque. Such an experiment is referred to as a *Creep* experiment. As opposed to the previous experiment, where the shear rate was specified, in this case, the shear-rate is held constant. The stress is instantaneously increased from zero to a constant value, i.e.,

$$\tau_{12} = \begin{cases} 0 & , t = 0 \\ \tau_0 & , t > 0. \end{cases} \tag{5.1}$$

During the period over which the stress is applied, the nature of deformation of the sample is observed in terms of the compliance function, $J(t)$. Polymeric liquids typically tend to

deform with the shear stress until a steady state of strain is reached. We shall refer to this steady strain rate as $\dot{\gamma}_\infty$. If we denote the steady state creep compliance by J_s^0, then we can write the compliance function in the form

$$J(t) = J_s^0 + \frac{t}{\eta_0}$$

where η_0 is the zero shear rate viscosity. The creep experiment is performed in conjunction with a *Recovery* test, where the constant stress τ_0 is removed after a sufficiently long time, t_r, usually after the steady state has been reached. At this time, the deformation process reverses as

$$\tau_{12} = \begin{cases} \tau_0 & , 0 < t < t_0 \\ 0 & , t \geq t_0. \end{cases} \tag{5.2}$$

In the recovery process, the recovery compliance function $J_r(t)$ is measured,

$$J_r(t) = \frac{\gamma_r(t)}{\tau_0}$$

where $\gamma_r(t)$ is the recoverable shear-strain. Additionally, we define the recoil function, $R(t, \tau_0)$ as

$$R(t, \tau_0) = J_r(t, \tau_0).$$

The eventual recoil function R_∞ is defined as

$$R_\infty = \lim_{t \to \infty} R(t, \tau_0).$$

The compliance function and recoil function related to each other by the relation

$$J(t) = R(t, \tau_0) + \frac{t}{\eta_0}. \tag{5.3}$$

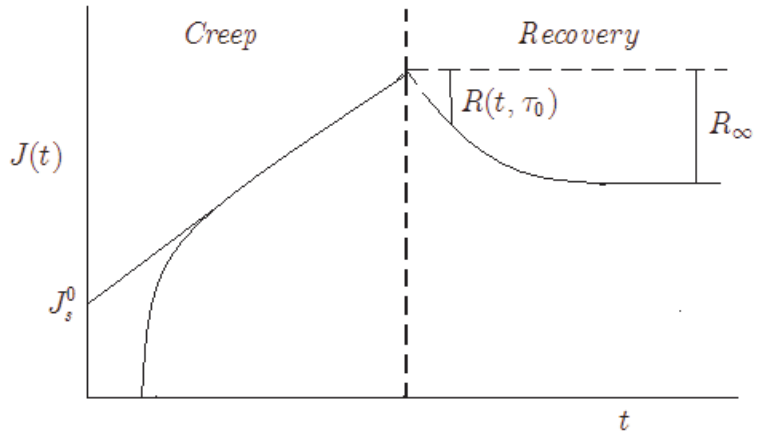

Figure 5.3. A sample sketch of a typical compliance versus time curve during Creep and Recovery tests.

The functions $J(t)$ and $R(t, \tau_0)$ are measured from the creep and recovery experiments respectively. Then using equation (5.3), we may evaluate the viscosity, η_0.

5.4 Small Amplitude Oscillatory Shear

In this experiment the sample is exposed a sinusoidal deformation (or strain) . As a result, the stress also changes sinusoidally, but with a time lag, ϕ. Therefore, we write

$$\gamma = \gamma_0 \sin(\omega t)$$

and

$$\tau = \tau_0 \sin(\omega t + \phi). \tag{5.4}$$

We decompose the stress into parts, one that is in phase with the strain and the other which is out of phase with the strain. Hence we may write,

$$\tau = \tau_0' \sin(\omega t) + \tau_0'' \cos(\omega t). \tag{5.5}$$

Hence, combining the equations (5.4) and (5.5), we have

$$\tan\phi = \frac{\tau_0^{''}}{\tau^{'}_0.}$$

We can also calculate the elastic moduli, the in-phase moduli,

$$G^{'} = \frac{\tau_0^{'}}{\gamma_0}$$

and the out-of-phase moduli,

$$G^{''} = \frac{\tau_0^{''}}{\gamma_0}.$$

From the earlier relations it is easy to see that

$$\tan\phi = \frac{G^{''}}{G^{'}}$$

and also

$$\tau = G^{'}\gamma_0 \sin(\omega t) + G^{''}\gamma_0 \cos(\omega t).$$

When measuring the properties of polymeric liquids, we may also introduce the dynamic viscosity material functions which are defined as

$$\eta^{'} = \frac{G^{''}}{\omega},\ \eta^{''} = \frac{G^{'}}{\omega}.$$

In studying a certain liquid sample, we typically plot the functions $G^{'}$, $G^{''}$, $\eta^{'}$ and $\eta^{''}$ versus ω. In case of a Newtonian liquid, the stress curve is seen to be in phase with the strain curve (i.e. $\phi = 0$). Also, $G^{'} = 0$ and $\eta^{'} = \eta$, the viscosity of the liquid. In case of a non-Newtonian liquid however, the phase lag, ϕ is non-zero and so are the two elastic moduli $G^{'}$ and $G^{''}$. One can use these clues and standard curves to determine the exact nature of the test liquid.

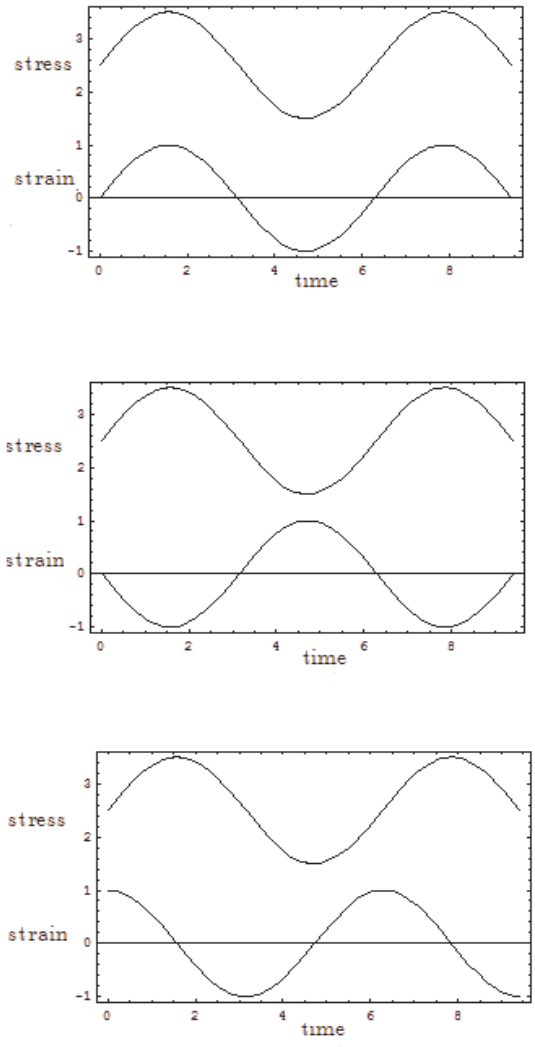

Figure 5.4. A certain deformation(stress) is applied to the sample and the responding strain is observed. The phase difference, δ, of (a) 0 degrees is a purely elastic response, (b) 90 degrees is a purely viscous response and (c) $0 < \delta < 90$ degrees corresponds to a viscoelastic response.

6.0 EXPERIMENTAL WORK

We discuss two kinds of experiments that we have performed. The first involves the sedimentation of particles in a vertical tank. Here, we try to reproduce the results of our predecessors. Additionally, we also wish to advance our understanding of this phenomenon by considering the sedimentation experiments in a variety of liquids, Newtonian and viscoelastic and with particles of different shapes. Our sedimentation experiments have also been carried out at higher Reynolds numbers where we make several interesting observations. In addition to observing the horizontal and vertical orientations and the tilt angle, we also notice oscillatory and turbulent behavior of particles at very high Re. The second experiment involves observations of particle behavior in the presence of a flow. Here, the particle is held fixed in the center of a flow chamber while we recycle water through the chamber. Here again, we make observations on the orientation behavior of the suspended particle at varying values of the Reynolds number. In this experiment, we observe the across-stream orientation at low Re and oscillatory motion at higher values of Re. In the following sections, we give a detailed account of the experiments performed with the results systematically tabulated. A comparison of these results with our theoretical analysis will be performed in the following chapter.

6.1 Sedimentation Experiments

6.1.1 Experimental Setup

The setup consists of a sedimentation tank of width 6 inches, breadth 6 inches and height 3 feet (see Figure 6.1) allowing for a volume of approximately 4.0 gallons. The tank is made of plexiglass which was cut and put together at the School of Engineering Machine shop.

The dimensions of the tank are chosen to be similar to previous experiments. The experiments are recorded using a digital camera (Cannon XL1) which is placed on a traversing system. The camera can be moved up or down on this system using a motor which is set at the top of the system, as shown in the Figure. The camera is in turn connected to a

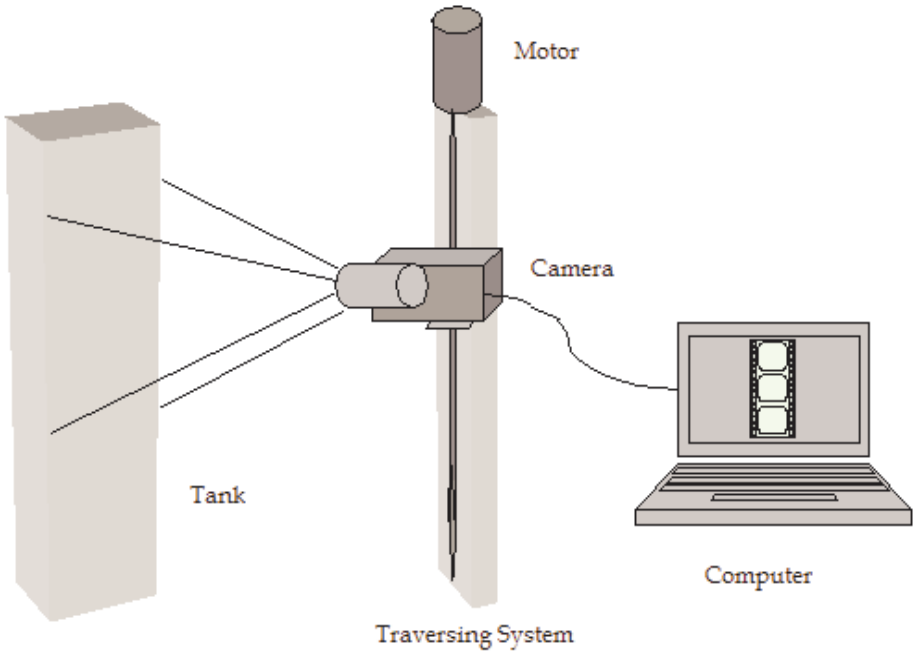

Figure 6.1. Setup of sedimentation experiment.

computer. A live feed of the experiment is captured on the computer which allows us to record the experiment and make accurate measurements of the speed of fall and terminal orientation of the sedimenting body.

6.1.2 Test Particles

The sedimentation experiment involved filling the tank with a liquid and dropping a rigid body in it. The liquid filled almost the entire tank the particle was dropped from rest.

The shape of the sedimenting body was either a prolate spheroid, a flat ended cylinder or a round ended cylinder (see Figure 6.2). The dimension and material of the particles were varied in order to change the rate of fall of the body in the liquids. The Table 6.1 lists the dimensions and materials of the particles. In case of ellipsoidal bodies, the Table also displays the eccentricity of the body which is given by the relation $e = \sqrt{1 - \frac{b^2}{a^2}}$, where b and a refer to the minor and major axis of the ellipsoid respectively. For future comparison,

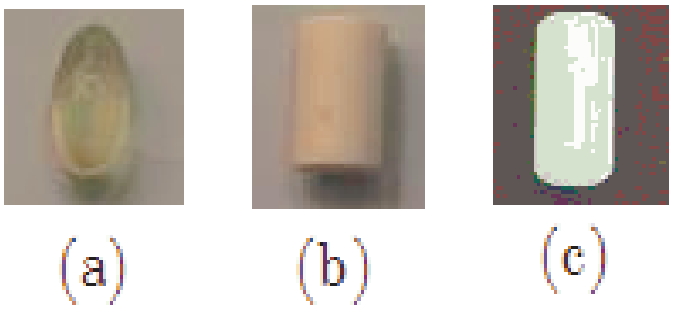

Figure 6.2. Particles of (a) prolate ellipsoidal, (b) flat ended cylindrical and (c) round ended cylindrical shapes used in the sedimentation experiments.

we also calculate an effective eccentricity for the cylindrical particles where, a refers to the length of the cylinder and b refers to the diameter of the cylinder.

Table 6.1. Particles used in sedimentation experiments.

Number	Shape	Name	Material	Major axis (in)	Minor axis (in)	e	Density g/cm^3	Hydraulic† Diam.(in)
1		E1	Si40	0.5	0.25	0.87	1.1	0.63
2		E2	Si40	1.0	0.5	0.87	1.1	0.91
3	Prolate	E3	Aluminum	1.0	0.5	0.87	2.70	0.91
4	Spheroid	E4	Steel	1.0	0.5	0.87	7.83	0.91
5		E5	Wax	1.0	0.5	0.87	0.93	0.91
6		E7	Plexiglass	1.0	0.5	0.87	1.29	0.91
7		CF1	Aluminum	0.5	0.06	-	2.70	0.16
8		CF2	Delrin	0.5	0.25	-	1.54	0.50
9	Flat	CF3	Delrin	0.75	0.375	-	1.54	0.75
10	Ended	CF4	PET	0.75	0.375	-	1.37	0.75
11	Cylinder	CF5	Delrin	1.0	0.5	-	1.54	1.0
12		CF6	PET	1.0	0.5	-	1.37	1.0
13	Round	CR1	Steel	0.9	0.4	-	7.83	0.83
14	Ended	CR2	Teflon	1.0	0.2	-	2.18	0.50
	Cylinder							

†-We compute hydraulic diameter using the formula $D_h = \frac{6 \times \text{Volume}}{\text{Wetted Area}}$ (36)

6.1.3 Test Liquids

Several different kinds of test liquids were used for the sedimentation experiments, Newtonian and Viscoelastic fluids. Table 6.1.3 summarizes the properties of these sample liquids. Also see Table 6.3 for a characterization of the rheological properties of these liquids. The primary objective of these experiments is to test the effect of inertia, viscoelasticity and shear-thinning on the orientation phenomenon. For this purpose, we choose liquids that possesses each of these properties. Whereas Newtonian liquids show only inertial effects, viscoelastic liquids exhibit inertial, elastic and shear-thinning effects.

The Newtonian liquids used were water and a 70% Glycerine solution in water. A third commercial liquid soap (Softsoap) was also employed. However, this is not included in the thesis since its properties were not ascertained. The three different Newtonian liquids were used in order to expose our experiment to different viscosities.

Two kinds on viscoelastic liquids of different concentrations (by volume) were used in our study. The first of these bears the chemical name Carboxymethylcellulose(Hercules Inc.) while the second polymer was Polyacrylamide(SNF Inc). Three different concentrations (0.5%,0.75% and 1%) of Carboxymethylcellulose(CMC) were prepared while in the case of Polyacrylamide(PAA), we made 1.0% solution of the PAAFS920SH sample and 0.56% of the sample PAAAN934SH in distilled water. Refer to Table 6.2 for detailed properties of the liquids used.

The dispersion technique for this polymer involves adding the polymer to a third of the total volume of water which is heated to about 90 degrees centigrade in a mixing vessel by means of a heating coil which is immersed in the vessel(see Figure 6.3). The mixture is agitated at about 500 rpm, initially. The heating is stopped once the polymer is completely added to water. The agitation speed in the meanwhile is reduced to about 50rpm. The

remaining amount of water is then added at a cold temperature. The agitation is continued for several hours until the polymer is completely dispersed. The sample is then allowed to sit for a few hours to let the sediments settle. At this stage the polymer is ready for experimentation. The polymer was finally transferred from the vessel to the sedimentation tank. The polymer is again allowed to sit in the sedimentation tank for about a couple of hours to allow the trapped bubbles to clear out.

Table 6.2. Liquids used in sedimentation experiments.

Number	Type	Liquid	Density (gm/mL)	Mol. Weight (gms/mole)	Viscosity† (Pa.s)
1	Newtonian	Water	1.0	-	0.001
2		Water-Glycerine(30%:70%)	1.13	-	0.5
3		CMC(0.5%)	1.01	700,000	
4	Shear-thinning	CMC(0.75%)	1.06	700,000	
5	Viscoelastic	CMC(1.0%)	1.1	700,000	
6		PAA-FS920SH (1.0%)	1.1	$(7\text{-}9)\times10^6$	
7		PAA-AN934SH (0.56%)	1.1	$(14\text{-}17)\times10^6$	

† - Viscosities of the viscoelastic liquids are provided in Table 6.3

Figure 6.3. A snapshot of the mixer and mixing vessel used to prepare the polymer.

6.1.4 Rheology of Test Liquids

Our rheological studies included the creep and recovery test, steady flow and oscillatory shear experiments. The results of these tests are discussed below and summarized in the Table 6.3. The essential objective of this test was to verify the nature of the liquids used and additionally to extract certain essential viscoelastic parameters such as the viscosity and relaxation times.

The tests were performed on the TA Instruments AR1000 Rheometer using a cone and plate geometry. The diameter and the angle of the steel cone used was 40mm and 2 degrees respectively. The flow experiment was conducted between 0.5968-59.68 Pa. The results of the steady flow experiment indicates that viscosity for all of these liquids is certainly a function of the applied shear. However the effect is particularly strong in the CMC(1%), PAA(1%) and the highest in the PAA(0.56%) solution. The flow curves are shown in the Figures 6.4 and 6.5. Following the work of Liu and Joseph[54] and Chiba et.al.,[14] we fit the viscosity curves with the Cross model

$$\eta = \eta_\infty + \frac{(\eta_0 - \eta_\infty)}{(1 + k|\dot{\gamma}|^n)}$$

where η_0 is the limiting viscosity at zero shear rate, η_∞ is the limiting viscosity at infinite shear rate and k is the consistency index. The results of the curve fitting are provided in the Table 6.3 at the end of the subsection.

The second analysis upon our liquids was the oscillatory shear test where the samples were put to a stress of 0.5968Pa. The oscillation of the cone was varied between 6.283-62.83 radians per second. Results of the experiment are shown in Figure 6.6 and 6.7. The two Figures compare the values of the storage and loss moduli, G' and G'' respectively, both of which are a function of the angular velocity. It is well known[56,72] that when G" dominates

G', then the sample displays liquid-like characteristics while if G dominates G'', then the liquid possesses elastic features. When the two quantities are of equal magnitude, then both viscous and elastic features exist in equal strength. Therefore, upon comparing the two quantities in our measurements, we see that in the case of CMC(0.5 %), the sample displays liquid like behavior over the entire frequency range. Hence, we may expect this sample to behave predominantly like a Newtonian liquid with little elasticity. In the next sample, CMC(0.75%), the material is liquid like at low frequencies and more solid like at higher frequencies, therefore, we may expect some viscoelastic behavior. The remaining samples show a significantly dominating G' over G'' and we may expect these samples, in particular, PAA(0.56%), to have noticeable viscoelastic properties. The oscillatory experiment allows us to compute the significant parameter, $_r$, the relaxation time. It can be seen from most elementary text books in Polymers and Rheology that the relaxation time obeys the empirical relationship

$$\lambda_r = \frac{G'}{\omega G''}.$$

We use this formula to evaluate λ_r for the different samples and these values are listed in Table 6.3. The results of this section will be crucial in obtaining the Re and We in the forthcoming sections. Following,[14,38,54] we define these two parameters as

$$Re = \frac{\rho U d}{\eta_0},\ We = \frac{\lambda_r U}{d}$$

where ρ is the density of the liquid, U the speed of fall of the body and d is the characteristic length of the sedimenting body, often given as the hydraulic diameter.

It must also be pointed out that there are some likely errors in our rheological measurements. The samples were tested for the material parameters several times over a period of a couple of weeks. Additionally preparation procedure errors, sediments in containers and evaporation of liquid samples may also contribute though perhaps minutely to our measured

Table 6.3. Rheological measurements of the liquid samples .

Liquid	η_0 $(Pa.s)$	η_∞ $(Pa.s)$	k	n	λ_r (sec)
CMC(0.5%)	0.693	0	0.21	0.563	0.044
CMC(0.75%)	0.814	0	0.1338	0.6096	0.041
CMC(1.0%)	18.68	0.286	0.9224	0.6318	0.105
PAA(0.56%)	90.067	1.88	50.17	1.5545	0.285
PAA(1.0%)	0.773	0.0114	0.4665	0.743	0.134

quantities. The relaxation time measured for CMC(0.5%) seems to be very slightly larger in magnitude to the relaxation time of CMC(0.75%). We attribute this to possible film formation upon evaporation of this dilute sample in the rheometer.

The results of the creep and recovery tests were performed at three different shear stress values, 0.1Pa, 0.5 Pa and 1.0 Pa and were in qualitative agreement with all the other experiments. The creep curves display a slight concavity at short times indicative of some viscoelastic behavior. This curvature is almost negligible in CMC(0.5%) and most pronounced in CMC(1.0%) and in the Polyacrylamide samples. The second test shows a low recovery for CMC(0.5%) sample indicating Newtonian like behavior. For the other samples, there is noticeable recovery, especially in the case of CMC(1.0%) and for both the PAA samples. We will refrain from going into the details of this experiment since we draw no specific parameters from this test.

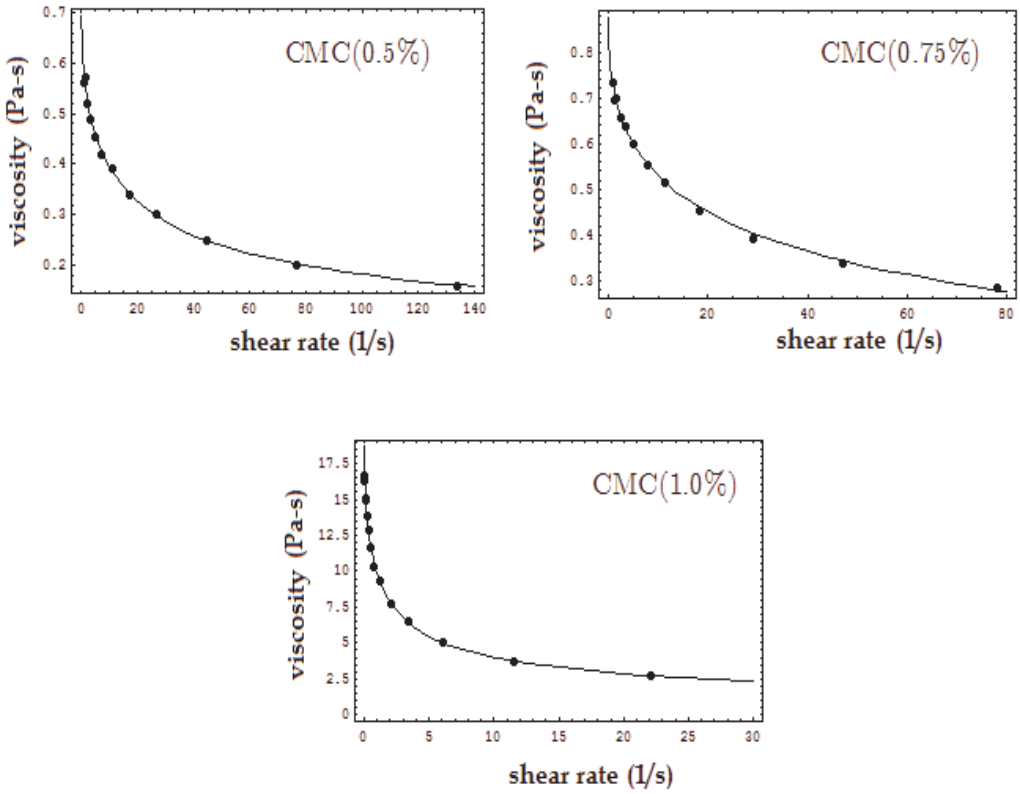

Figure 6.4. Viscosity versus shear rate for CMC.

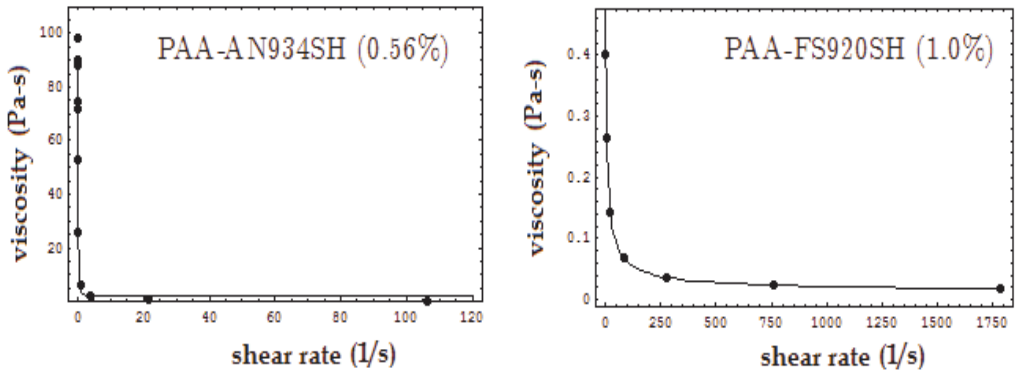

Figure 6.5. Viscosity versus shear rate for PAA.

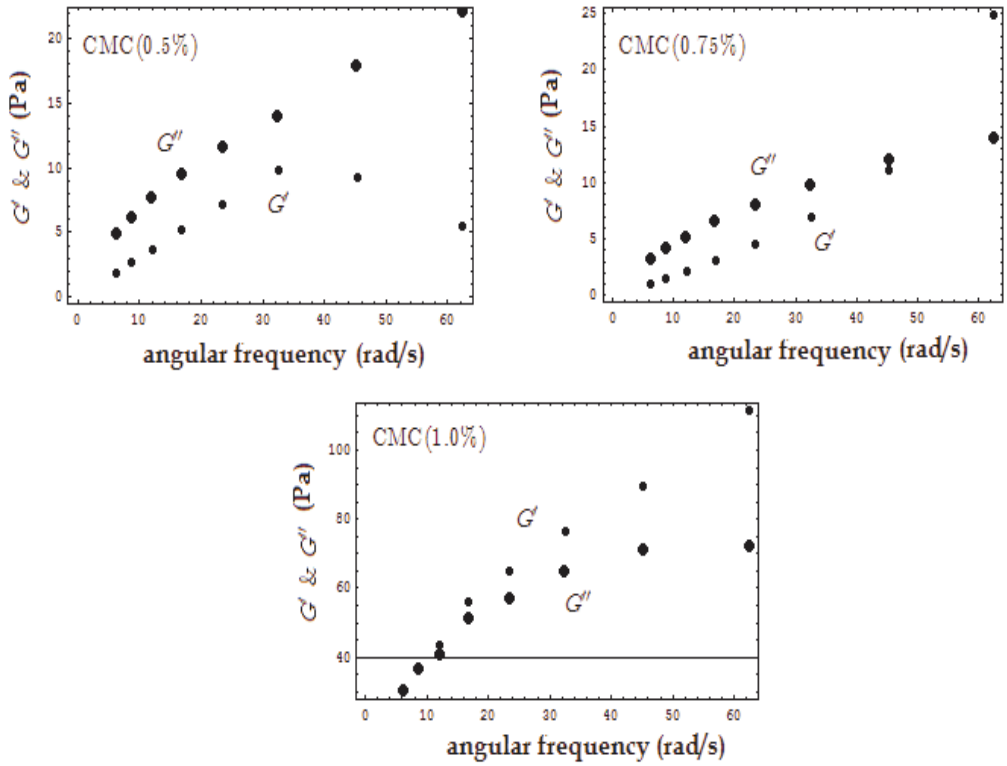

Figure 6.6. Viscosity versus shear rate for CMC.

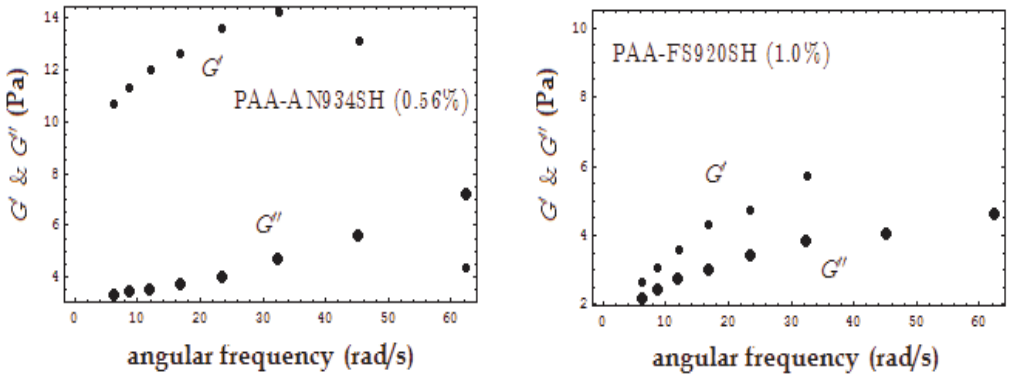

Figure 6.7. Viscosity versus shear rate for PAA.

6.1.5 Observations and Discussion

In this section we discuss the results of our sedimentation experiments. The data obtain from each run is tabulated with detailed measurements. We are able to reproduce the orientation phenomenon which has been observed in previous experiments. The observations can be summarized as follows:

- In the soap solution, we observe that the particle maintains its initial orientation for all future times. Therefore we believe this experiment to be in the Stokes regime[1]
- In the Newtonian solution, the particles were seen to adopt a terminal orientation with their broadside eventually aligning perpendicular to gravity. At higher values of Re, we observed oscillatory behavior and even turbulent motion.
- In the strongly viscoelastic solutions, the particles aligned with their broadside parallel to the direction of gravity. For certain light cylindrical particles the tilt-angle was also observed.

In the Tables below we record the fall times, the Reynolds number, Weissenberg number, initial and final orientation of different particles in the different test liquids. The fall time recorded is the average of three trials in each case. The orientation of the body is the angle between the longer axis and the horizontal.

From Table 6.4, we infer the following. The particles used in this experiment give rise to a very high Reynolds numbers, due to the low viscosity, high fall speeds and high densities of the particles. Therefore the stable horizontal orientation of the particle is not observed. Instead, due to the high Re, the particle is seen to oscillate about the horizontal position. In the case of the particles E3 and E4, the particle speeds were too high to be measured. For the particles E7, CF1 and CR2, which exhibit Re of 2288.2, 402.3 and 2041.9 respectively,

[1] As mentioned earlier, details of this experiment are not given since the properties of the liquid are not known.

the particles begin to exhibit unsteady oscillations. In our final observation where Re is very high, 9890, the particle falls in a chaotic manner.

In the second experiment in glycerine-water solution, we are able to see the horizontal terminal orientation with particles E7 and CF1 (see Table 6.5). The Reynolds numbers for these two particles lies well below 500. The rest of the particles begin to oscillate in an unsteady manner in their terminal states.

In the third experiment (see Table 6.6), we employ a 0.5% solution of the Carboxymethylcellulose solution. At these low concentrations, the liquid seems to behave more like a Newtonian liquid. The particles, are dropped with a initial orientation of both 0 degrees and 90 degrees and in both cases, we see that all of the particles acquire a terminal orientation of 0 degrees as might be expected in a Newtonian liquid. A likely explanation for this phenomenon is that the elastic effects of this solution being small, the inertial effects dominate making the particles turn their broadside perpendicular to the direction of gravity.

The fourth experiment was performed using a 0.75% solution of the CMC polymer. The results are summarized in Table 6.7. The viscoelastic effects seem to emerge more strongly than in the previous case. Except for the one case of particle E3, all other particles either exhibit a vertical orientation or the tilt angle. The orientation phenomenon as an interplay of inertia, viscoelasticity and shear-thinning effects seems more plausible in this case.

The fifth experiment was performed using a 1.0% solution of the Carboxymethylcellulose solution. The results of this experiment are summarized in Table 6.8. The elastic effects at this concentration are now noticeable since we see most particles taking on a vertical orientation in their terminal states. In fact, we note that two particles, CF2 and CF3 exhibit the tilt angle phenomenon. The increased viscous effect of this sample compared to the previous

one is apparent from the significantly longer fall times that the particles take to cover the length of the tank.

In the case of the particle CF3, we can see the continuous transition of the orientation from 0 degrees to the tilt angle to eventually 90 degrees (see Figure 6.8). This transition is not apparent in other particles due to several reasons. Firstly the density and material of the particle may not be appropriate to exhibit this change within the available concentrations of the test liquids. It would be valuable to repeat our experiments with polymeric, shear-thinning liquids whose concentrations vary over a wider range of values. Several more samples would be required for this purpose. However time constraint prevents us from delving into this project at this point. The Figure 6.8 is similar to that of[13,14] where they have managed to obtain several more data points.

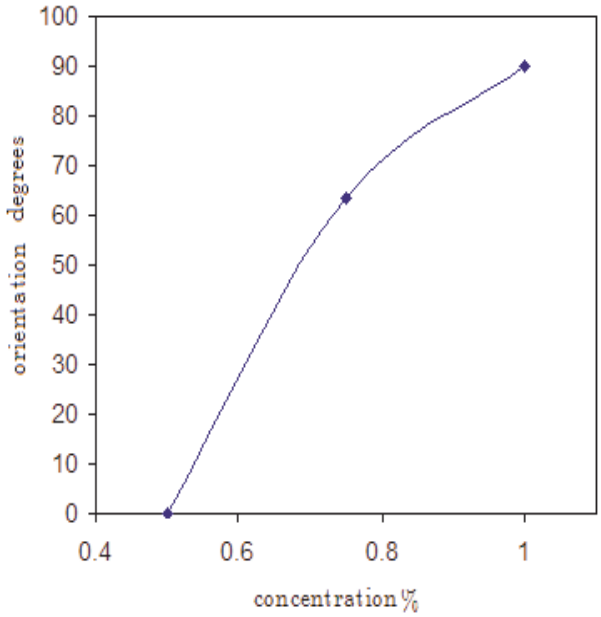

Figure 6.8. Variation of orientation angle with concentration of Carboxymethylcellulose solution.

Note that the tilt-angle is observed only for flat ended cylinders and for not for any other particle shape. The round ended bodies do not display this behavior. Furthermore, the tilt angle is always an edge-edge alignment and hence the angle can be computed directly from the dimensions of the particles. We attribute our lack of tilt angle observations in round-ended bodies to the sparse liquid samples. We would need to prepare several samples of the liquid at varying concentrations, in order to see this phenomenon.

Our final set of experiments were performed with Polyacrylamide samples. The results of our observations are mentioned in Tables 6.9 and 6.10. In the case of PAA(1.0%), some of the heavier particles assumed a final horizontal state, while others took on a vertical orientation in the steady state. In PAA(0.5%), however, all particles assumed the vertical state, due to the predominant viscoelastic character of the fluid. Time of fall in this liquid ranged from a few minutes to several hours, putting the experiment at extremely low Reynolds numbers. Due to the long observation times of sedimenting bodies in the PAA(0.56%) polymer, we have the benefit of tracking the progress of certain particles which move very slowly and observe the orientation angle as a function of time. The Figure 6.9 shows the variation of the tilt angle with time for particles CF3 and CF6.

The typical observation times in these earlier experiments have not been nearly as long as ours. The cylinders begin at rest at a horizontal orientation to gravity. In the initial stage the particles move very slowly retaining their initial angle for several minutes. In the second stage, the particle goes through a change in angle, accompanied by a drift along the tilt, which lasts for several minutes. The particle finally acquires a vertical state which is the steady orientation which it retains for the rest of the fall time. In Figure 6.10, we provide snapshots of the motion of particle CF3 in PAA(0.56%).

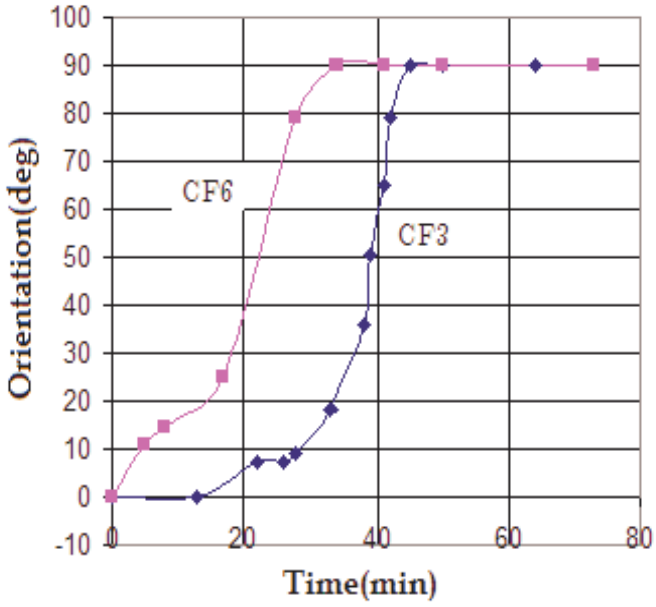

Figure 6.9. Transition of orientation angle with time.

This observation has implications upon the shape-tilting observations in polymeric liquids which was introduced in Section 2.1. It is claimed that shape-tilting is directly proportional to the ratio, a/b, of length to the diameter of the particle and varies continuously with this parameter.[81] We have conducted experiments with the particle CF3 ($a/b = 2.0$) and with two additional flat cylinders with ratios 0.75 and 1.5 in the PAA(0.56%) solution. The sedimentation process for the particle CF3 is explained earlier. For the remaining two particles, the sedimentation process takes approximately 4 hours and 2.5 hours respectively, with no shape-tilting in either case. This observation needs to be confirmed with more elaborate experiments, however our preliminary tests seem to indicate that shape-tilting is merely a transient phenomenon. The earlier sedimentation experiments were performed in Polyox solutions of lower molecular weight and with particles of much higher densities and therefore have very short observation times when compared to our experiments. As we can see from Figure 6.9, it can take several minutes for the particle to turn completely and reach a stable orientation. In fact, some of our observations take up to two hours or more to fall

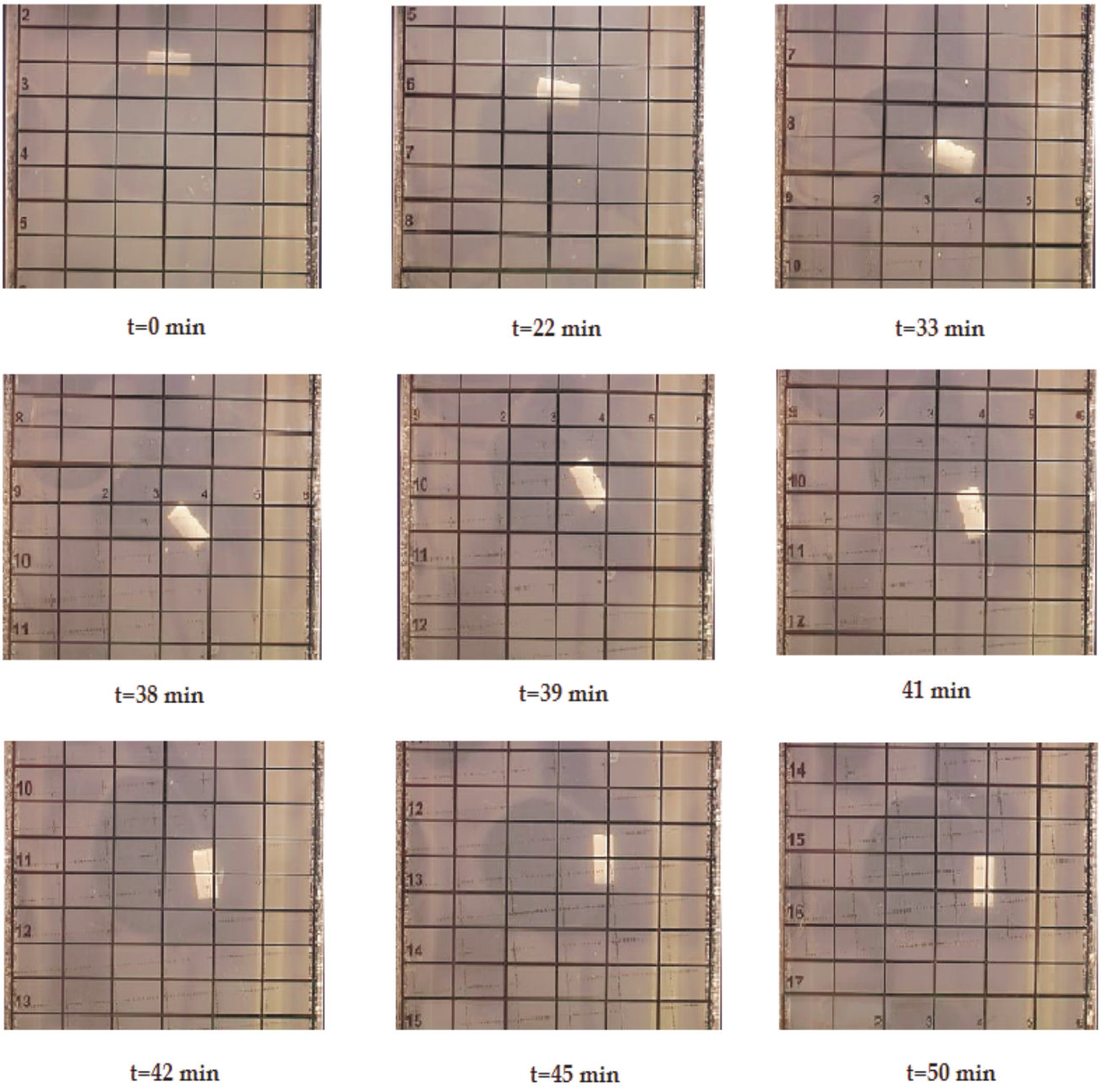

Figure 6.10. Motion of particle CF3 in PAA(0.56%).

through the sedimentation tank. Therefore, in the span of a few minutes which is typical in previous studies, it is plausible, that the cylinders are still in the transient state. We identify three possible ways of getting around this problem. Firstly, we choose to work with a highly viscoelastic liquid, which allows for very slow fall. Secondly, we use particles with much lower densities than in previous studies and finally, we design an alternative setup, a flow experiment whereby it is much easier to extend observations to very long times.

In general, our experimental observations are for the most part compatible with our rheological analysis of the liquid samples. We expect, qualitatively, for the particles to orient horizontally when the Re exceeds the We and to orient vertically when We is the higher number. However, we do observe a few contradictions to this expectation. Observations (2) from Table 6.6, (1) from Table 6.7 and the tilt angle observations from Table 6.7 do not behave as expected. We attribute this mismatch of observation and rheological analysis to measurement errors. As we noted earlier, the relaxation time for CMC(0.75%) is smaller than that for CMC(0.5%). The error is relaxation time calculation can very likely be reason for the discrepancies of Table 6.7. A higher value of λ_r could yield better results. Another possible reason for the errors is likely to be due to our use of the average speed of fall in the Reynolds numbers whereas, the terminal speed would perhaps render more accurate results. However, besides the few bad data that we mention above all other data are in agreement with previous experiments and with the results of Table 6.3. In a forthcoming chapter, we make a comparison of the results here with those of our theoretical analysis.

Table 6.4. Results of sedimentation experiment in water occupying a height of 34 inches in the sedimentation tank. .

Number	Particle	Fall Time(sec)	Speed U(cm/sec)	Re	Initial Orientation(deg)	Final Orientation(deg)
1	E3†	-		-	90	Oscillation
2	E4†		-	-	90	Oscillation
3	E7	5	17.72	2288.2	90	Oscillation
4	CF1	5	17.72	402.3	90	Oscillation
5	CR1	2	43.18	5085.6	90	Turbulent
6	CR2	3	28.78	2041.9	90	Oscillation

† Due to the high density of these particles the fall time through the chamber was not possible to record. The high Reynolds number of fall induces highly unsteady oscillations in these particles

Table 6.5. Results of sedimentation experiment in glycerine-water solution occupying a height of 34 inches in the sedimentation tank..

Number	Particle	Fall Time(sec)	Speed U(cm/sec)	Re	Initial Orientation(deg)	Final Orientation(deg)
1	E7	14	6.17	3.16	90	0
2	CF1	5	17.28	1.56	90	0
3	CR1	1.5	57.6	26.90	90	Oscillation
4	CR2	3	28.8	8.10	90	0

Table 6.6. Results of sedimentation experiment in 0.5% concentration of Carboxymethylcellulose solution occupying a height of 32 inches in the sedimentation tank.

Number	Particle	Fall Time(sec)	Speed U(cm/sec)	Re	We	Initial Orientation(deg)	Final Orientation(deg)
1	E7	10.1	8.04	2.71	0.15	0,90	0
2	CF1	12.69	6.04	0.36	0.65	0,90	0
3	CF2	4.5	18.06	3.34	0.62	0,90	0
4	CF3	6.3	12.90	3.58	0.30	0,90	0
5	CR2	3.87	21.00	3.88	0.73	0,90	0

Table 6.7. Results of sedimentation experiment in 0.75% concentration of Carboxymethylcellulose solution occupying a height of 33.5 inches in the sedimentation tank.

Number	Particle	Fall Time(sec)	Speed U(cm/sec)	Re	We	Initial Orientation(deg)	Final Orientation(deg)
1	E2	19.84	4.28	1.28	0.07	0	90
2	E3	2.75	30.94	9.3	0.53	0	0
3	CF1	13.23	6.43	0.34	0.63	0	90
4	CF2	13.18	6.45	1.06	0.20	0	Tilt
5	CF3	14.81	5.74	1.42	0.12	0	Tilt
6	CF4	19.26	4.41	1.09	0.09	0	Tilt
7	CF6	16.53	5.14	1.70	0.08	0	Tilt

Table 6.8. Results of sedimentation experiment in 1.0% concentration of Carboxymethylcellulose solution occupying a height of 33.5 inches in the sedimentation tank.

Number	Particle	Fall Time(sec)	Speed U(cm/sec)	Re	We	Initial Orientation(deg)	Final Orientation(deg)
1	E1	128.0	0.66	0.006	0.04	0	90
2	E2	32.24	2.63	0.035	0.12	0	90
3	E3	3.69	23.05	0.31	1.06	0	90
4	CF1	55	1.54	0.003	0.39	0	90
5	CF2	20.27	4.19	0.03	0.35	0	Tilt
6	CF3	37.0	2.29	0.025	0.13	0	Tilt
7	CF4	22.0	3.86	0.04	0.19	0	90
8	CR2	9.3	9.14	0.068	0.75	0	90

Table 6.9. Results of sedimentation experiment in 0.56% concentration of Polyacrylamide solution occupying a height of 33.5 inches in the sedimentation tank.

Number	Particle	Fall Time(sec)	Speed U(cm/sec)	Re	We	Initial Orient.(deg)	Final Orient.(deg)
1	E2	12780	0.0066	1.8×10^{-5}	2.1×10^{-3}	0	90
3	E3	9	9.454	0.026	1.16	0	90
4	CR1	14	6.077	0.015	0.82	0	90
5	CR2	115	0.739	0.001	0.17	0	90
6	CF5	4620†	0.016	4.9×10^{-5}	1.78×10^{-3}	0	90
7	CF2	4500	0.0189	2.9×10^{-5}	0.004	0	90

† - The time indicated here pertains to a height of 30 inches

Table 6.10. Results of sedimentation experiment in 1.0% concentration of Polyacrylamide solution occupying a height of 33.5 inches in the sedimentation tank.

Number	Particle	Fall Time(sec)	Speed U(cm/sec)	Re	We	Initial Orientation(deg)	Final Orientation(deg)
1	E1	59	1.44	0.32	0.12	0	90
2	CF5	2	38.1	13.77	2.00	0	0
3	CF6	9	9.45	3.41	0.49	0	0
4	CF1	5	17.02	0.98	5.61	0	90
5	CR2	7	12.15	2.19	1.26	0	90

6.2 Flow Experiments

As can be seen from the previous sections, the fall times for the particles in the sedimentation tank varies typically between a few seconds to a few minutes at the most, except in the case of the PAA(0.56%) sample. In fact, there are only two cases where the time exceeds a minute in our other liquids and this is achieved with the particle E1 whose density is low (see Table 6.1) and dimensions are very small. The difficulty and cost in machining these particles prohibits us from acquiring smaller and lighter particles like E1. Furthermore, even in a sample like PAA(0.56%), the fall time still finite and about a couple of hours at the most. To achieve longer fall would require using particles with much lower densities or liquids with much higher molecular weights which will have to be pursued in the future. Another feasible idea to increase the observation time, which we have done, is to design a flow chamber where the particle is at rest and instead, the liquid moves past the body. The details of the design and setup are explained in the following subsection. In such an experiment, we have managed to extend our observation times to several hours.

The flow chamber experiment is obviously different from the sedimentation experiment in that whereas in the former, we are dealing with the motion of the body in a quiescent liquid, the latter, we have a uniform flow past the body. However, we can expect the results of the two experiments to be similar.

6.2.1 Experimental Setup

The experimental setup consists of a flow chamber with length of 3 feet and a cross-section 5 inches $\times$ 5 inches (see Figures 6.11,6.12). One end of the chamber is attached to a reservoir while the other end is connected to a tube which leads the liquid back to the reservoir tank. Therefore the flow is recycled and we are able to carry out the experiment and extend the observation times to as long as required.

The liquid enters the chamber from the reservoir through a honeycomb which is placed in order to maintain a uniform flow at the entrance. The flow is driven by a pump which is connected to a rheostat by which we may vary the flow rate in the chamber. The liquid used in the flow experiments is water. We have not used any viscoelastic liquid for fear that the pump may shear and hence degrade the polymer.

Perhaps the most challenging aspect of the setup was the particle suspension (see Figure 6.13). The only disadvantage of the flow chamber is that the particle needs to be held in the middle of the chamber at a suitable distance from the entrance and exit by some means. The particles used in this experiment were prolate spheroidal particles made of wax, plexiglass, aluminum and steel. For purpose of suspension, a thin copper wire of thickness 0.006 inches was inserted through tiny holes made in the particles. The ends of the copper wire were then inserted through the walls of the chamber and made taut and sealed on the outer walls of the chamber. The copper wire was chosen due to its thickness, which does not affect the flow past the body and also due to the absence of torsional effects which may contribute to the orientation phenomenon. As is apparent, the particle is restricted to rotate only about the suspending wire.

Two different suspension mechanisms were used as shown in the Figure 6.13. In the first one, the particle is suspended vertically and the particle is held in place by means of a stopper placed below it. In the second mechanism, the particle is suspended horizontally thereby eliminating the use of a stopper. We find that the second mechanism is preferable to the first one since it reduces friction and allows the particle to turn more freely.

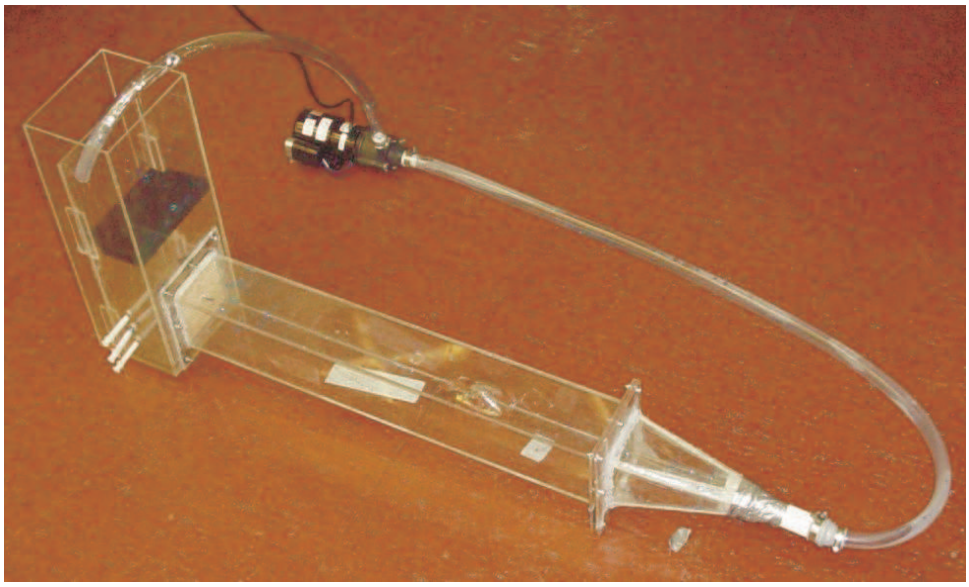

Figure 6.11. A snapshot of the flow chamber.

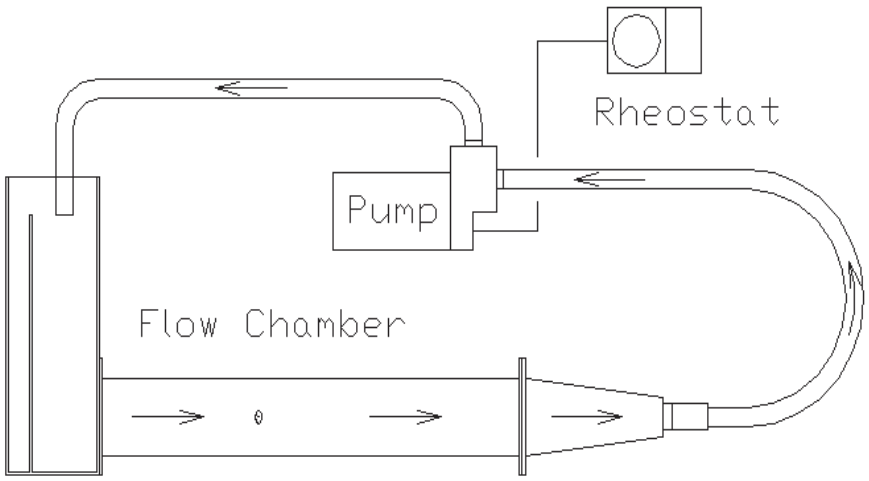

Figure 6.12. The experimental setup.

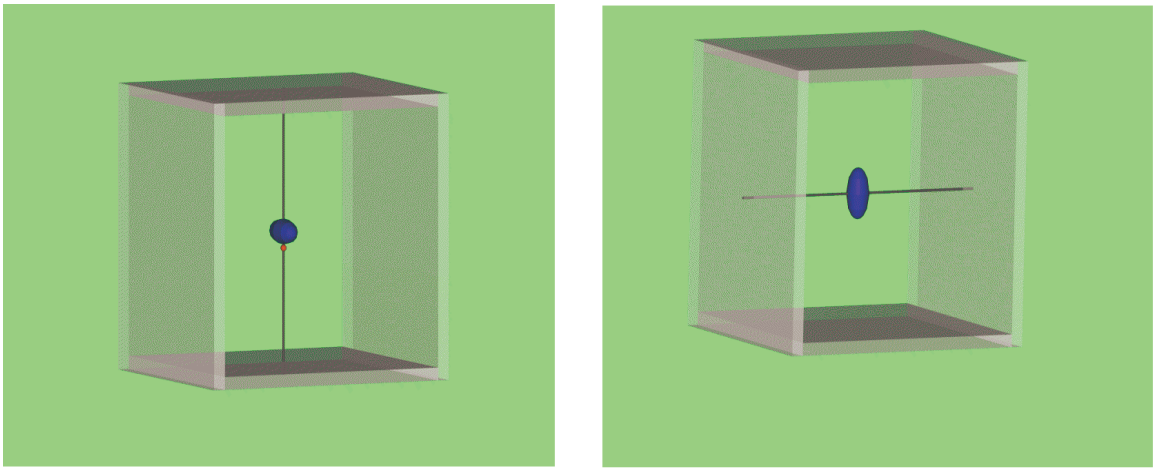

Figure 6.13. A schematic of the suspension mechanism of the particle.

Table 6.11. Particles used in flow chamber experiments.

Number	Shape	Name	Material	Major axis (in)	Minor axis (in)	e	Density
1	Ellipsoid	E1	Wax	1.0	0.5	0.87	0.93
2	Ellipsoid	E2	Plexiglass	1.0	0.5	0.87	1.29
3	Ellipsoid	E3	Aluminum	1.0	0.5	0.87	2.70
4	Ellipsoid	E4	Steel	1.0	0.5	0.87	7.83
5	Cylinder(R)	CR2	Teflon	1.0	0.2	-	2.18
6	Cylinder(R)	CR1	Steel	0.9	0.4	-	7.83

6.2.2 Observations and Discussion

We first identify two essential parameters in this experiment. The first is Re_p, the particle Reynolds number and the second is Re_f, the Reynolds number for the flow chamber. They are determined by the following equations,

$$Re_p = \frac{\rho Q d}{A\mu}, \; Re_f = \frac{\rho Q D}{A\mu}$$

Table 6.12. Critical Reynolds numbers at which particles turn in the flow chamber.

Number	Name	Flow rate(m^3/s)	Re_c
1	E1	2.7×10^{-5}	27.2
2	E2	5.6×10^{-5}	55.8
3	E3	8.4×10^{-5}	83.7
4	E4	1.1×10^{-4}	104.6

where Q is the flow rate, A is the cross-sectional area of the chamber, d measures the diameter of the body, D is the hydraulic diameter of the flow chamber[2], ρ is the density of the liquid and μ is its viscosity.

The particle is initially fixed so it is oriented with its major axis along the direction of flow. The chamber is then slowly filled with water while maintaining the orientation of the particle. Once the chamber is filled with the liquid, the pump is turned on and the liquid is allowed to flow. The experiment is maintained at each fixed flow rate for several minutes to observe any possible change in the orientation of the particle. If none is observed, then the flow rate is incremented by a small amount. This process is continued until, at a particular flow rate the body is seen to change its orientation such that its major axis is perpendicular to the direction of flow. We tabulate below (Table 6.12) the results of this experiment giving the particles and the critical Reynolds numbers of the particles (Re_c) at which they turn to such that their longer axis is perpendicular to the length of the flow chamber.

In Figure 6.14, the data from the above Table 6.12 is plotted. The data points are seen to lie along an 'almost straight' line. Additionally, we can see that the line connecting the data points divides the graph into two regimes. The region below the critical line, we refer to as the *Stokes regime* since for $Re_p < Re_c$ the particle maintains its initial orientation, like

[2]The hydraulic diameter of a flow chamber of width W and Height H is given by $D = \frac{2WH}{W+H}$.

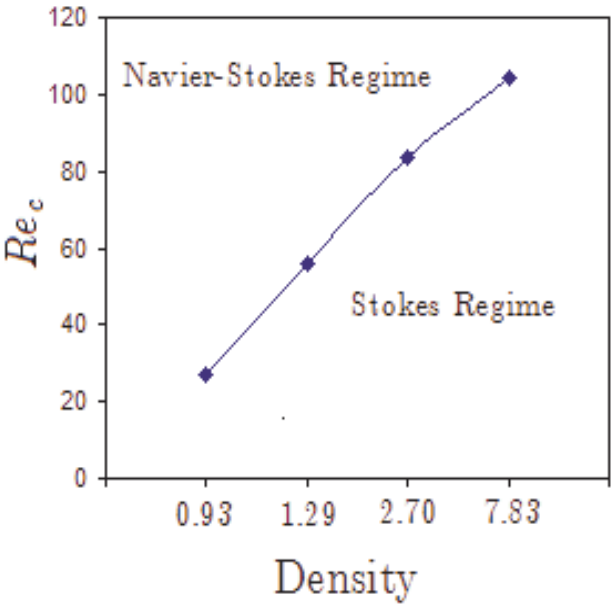

Figure 6.14. Critical Reynolds numbers at which particles turn.

in the sedimentation experiments. As $Re_p > Re_c$, we note that the stable orientation of the particle changes to the one that we see in a Newtonian liquid in sedimentation experiments. For this reason the region above the critical line is referred to as the *Navier-Stokes regime*. It is easily seen from Figure 6.14 that the value of Re_c increases with the density of the particle used. If we extrapolate the curve to $\rho \to 0$, i.e. for a body with zero buoyancy, the particle should turn for very small, non-zero Reynolds numbers. This points to the possibility of increasing frictional resistance to the turning of the particle, with increasing density of the particle.

The second of the flow chamber experiments involved observing the behavior of the particles at higher flow rates, i.e. at higher Reynolds numbers, than in the previous experiment. Though our primary objective is restricted to the interaction of particles and fluids at low Reynolds numbers, we come across some very interesting results, upon increasing the Reynolds numbers to intermediate values. We observe that as the Reynolds number of the

Table 6.13. Observations of periodic oscillations of particles in the flow chamber.

Number	Name	Re	Amplitude(deg)	Period(sec)
1	E1	282.6	5	2
2	E1	470.5	14	1.7
3	E1	754.1	19	1.45
4	E2	282.6	7	3.2
5	E2	470.5	15	1.5
6	E2	754.1	27	1.5
7	E3	754.1	6	1.67
8	CR1	470.5	6.5	0.7
9	CR1	754.1	17.5	0.6
10	CR2	470.5	2	0.7
11	CR2	754.1	5	0.7

particle is increased sufficiently above the Re_c value, the particle begins to exhibit oscillatory behavior and for sufficiently large Re_p, it begins to move in a chaotic manner. In the Table below, Table 6.13, we record the oscillatory behavior of different particles as we vary the Reynolds number over 100. Re_p is slowly increased beyond the point where the particle is oriented with its longer axis perpendicular to the flow. There is a second critical value of Reynolds number, denoted Re_{c-o} where the particle first begins to oscillate periodically about its previously stable position. The oscillatory behavior continues until a third critical value Re_{c-t}, is reached, beyond which the particle begins to oscillate in a turbulent manner. Our experiment is merely a first step in unraveling details of this phenomenon. In this thesis, we restrict ourselves to some preliminary results on these experiments at intermediate Reynolds numbers. More elaborate experiment needs to be designed which can help determine the critical parameters Re_c, Re_{c-o} and Re_{c-t} accurately. We are restricted to certain fixed values of the Reynolds numbers (as in Table 6.13) due to the design of the flow chamber and the pump used in the experiment.

6.3 Wall Effects

It is well known that the presence of walls in sedimentation experiments can result in dramatically different results when compared to those without walls.[7,13,36] We need to be certain that the orientation results that we observe in our experiments are not effected by the presence of walls. The effect of the walls on the terminal orientation of sedimenting bodies is not available in the literature. Most work in this area is restricted to comparing the settling velocities of bodies of different shapes, sizes and composition, in the presence of walls, with those in the absence of walls.[11–13] Financial and time constraints prevent us from conducting our own investigation into this subject. However, as justification for our choice experimental parameters, we compare (see Table 6.14) the typical dimensions of particles and setup in our experiment with those of D.D. Joseph and his co-workers.[38]

Table 6.14. Comparison of experimental parameters.

Group	Particle Shapes†	Minor axis of Particle(in)	Major axis of Particle(in)	Dimension of Tank(in)
Joseph et.al.	Cylinders (F,R,C)	0.02-0.4	0.4-1.0	0.44×6.5×23 0.28×4.0×25
Galdi,Vaidya	Ellipsoids, Cylinders (F,R)	0.06-0.5	0.5-1.0	6.0×6.0×36.0

† F represents a cylinder with flat ends, R with rounded ends and C with conical ends.

Comparing the two columns of the Table 6.14 we see that the dimensions used for the particles are in fact, very similar. On the other hand, those for the sedimentation tank are actually much bigger in comparison. Since Joseph and co-workers claim no effect upon their orientation observations due to the presence of walls, we too make the same assumption. We use this as sufficient tentative justification that wall effects play no role in our experiments until further evidence is available.

It is seen that in case of Newtonian liquids, walls tend to repel sedimenting particles away from them, while in viscoelastic liquids, the particles are attracted to the walls, provided the initial distance of the particles from the wall is less than a critical distance at which point the particles feels the presence of the wall. Besides the lateral drift of particles, walls have the additional better known ability of reducing the settling speeds of sedimenting particles. However, as mentioned earlier, no such study is available on the effect of walls on terminal orientations. In our experiments, we observe lateral drifts of particles towards walls, however, we see no noticeable reason to believe from our observations that the orientation angle is in any way altered near the walls. Horizontal and vertical alignments of particles continue to remain so even as the particle approaches the wall. The only case of tilt angles that are observed are with the flat ended cylindrical particles which tend to align edge to edge (shape tilt) and maintain such an orientation even if near the wall. Since the fall times for these observations are not long enough, we cannot claim with any certainty that the tilt angle will in fact be maintained for all future times. Hence it is not possible to verify based upon current observations what kind of effect the wall has upon our experiments. The effect of walls upon the terminal orientations of bodies needs independent study. We therefore suggest this as part of the future work that must be undertaken in this area.

Though we may temporarily overlook this matter of wall effects on our experimental observations, we need to justify this assumption in our theory. Our mathematical theory, which we conduct in the forthcoming chapters works on the assumption of sedimentation in an unbounded fluid domain in the absence of any walls. This assumption has the advantage of simplifying the mathematical analysis to a certain extent. However, there is also a strong physical justification for this which permits us the use of some simple and elegant theoretical analysis. Studies on the effects of walls[13] indicate that for the aspect ratios (ratio of particle to tank diameter) less than a certain value, the particle does not recognize the wall and the

sedimentation occurs as if in an unbounded domain. Several of the previous experimental studies of[13,14] and even to some extent[54] have been conducted with aspect ratios less than the critical value with expected results. Therefore, our it is sufficient that we pursue our theoretical studies in this framework.

7.0 FORMULATION OF PROBLEM

7.1 Equations in Inertial Frame

In this chapter, we identify the appropriate setting which renders a convenient theoretical analysis. We consider a rigid body, $\mathcal{B}$, of arbitrary shape falling in a fluid $\mathcal{F}$ of density ρ under the action of the acceleration due to gravity, g. In general, the body can be inhomogeneous, that is, of varying density. We assume that the body-fluid system is in a steady state, that is, the translational velocity, ξ and angular velocity, ω of $\mathcal{B}$ are constants in time. We may consider the problem from two possible frames, the inertial frame $\mathcal{I}$ or the body frame $\mathcal{S}$. We will formulate the equations in both of these frames and we shall show that the problem stated in frame $\mathcal{S}$ is more desirable. In the frame $\mathcal{S}$, we place the origin at the centroid or geometric center of the body, which we denote by $\mathcal{O}$. The center of mass of $\mathcal{B}$ is denoted by $\mathcal{M}$. R denotes the vector from $\mathcal{O}$ to $\mathcal{M}$(see Figure 7.1). Note that for a homogeneous body, R vanishes since the center of mass now coincides with the geometric center of the body. The problem of sedimentation of a rigid body in a fluid must be frame mathematically as a coupled fluid-structure problem. Therefore, the problem contains equations for the fluid and equations for the rigid body. We consider the problem in an Inertial frame, $\mathcal{I}$,

$$\left.\begin{aligned} \rho\left(\frac{\partial v}{\partial t}\right) &= \text{div } \left(\hat{T}(v,p) + \rho\hat{f}\right) \\ \text{div } v &= 0 \\ \lim_{|x|\to\infty} v(x,t) &= 0 \\ v(x,t)|_{\Sigma} &= \eta(t) + \Omega(t) \times x \end{aligned}\right\} \tag{7.1}$$

where v is the velocity field, p the pressure field, η the translatory motion of the body and Ω the rotation of the rigid body. Additionally, equations for the body, in frame $\mathcal{I}$. These

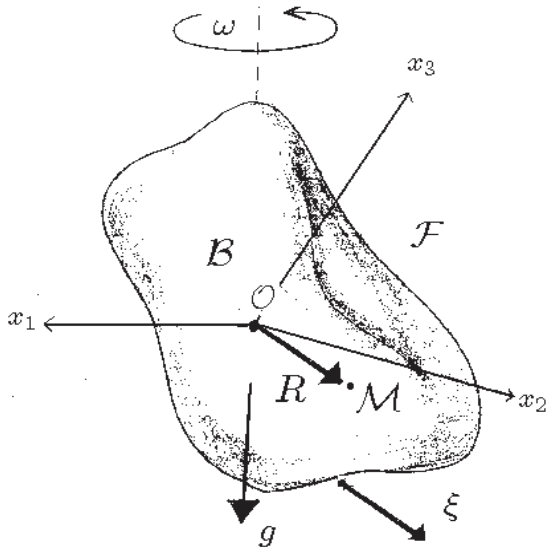

Figure 7.1. Physical setting of a body, $\mathcal{B}$ freefalling in a fluid, $\mathcal{F}$.

are given by

$$m\frac{d\eta}{dt} = -\int_{\hat{\Sigma}} \hat{T}(v,p)\cdot N + F \tag{7.2}$$

$$\frac{d(J\cdot\Omega)}{dt} = -\int_{\hat{\Sigma}} (x-c)\times\hat{T}(v,p)\cdot N + M_c \tag{7.3}$$

where F is the external force, M_c is the external torque, c refers to the position of the center of mass of the rigid body and J is the inertial tensor. The above equations constitute the full set of equations for our problem.

7.2 Equations in a Body-Frame

In this section, we will reformulate the problem in a frame $\mathcal{S}$, which is attached to the body. The specific advantage of this transformation is that in the new frame $\mathcal{S}$, the fluid domain is independent of time, since Ω is unbounded. However, in this frame g becomes an unknown. Since the frames $\mathcal{I}$ and $\mathcal{S}$ vary by an orthogonal transformation, Q, we may

define the following:

$$\begin{aligned} y(t) &= Q^T \cdot (x(t) - c(t)) \\ \xi(t) &= Q^T \cdot \eta(t) \\ \omega(t) &= Q^T \cdot \Omega(t) \\ w(y,t) &= Q^T \cdot v(Q^T \cdot y, t) \\ \pi(y,t) &= p(Q^T \cdot y, t) \\ n &= Q^T \cdot N \\ T(w,\pi) &= Q^T \cdot \hat{T}(Q^T \cdot w, p) \cdot Q \end{aligned}$$

where $y(t)$, $\xi(t)$, (t), $w(y,t)$, $\pi(y,t)$, n and $T(w,\pi)$ are the position vector, translation vector, rotation vector, velocity field, pressure field, outer unit normal to the surface and stress tensor respectively in the frame $\mathcal{S}$.

Remark 7.2.1 *We will need a few useful properties of orthogonal transformations here to rewrite the equations for the problem in frame $\mathcal{S}$.*

1. $\dot{Q}Q^T \cdot a = \Omega \times a$

2. $Q^T\dot{Q} \cdot a = \omega \times a$

3. $(Q \cdot a) \times (Q \cdot b) = Q \cdot (a \times b)$.

We first note that the term

$$\begin{aligned} \frac{Dv}{Dt} &= \frac{D(Q \cdot w)}{Dt} \\ &= \dot{Q} \cdot w + Q \cdot (\frac{\partial w}{\partial t} + \dot{y}\text{grad }_y w) \\ &= Q \cdot (\omega \times w) + Q \cdot \frac{\partial w}{\partial t} + Q \cdot (w - \xi - \omega \times y)\text{grad } w \end{aligned} \tag{7.4}$$

where we use property 2 of Remark 7.2.1. Also,

$$\text{div } {}_x\hat{T}(v,p) = \text{div } {}_yT(w,\pi), \tag{7.5}$$

hence we may write the transformed equation of the fluid in the form

$$\rho(\frac{\partial w}{\partial t} + (w - \xi - \omega \times y) \cdot \text{grad } w + \omega \times w) = \text{div } {}_yT(w,\pi) + \rho Q^T f(x,t). \tag{7.6}$$

Also, we have

$$\left.\begin{array}{rcl} \text{div } w & = & 0 \\ \lim\limits_{|x|\to\infty} w(y,t) & = & 0 \\ w(y,t)|_{\,\Sigma} & = & \xi(t) + \omega(t) \times y. \end{array}\right\} \tag{7.7}$$

Similarly the equations for the body in the frame $\mathcal{S}$ can be given in terms of the new quantities defined above.

$$m\frac{d\eta}{dt} \;=\; m\frac{d(Q\cdot\xi)}{dt} = mQ\cdot(\dot{\xi} + \omega \times y)$$

and

$$\int_{\hat{\Sigma}} \hat{T}(v,p)\cdot N = Q\cdot\int_{\Sigma} T(w,\pi)\cdot n \tag{7.8}$$

Therefore, combining the two above equations, we get

$$m\left(\frac{d\xi}{dt} + \omega\times\xi\right) = \int_{\Sigma} T(w,\pi)\cdot n. \tag{7.9}$$

Similarly,

$$\frac{d(J\cdot\Omega)}{dt} \;=\; Q\cdot(\omega\times I\omega) + Q\cdot I\dot{\omega})$$

and also, we note that

$$\begin{aligned}\int_{\hat{\Sigma}} x \times \hat{T}(v,p)\cdot N &= \int_{\Sigma} Q\cdot y \times (Q\cdot T(w,\pi)\cdot Q^T)\cdot n \\ &= Q\cdot \int_{\Sigma} y\times T(w,\pi)\cdot n.\end{aligned}$$

Therefore, combining the last two equations above we have,

$$\omega \times I\omega + I\dot{\omega} = -\int_{\Sigma} y\times T(w,\pi)\cdot n - \rho Q^T M_c. \tag{7.10}$$

Hence equations (7.9) and (7.10) constitute the two equations for $\mathcal{B}$ in the frame $\mathcal{S}$. We find some important consequences for choosing to work with the frame $\mathcal{S}$ which we provide below in the form of two Lemmas below.

Lemma 7.2.1 *Let $\hat{T}(v,p)$ refer the stress tensor corresponding to a Newtonian liquid. Then*

$$\hat{T}(v,p)|_{w,\pi} = T(w,\pi)$$

is frame $\mathcal{S}$.

Proof:

Let us write $\hat{T}(v,p) = \hat{T}_{NS}(v,p)$. Then

$$\hat{T}_{NS}(v,p) = (-pI + 2\eta D(v)) \tag{7.11}$$

by definition. However, we also have

$$\begin{aligned}Q^T\cdot \hat{T}(v,p)\cdot Q &= T(w,\pi) \\ &= -\pi I + 2\eta D(w) = \hat{T}(v,p)|_{(w,\pi)}.\end{aligned} \tag{7.12}$$

□

Lemma 7.2.2 *Let $\hat{S}(v) \equiv \hat{T}_E$, refer to the extra stress tensor corresponding to a Second order fluid. Then, in the frame, $\mathcal{S}$, attached to the body,*

$$\hat{S}(v) = S(u)$$

where $u = w - (\xi + \omega \times y)$ is the relative velocity.

Proof:

In the inertial frame, the extra stress tensor for the Second order fluid is written as

$$\hat{S}(v) = \alpha_1[\frac{dA_1(v)}{dt} + A_1(v) \cdot L^T(v) + L(v) \cdot A_1(v)] + \alpha_2 A_1(v) \cdot A_1(v).$$

The equivalent quantity in the frame $\mathcal{S}$ attached to the body can be given by the transformation

$$S(w) = Q^T \cdot \hat{S}(Q \cdot w) \cdot Q.$$

Hence, on calculation, we see that $S(w)$ takes the form

$$\begin{aligned} S(w) &= \alpha_1[Q^T \cdot \dot{Q} \cdot A_1(w) - A_1(w) \cdot Q^T \cdot \dot{Q}] \\ &+ \alpha_1[\frac{\partial A_1(w)}{\partial t} + (w - \xi - \omega \times y) \cdot \text{grad } A_1(w) + A_1(w) \cdot L^T(w) + L(w) \cdot A_1(w)] \\ &+ \alpha_2 A_1(w) \cdot A_1(w) \end{aligned}$$

and so it follows that the extra stress tensor in the two frames, $\mathcal{I}$ and $\mathcal{S}$ are not equivalent. For this reason we introduce the relative velocity $u \equiv w - \xi - \omega \times y$. Then, since $A_1(\xi + \omega \times y) = 0$, we see upon some manipulation that

$$S(u) = \alpha_1[\frac{\partial A_1(u)}{\partial t} + u \cdot \text{grad } A_1(u) + A_1(u) \cdot L^T(u) + L(u) \cdot A_1(u)] + \alpha_2 A_1(u) \cdot A_1(u).$$

7.3 Equations for the Freefall Problem

Since in this thesis we are specifically discussing the problem of freefall of a body in a liquid, we must provide the appropriate equations for this problem. A body $\mathcal{B}$ is said to execute freefalling motion in a liquid if the following conditions are met[31]

1. The boundary of $\mathcal{B}$ is impermeable.

2. Gravity is the only external force acting on $\mathcal{B}$.

3. $\mathcal{B}$ is moving in a quiescent liquid.

One important aspect of the freefall equation is that, in the frame $\mathcal{S}$, the direction of gravity $g(t)$ is an unknown in the problem. Therefore, we must provide appropriate equations for g. Let G be the gravity vector in the frame $\mathcal{I}$, then $g = Q^T \cdot G$. Hence,

$$\begin{aligned} \frac{dg}{dt} &= \dot{Q}^T \cdot G \\ &= \dot{Q}^T Q g \\ &= g \times \omega. \end{aligned}$$

Since, the problem considered in this thesis pertains to the terminal or steady state orientation behavior of $\mathcal{B}$ in the liquid, we may rewrite the steady fluid-body equations in the non-dimensional form as

$$\left.\begin{aligned} \mathrm{Re}((w - \xi &- \omega \times y) \cdot \mathrm{grad}\ w + \omega \times w) = \mathrm{div}\ T(w, \pi) + g \\ \mathrm{div}\ w &= 0 \\ \lim_{|x| \to \infty} w(y,t) &= 0 \\ w(y,t)|_{\Sigma} &= \xi + \omega \times y. \end{aligned}\right\} \tag{7.13}$$

and

$$\left.\begin{array}{rcl} \mathrm{Re} m\omega \times \xi & + & \displaystyle\int_\Sigma T(w,\pi)\cdot n = mg \\ \mathrm{Re}\omega \times I\omega & + & \displaystyle\int_\Sigma y \times T(w,\pi)\cdot n = 0 \\ \omega \times g & = & 0. \end{array}\right\} \tag{7.14}$$

We may write the equations (7.13)-(7.14) in terms of a new variable $u = w - (\xi + \omega \times y)$ for future convenience, as follows:

$$\left.\begin{array}{rcl} \mathrm{Re}(u \cdot \mathrm{grad}\ u + 2\omega \times u + \omega \times (\xi + \omega \times y)) & = & \mathrm{div}\ T(u,\pi) + g \\ \mathrm{div}\ u & = & 0 \\ \lim\limits_{|x|\to\infty} (u + \xi + \omega \times y) & = & 0 \\ u|_\Sigma & = & 0. \end{array}\right\} \tag{7.15}$$

and

$$\left.\begin{array}{rcl} \mathrm{Re} m\omega \times \xi & + & \displaystyle\int_\Sigma T(u,\pi)\cdot n = mg \\ \mathrm{Re}\omega \times I\omega & + & \displaystyle\int_\Sigma y \times T(u,\pi)\cdot n = 0 \\ \omega \times g & = & 0. \end{array}\right\} \tag{7.16}$$

Remark 7.3.1 *If we take into account that $\omega \times g = 0$, then we have that $\omega = \lambda g$ where λ is a scalar. Therefore, with this restriction, we have ten scalar unknowns, w, π, ξ, ω and λ. Also, equations (7.13) and (7.14) constitute the set of ten scalar equations. Hence our problem is well posed.*

8.0 FREEFALL IN A SECOND ORDER FLUID AT $RE = 0$

In this chapter we study the existence and uniqueness of solutions to the freefall problem in a Second order fluid at $Re = 0$. We will present two different arguments to establish existence of solutions. The first is based upon a Lemma due to Rabier and Serre and the second argument follows independently from the Implicit function theorem, both, with the restriction $\alpha_1 + \alpha_2 = 0$. In the final section, we show existence of solutions to the freefall problem at zero Reynolds number but for arbitrary $\alpha_1 + \alpha_2$ values. The restriction $\alpha_1 + \alpha_2 = 0$ can also be written in terms of a new parameter ϵ which is defined as $\epsilon = \frac{\alpha_2}{\alpha_1}$. The case $\epsilon = -1$ is a special case of the more general result that we obtain in the final section. However, we still deem it necessary to include the former result since the argument used is considerably simpler. Also, in the case $\epsilon = -1$, we have from Giesekus' theorem and also independently shown by us, that the velocity field coincides with the Stokes velocity. This has some immediate consequences which is not very evident in the more general case and requires very heavy handed tools. In the second section we provide an alternative proof of existence for the case $\epsilon = -1$ based upon the Implicit Function theorem. Once again, the results of the section are of course known from earlier arguments, yet the technique manages to elucidate certain features of the problem which are not apparent otherwise.

8.1 Existence and Uniqueness for $\alpha_1 + \alpha_2 = 0$

Following Giesekus,[34] we assume that $\epsilon = -1$ (i.e. $\alpha_1 + \alpha_2 = 0$) in the constitutive equation for the Second order fluid. The equation of motion of the fluid in non-dimensional form is given by (7.13) and (7.14) with $T(v, p) = T_N(v, p) - \mathrm{We}S(u)$ the stress tensor corresponding to the Second order fluid model, with T_N representing the Newtonian part of the stress tensor and S, the viscoelastic part. However, if in equation (7.15-7.16) we take $\epsilon = -1$

and $\mathrm{Re} = 0$, then upon some manipulation, the governing equations may written as

$$\left.\begin{array}{c} \Delta u - \text{grad } \Pi - We\Delta(\text{curl} u) \times u = 0 \\ \text{div } u = 0 \\ u|_\Sigma = 0 \\ \lim_{|x|\to\infty}(u + v_\infty) = 0 \end{array}\right\} \tag{8.1}$$

where

$$\Pi = p - g \cdot y + We(u \cdot \Delta u + \frac{1}{4}|A_1(u)|^2)$$

and $v_\infty = \xi + \omega \times y$. A significant contribution to approaching this problem is provided in[27,28,31] where the equations of the body are decoupled from those of the fluid by the introduction of auxiliary fields $(h^{(i)}, p^{(i)})$ and $(H^{(i)}, P^{(i)})$, corresponding to elementary translation and rotation respectively. It is now easily verified that the fields $\hat{u}$ and $\hat{p}$ in the form

$$\hat{u} = \xi_i h^{(i)} - \xi + \omega_i H^{(i)} - \omega \tag{8.2}$$

$$\hat{p} = \xi_i p^{(i)} + \omega_i P^{(i)} + g \cdot y - We(\hat{u} \cdot \Delta\hat{u} + \frac{1}{4}|A_1(\hat{u})|^2) \tag{8.3}$$

satisfy the problem (8.1). This problem can be reformulated in a more convenient manner. If we now multiply equation $(7.15)_1$ by $h^{(i)}$ and integrate by parts over Ω, we obtain

$$\int_\Sigma (e_i \cdot T_N(u,p) \cdot n + e_i \cdot ng \cdot x) = \int_\Sigma A_1(u) : A_1(h^{(i)}) + We\mathcal{F} \tag{8.4}$$

where

$$\mathcal{F} = \int_\Omega h^{(i)} \cdot \text{div } S(u) \tag{8.5}$$

$i = 1, 2, 3$. Similarly multiplying the equation $(7.15)_1$ by $H^{(i)}$ and integrating by parts over Ω again, we have the expression

$$\int_\Sigma \{(e_i \times x) \cdot T_N \cdot n + (e_i \times x) g \cdot x\} = \int_\Sigma A_1(u) : A_1(H^{(i)}) + We\mathcal{M} \tag{8.6}$$

where

$$\mathcal{M} = \int_\Omega H^{(i)} \cdot \text{div } S(u) \tag{8.7}$$

$i = 1, 2, 3$. Now multiplying equations (3.3) and (3.4) by $(u + v_\infty)$ and integrating over Ω, gives us, upon routine manipulation,

$$\begin{aligned} \int_\Sigma A_1(u) : A_1(h^{(i)}) &= \int_\Sigma v_\infty \cdot T_N(h^{(i)}, p^{(i)}) \cdot n \\ \int_\Sigma A_1(u) : A_1(H^{(i)}) &= \int_\Sigma v_\infty \cdot T_N(H^{(i)}, p^{(i)}) \cdot n. \end{aligned}$$

Substituting these equations into equations (8.4) and (8.6) respectively, and collecting all the terms, we obtain upon some rearrangement,

$$K \cdot \xi + C \cdot \omega = m_e g + We\mathcal{F}(u) \tag{8.8}$$

$$C^\dagger \cdot \xi + \Omega \cdot \omega = R \times g + We\mathcal{M}(u) \tag{8.9}$$

$$\omega \times g = 0 \tag{8.10}$$

where the tensors K, C and Ω are defined by

$$K_{ij} = \int_\Sigma \left(T(h^{(i)}, p^{(i)}) \cdot n\right)_j \tag{8.11}$$

$$C_{ij} = \int_\Sigma \left(x \times T(h^{(i)}, p^{(i)}) \cdot n\right)_j \tag{8.12}$$

$$\Omega_{ij} = \int_\Sigma \left(x \times T(H^{(i)}, P^{(i)}) \cdot n\right)_j \tag{8.13}$$

and depend simply on the shape, size or symmetry of $\mathcal{B}$. We shall elaborate on the terms

$\mathcal{F}$ and $\mathcal{M}$ in the following sections. The above equations now represent the central equations for our problem. In the Lemma below, we show that solving the equations (8.8)-(8.10) is equivalent to solving the problems (8.1) and (7.16).

Lemma 8.1.1 *The problem (8.1) has at least one solution if and only if the equations (8.8)-(8.10) can be solved for ξ, ω and g.*

Proof :

If problem (8.1) has a solution $\{u, p, \xi, \lambda, \omega, g\}$ then it follows that $\{\xi, \lambda, g\}$ automatically solve equations (8.8)-(8.10). For the converse argument, recall that if equations (8.8) and (8.10) can be solved then, equations (8.2), (8.3) provides a solution to problem (8.1). □

8.1.1 A Uniqueness Property

We define the class $\mathcal{A}$, of the pair (u, p) such that

$$u \in C^2(\bar{\mathcal{D}'}) \bigcap W^{2,3}_{loc}(\mathcal{D}), \quad p \in C^0(\bar{\mathcal{D}'}) \bigcap W^{1,2}_{loc}(\mathcal{D})$$

where $\mathcal{D}'$ is an bounded subset of $\mathcal{D}$ and the asymptotic behavior of the pair (u, p) is given by

$$D^\beta(u(y) + v_\infty(y)) = O(|y|^{-1-|\beta|}), \quad 0 \leq |\beta| \leq 3$$

$$p - g \cdot y = p_0 + O(|y|^{-2})$$

where $p_0 \in \mathbf{R}$. We also require that the body, $\mathcal{B}$, be of class $\mathcal{C}^3$.[(25)] In this section we show that for small Weissenberg numbers, the velocity field, u which satisfies problem (8.1) coincides with the Stokes velocity field, $\hat{u}$, in the class $\mathcal{A}$. This result is crucial to our following sections where we analyze the problem for specific symmetries of $\mathcal{B}$. Supposing

(u, p) is another solution to problem (8.1), then it follows that

$$\Delta v - We[\Delta\omega \times u] + We[\Delta\hat{\omega} \times \hat{u}] = \text{grad}\pi \tag{8.14}$$

where $v = (u - \hat{u})$, $\pi = (p - \hat{p})$, $\omega = \text{curl } u$ and $\hat{\omega} = \text{curl } \hat{u}$. Adding and subtracting term $We[\Delta\hat{\omega} \times u]$ yields after some manipulation

$$\Delta v + We\Delta\bar{\omega} \times u = \text{grad}\pi \tag{8.15}$$

where $\bar{\omega} = \hat{\omega} - \omega$ and $\Delta\hat{\omega} = 0$ follows from taking $\hat{u}$ to be the Stokes velocity field.

Lemma 8.1.2 *If u is defined as a solution to problem (8.1), $\hat{u}$ the solution to the Stokes problem and v_∞, the terminal velocity, then we have the following estimates*

$$(i) \quad ||\Delta A_1(u)|| \leq c_1(|\xi| + |\omega|) \tag{8.16}$$

and

$$(ii) \quad \sup |A_1(u)| \leq c_2(|\xi| + |\omega|). \tag{8.17}$$

Proof :

(i) Let us write $w = u - v_\infty$, then $A_1(w) = A_1(u) - A_1(v_\infty) = A_1(u)$. We begin with the fundamental inequality[(25)]

$$||\Delta A_1(u)||_{\frac{3}{2}} \leq c|w|_{3,\frac{3}{2}}.$$

Then, using [25, Theorem 2.8,Ch.5] with $m = 1$ and $q = \frac{3}{2}$, we obtain

$$|w|_{3,\frac{3}{2}} \leq c(||v_\infty||_{2-\frac{1}{t},t} + ||v_\infty||_{\frac{7}{3},\frac{3}{2}}).$$

Therefore it follows that

$$||\Delta A_1(u)|| \leq c_1(|\xi| + |\omega|).$$

(ii) Let $f = \nabla w$. Then for $r = \frac{3t}{3-t}$, $1 < t < \frac{3}{2}$ and $1 < q < \infty$, $f \in L^r$ and $Df \in L^q$. We then have[25]

$$\begin{aligned} |f| &\leq c(||f||_{1,B_1(x)} + ||\nabla f||_{q,\Omega}) \\ &\leq c_2[||f||_{r,\Omega} + ||\nabla f||_{q,\Omega}]. \end{aligned}$$

Therefore applying [25, Theorem 4.3,Ch.5] once again, with $m = 0$, $q > 3$ and $k = 0$ we get

$$\sup |A_1(u)| \leq c_2(|w|_{1,r} + |w|_{2,q}) \leq c_3(||v_\infty||_{2-\frac{1}{t},t} + ||v_\infty||_{2-\frac{1}{q},q}) \leq c_2(|\xi| + |\omega|).$$

□

Theorem 8.1.1 *The velocity field $\hat{u}$ given by equation* (8.2) *is unique in the class $\mathcal{A}$ if*

$$|We|\,(|\xi| + |\omega|) \leq c.$$

Proof :

Multiplying equation (8.15) by v and integrating over a ball of radius r, B_r, we have

$$\int_{B_r} v \cdot \Delta v + We \int_{B_r} v \cdot (\Delta\bar{\omega} \times u) = \int_{B_r} v \cdot \mathrm{grad}\pi \tag{8.18}$$

To simplify equation (8.18) we further integrate by parts. Then the first and third terms of the above equation become

$$\begin{aligned} \int_{B_r} v \cdot \Delta v &= \int_{\partial B_r} v \cdot \mathrm{grad}v \cdot n - \int_{B_r} |\mathrm{grad}v|^2 \\ \int_{B_r} v \cdot \mathrm{grad}\pi &= \int_{\partial B_r} (v \cdot n)\pi \end{aligned} \tag{8.19}$$

while second term, upon some manipulation[18] becomes

$$\int_{B_r} v \cdot (\Delta\bar{\omega} \times u) = \int_{B_r} v \cdot \Delta(\mathrm{grad}v - \mathrm{grad}^T v) \cdot u.$$

Therefore the equation (8.18) simplifies to

$$\int_{\partial B_r} v \cdot \mathrm{grad}v - \int_{B_r} |\mathrm{grad}v|^2 + We \int_{B_r} v \cdot \Delta(\mathrm{grad}v - \mathrm{grad}^T v) \cdot u = \int_{\partial B_r} (v \cdot n)\pi \qquad (8.20)$$

which in the limit $r \to \infty$ becomes

$$\int_{\Omega} |\mathrm{grad}v|^2 = We \int_{\Omega} v \cdot \Delta(\mathrm{grad}v - \mathrm{grad}^T v) \cdot u \qquad (8.21)$$

since v is solenoidal and zero on the boundary. We further simplify this equation by integrating by parts the right hand side of equation (8.21) several times as shown below in indicial form. We consider the two terms separately. First,

$$\begin{aligned} \int_{\Omega} \partial_j \partial^2{}_k v_i v_j u_i &= -\int_{\Omega} \partial^2{}_k v_i \partial_j v_i u_j \\ &= 2\int_{\Omega} \partial_j v_i \partial_k u_j \partial_k v_i + \int_{\Omega} u_j \partial_j v_i \partial^2{}_k v_i. \end{aligned} \qquad (8.22)$$

The final step follows after integrating by parts twice. This then suggests that

$$\int_{\Omega} \partial_j \partial^2{}_k v_i v_i u_j = \int_{\Omega} \partial_j v_i \partial_k u_j \partial_k v_i. \qquad (8.23)$$

The second term in the right hand side of equation (8.21) can be rewritten as

$$\begin{aligned} \int_{\Omega} \partial_i \partial^2{}_k v_j v_i u_j &= -\int_{\Omega} v_i \partial^2{}_k v_j \partial_i u_j \\ &= \int_{\Omega} \partial_k v_i \partial_k v_j \partial_i u_j - \int_{\Omega} v_i v_j \partial^2{}_k \partial_i u_j + \int_{\Omega} \partial_i v_j \partial_k v_i \partial_k u_j. \end{aligned} \qquad (8.24)$$

Therefore, upon combining these two results, we have that

$$\begin{aligned}\int_\Omega |\text{grad}v|^2 &= \frac{We}{2}[\int_\Omega \text{grad}^T v \cdot A_1(u) \cdot \text{grad}v + \int_\Omega v \cdot \Delta A_1(u) \cdot v \\ &\quad -2\int_\Omega \text{grad}v \cdot A_1(u) \cdot \text{grad}v - \int_\Omega \text{grad}^T v \cdot A_1(u) \cdot \text{grad}^T v] \qquad (8.25) \\ &\leq 2|We|\int_\Omega |\text{grad}v|^2|A_1(u)| + |\frac{We}{2}|\int_\Omega |v|^2|\Delta A_1(u)| \\ &\leq 2|We|\int_\Omega |\text{grad}v|^2|A_1(u)| + |\frac{We}{2}|(\int_\Omega |v|^6)^{\frac{1}{3}}(\int_\Omega |\Delta A_1(u)|^{\frac{3}{2}})^{\frac{2}{3}}\end{aligned}$$

where we have used the Holder's inequality in the final step. Furthermore, by a simple application of the Sobolev Inequality we get

$$||\text{grad}v||_2^2 \leq 2|We|M_1||\text{grad}v||_2^2 + \frac{2}{3}|We|||\Delta A_1(u)||_{\frac{3}{2}}||\text{grad}v||_2^2$$

where we define $M_1 = sup|A_1(u)|$. Therefore

$$(1 - |We|M_1 + \frac{2}{3}|We|||\Delta A_1(u)||_{\frac{3}{2}})||\text{grad}v||_2^2 \leq 0.$$

Using Lemma 8.1.2 it then follows that $u = \hat{u}$ if

$$|We|\,(|\xi| + |\omega|) \leq c_3. \qquad (8.26)$$

Therefore as long as the condition provided by equation (8.26) is satisfied, the velocity field u corresponding to equation (8.1) coincides with the Stokes velocity field. □

8.1.2 Existence of Steady Fall

In this section we shall prove existence of solutions to the problem (8.8)-(8.10) for small Weissenberg numbers. From now on, as a consequence of the uniqueness result, we will take u to be the Stokes velocity field. We have seen in section 2.1 that the problem (8.1)

and (7.16) can be rewritten as equations (8.8)-(8.10) and we have also established that the two problems are in fact equivalent. The remarkable feature of this method is that though we are restricted to the case of small We, yet, we can predict significant departures from the Stokes problem and as we shall see in the following sections, certain interesting aspects of the problem can be elucidated. We begin with a simplification of the nonlinear terms that arise as a result of the Second order fluid model, by exploiting the symmetries of the Stokes velocity field, which allows for a very convenient analysis of the equations. We have seen the terms $\mathcal{F}$ and $\mathcal{M}$ first emerge in section 2.1, which we shall henceforth refer to as the viscoelastic force and torque coefficients, respectively. In the case of slow motion approximation, these terms can be written in the form[31]

$$\mathcal{F} = \frac{1}{2}\int_{\Sigma} |\mathrm{curl}(\hat{u})|^2 n$$

and

$$\mathcal{M} = \frac{1}{2}\int_{\Sigma} |\mathrm{curl}(\hat{u})|^2 y \times n$$

where $y \in \Sigma$. It is easy to show that these terms are quadratic functions of ξ and ω with coefficients that depend only upon the geometry of the body, $\mathcal{B}$. To this end, we write

$$Z_1^{(i)} = \mathrm{curl} h^{(i)}, \quad Z_2^{(i)} = \mathrm{curl} H^{(i)}.$$

Let us also define the terms

$$\begin{aligned}
\mathbf{A}_T^{(i,j)} &= \frac{1}{2}\int_\Sigma Z_1^{(i)} \cdot Z_1^{(j)} n \\
\mathbf{B}_T^{(i,j)} &= \frac{1}{2}\int_\Sigma (Z_2^{(i)} \cdot Z_2^{(j)} - 4Z_{2j}^{(i)}) n \\
\mathbf{C}_T^{(i,j)} &= \int_\Sigma (Z_1^{(i)} \cdot Z_2^{(j)} - 2Z_{1j}^{(i)}) n \\
\mathbf{A}_R^{(i,j)} &= \frac{1}{2}\int_\Sigma Z_1^{(i)} \cdot Z_1^{(j)} y \times n \\
\mathbf{B}_R^{(i,j)} &= \frac{1}{2}\int_\Sigma (Z_2^{(i)} \cdot Z_2^{(j)} - 4Z_{2j}^{(i)}) y \times n \\
\mathbf{C}_R^{(i,j)} &= \int_\Sigma (Z_1^{(i)} \cdot Z_2^{(j)} - 2Z_{1j}^{(i)}) y \times n.
\end{aligned} \tag{8.27}$$

Therefore we can write the nonlinear terms in the following convenient indicial form

$$\mathcal{F}_k = \xi_i \xi_j A_{Tk}^{(i,j)} + \omega_i \omega_j B_{Tk}^{(i,j)} + \xi_i \omega_j C_{Tk}^{(i,j)} \tag{8.28}$$

$$\mathcal{M}_k = \xi_i \xi_j A_{Rk}^{(i,j)} + \omega_i \omega_j B_{Rk}^{(i,j)} + \xi_i \omega_j C_{Rk}^{(i,j)}. \tag{8.29}$$

where $k = 1, 2, 3$. Note that the terms $\mathcal{F}$ and $\mathcal{M}$ are quadratic in ξ and ω while the coefficients depend merely on the geometric properties of the body. Now, to show existence, we begin with the result of Property 3.4.3 that the 6×6 matrix

$$\begin{pmatrix} K & C \\ C^\dagger & \Omega \end{pmatrix}$$

is positive definite and invertible.[36] We next quote a Lemma due to P. Rabier.[25] A less general form of this Lemma is proved by Serre [68, Lemma 4.4] which would suffice for our purposes.

Lemma 8.1.3 *Let the maps*

$$\Pi : \hat{B}_R \times S^2 \to \mathbf{R}^n$$

$$\tau : \hat{B}_R \times S^2 \to \mathbf{R}^3$$

be continuous. Suppose also that

$$\Pi(c, g) \cdot c > 0$$

for all $(c, g) \in \partial B_R \times S^2$ *and*

$$\tau(c, g) \cdot g = 0$$

for all $(c, g) \in B_R \times S^2$. *Then there is a* $(c, g) \in B_R \times S^2$ *such*

$$\Pi(c, g) = 0, \quad \textit{and } \tau(c, g) = 0.$$

Theorem 8.1.2 (Existence Theorem 1) *Let* $\mathcal{B}$ *be a body of class* $\mathcal{C}^3$. *Then, the steady fall problem (8.8)-(8.10) has at least one solution, provided*

$$We < \frac{\lambda^2}{4\beta_1\beta_2}$$

where λ, β_1 *and* β_2 *are parameters depending only upon the geometry of the body.*

Proof :

Set $c := (\xi, \omega)$ and the maps τ and Π as follows:

$$\tau(c, g) := \omega \times g$$

$$\Pi(c, g) := \begin{pmatrix} K \cdot \xi + C \cdot \omega - m_e g - We\mathcal{F} \\ C^\dagger \cdot \xi + \Omega \cdot \omega - R \times g - We\mathcal{M} \end{pmatrix} \tag{8.30}$$

then the condition $\omega \times g = 0$ gives us $\tau(c,g)\cdot g = 0$ for all $(c,g) \in B_R \times S^2$. Furthermore, we have

$$\Pi(c,g)\cdot c = \xi\cdot K\cdot\xi + \omega\cdot\Omega\cdot\omega + 2\xi\cdot C\cdot\omega - m_e\xi\cdot g - We(\xi\cdot\mathcal{F} + \omega\cdot\mathcal{M}) \tag{8.31}$$

where

$$\begin{aligned} \xi\cdot\mathcal{F} &= \xi_i\xi_j\xi_k A^{(i,j)}_{Tk} + \omega_i\omega_j\xi_k B^{(i,j)}_{Tk} + \xi_i\omega_j\xi_k C^{(i,j)}_{Tk} & (8.32)\\ \omega\cdot\mathcal{M} &= \xi_i\xi_j\omega_k A^{(i,j)}_{Rk} + \omega_i\omega_j\omega_k B^{(i,j)}_{Rk} + \xi_i\omega_j\omega_k C^{(i,j)}_{Rk}. & (8.33) \end{aligned}$$

Denoting by $\beta_2 = \beta_2(\mathcal{B})$, an upper bound for the entries of the matrices in equation (8.27), we have

$$|\xi\cdot\mathcal{F}| + |\omega\cdot\mathcal{M}| \le \beta_2 R^3$$

for $c \in \partial B_R$. Notice that β_2 depends only upon the geometric properties of $\mathcal{B}$. Also, since the matrix

$$\begin{pmatrix} K & C \\ C^\dagger & \Omega \end{pmatrix}$$

is positive definite and symmetric, its eigenvalues are real and positive.[82,83] Then

$$\xi\cdot K\cdot\xi + \omega\cdot\Omega\cdot\omega + 2\xi\cdot C\cdot\omega = \begin{pmatrix} \xi \\ \omega \end{pmatrix}^T \cdot \begin{pmatrix} K & C \\ C^\dagger & \Omega \end{pmatrix} \cdot \begin{pmatrix} \xi \\ \omega \end{pmatrix}$$

$$\ge \lambda \begin{pmatrix} \xi \\ \omega \end{pmatrix}^T \cdot \begin{pmatrix} \xi \\ \omega \end{pmatrix} = \lambda(\xi^2 + \omega^2)$$

where $\lambda > 0$ is the least eigenvalue of the above 6×6 matrix. Hence, we have

$$\Pi(c,g)\cdot c \ge \lambda R^2 - \beta_1 R - \beta_2 R^3$$

where $\beta_1 = m_e$. We also make use of the fact that $|g| = 1$ here. Therefore a solution to the problem under investigation exists if there is a $R > 0$ such that

$$\lambda R - \beta_1 - \beta_2 R^2 > 0. \tag{8.34}$$

Now, equation (8.34) is satisfied for

$$\frac{\lambda + \sqrt{\lambda^2 - 4We\beta_1\beta_2}}{2We\beta_2} > R > \frac{\lambda - \sqrt{\lambda^2 - 4We\beta_1\beta_2}}{2We\beta_2}. \tag{8.35}$$

Therefore the requirement that R must be real and positive yields the condition $We < \frac{\lambda^2}{4\beta_1\beta_2}$. □

8.2 Alternative Proof of Existence for $\alpha_1 + \alpha_2 = 0$

In this section, we provide an alternative proof for the freefall of a rigid body in a Second order liquid with the restrictions $\epsilon = -1$ and $\mathrm{Re} = 0$. The proof is based upon the Implicit Function theorem and has some interesting consequences which are not apparent from our previous argument. Before delving into the proof, we shall rewrite the governing equations for the rigid body in a more appropriate form. We see from the formulation of the problem that the governing equations (8.8)-(8.10) depend upon the positive definite, 6×6 matrix

$$\begin{pmatrix} K & C \\ C^\dagger & \Omega \end{pmatrix}.$$

Since K, Ω and C are in general invertible we may use the governing equations to solve for ξ. Hence,

$$\xi = K^{-1}(m_e g - \lambda C \cdot g + \mathrm{We}\mathcal{F}) \tag{8.36}$$

and replacing this in equation (8.10) we obtain

$$\begin{aligned} m_e C^\dagger K^{-1} \cdot g - r \times g - \lambda(C^\dagger K^{-1} C - \Omega) \cdot g &= \mathrm{We}(C^\dagger K^{-1} \mathcal{F} + \mathcal{M}) \\ \Rightarrow (C^\dagger K^{-1} C - \Omega)^{-1}(m_e C^\dagger K^{-1} - R) \cdot g &= \lambda g - \mathrm{We}(C^\dagger K^{-1} C - \Omega)^{-1}(C^\dagger K^{-1} \mathcal{F} + \mathcal{M}) \end{aligned}$$

which we rewrite in the form

$$A \cdot g = \lambda g - \mathrm{We} G(\xi, \lambda, g) \tag{8.37}$$

where we define

$$A = (C^\dagger K^{-1} C - \Omega)^{-1}(m_e C^\dagger K^{-1} - R),\ G = \mathrm{We}(C^\dagger K^{-1} C - \Omega)^{-1}(C^\dagger K^{-1} \mathcal{F} + \mathcal{M}).$$

We define here $R = r \times I$ as in[36] where $|R|$ represents the inhomogeneity of $\mathcal{B}$. For a homogeneous body $R \equiv 0$. In terms of these new variables then, the governing equation may be represented as

$$K \cdot \xi + \lambda C \cdot g - m_e g - \hat{\epsilon} \mathcal{F}(\xi, \lambda, g) = 0 \tag{8.38}$$

$$A \cdot g - \lambda g = \hat{\epsilon} G(\xi, \lambda, g) \tag{8.39}$$

This defines a map $\Psi(\hat{\epsilon}, w) : [0,1] \times R \times R^3 \times S^2 \to R^3 \times R^3$ and $w = (\xi, \lambda, g)$ where the non-linear term appears as the coefficient of $\hat{\epsilon}$. Existence can now be shown by a straightforward application of the Implicit Function Theorem (see Theorem 3.3.3). At $\hat{\epsilon} = 0$ and $w = w_0$, the central equations become a linear eigenvalue problem and can be written as

$$K \cdot \xi_0 + \lambda C \cdot g_0 - m_e g_0 = 0 \tag{8.40}$$

$$A \cdot g_0 = \lambda_0 g_0 = 0. \tag{8.41}$$

Since A is a well defined, real, 3×3 matrix, it has at least one real solution. Therefore the linearized version of the governing equations have a solution (ξ_0, λ_0, g_0). We now show that the nonlinear problem also has a solution.

Lemma 8.2.1 *The problem (8.39) has at least one solution if and only if the equation (8.1) has a solution.*

Proof :

If problem (8.39) has a solution $\{\xi, \lambda, \omega, g\}$ then it follows that substituting them in equations (8.2) and (8.3) provides a solution to problem (8.1). Conversely, if problem (8.1) can be solved for (u, p, ξ, λ, g) then it follows that $\{\xi, \lambda, g\}$ automatically satisfies the equation (8.39). $\square$

First we need to rewrite the governing equations obtained above. We define the map $\Phi(\hat{\epsilon}, w) : R^7 \to R^7$ by

$$\Phi(\hat{\epsilon}, w) = \begin{pmatrix} \mathrm{K}\cdot\xi + \lambda C \cdot g - m_e g \\ \mathrm{A}\cdot g - \lambda g \\ <\mathrm{g},\mathrm{g}>\text{-}1 \end{pmatrix}.$$

At the point $(0, w_0)$ we then have the linear equation $\Phi(0, w_0) = 0$. Then the Frechet derivative at the point $(0, w_0)$ is given by

$$\Phi_w(0, w_0) = \begin{pmatrix} \xi + K^{-1}[\lambda_0 C g + \lambda C g_0 - m_e g] \\ \mathrm{A}\cdot g - \lambda_0 g - \lambda g_0 \\ 2 < \mathrm{g}_0, g > \end{pmatrix} \begin{pmatrix} \mathrm{f}_1 \\ \mathrm{f}_2 \\ \mathrm{f}_3 \end{pmatrix}.$$

say. To show existence of solutions to the nonlinear problem the Implicit Function Theorem suggests that the mapping $\Phi_w(0, w_0)$ be bijective. For the proof we shall adopt the technique used by Lusternik and Sobolev.[55] We now consider a useful Lemma concerning the multiplicity of the eigenvalue of the matrix A defined earlier.

Lemma 8.2.2 *Let A be a 3×3 matrix with a simple eigenvalue λ_0 and corresponding vector g_0. Furthermore, if there exist vectors g and $\tilde{g}$ which satisfy*

$$Ag - \lambda_0 g = \lambda g_0 \tag{8.42}$$

$$< g, g_0 > = 0 \tag{8.43}$$

then $< \tilde{g}, g_0 > \neq 0$.

Proof :

The Fredholm alternative tells us that the equation (8.44) has at least one solution iff $< \tilde{g}, g_0 >= 0$. Therefore if we assume this orthogonality condition to be true and apply $(A - \lambda_0 I)$ on both sides of (8.44), we obtain

$$(A - \lambda_0 I)^2 g = \lambda (A - \lambda_0 I) g_0 = 0$$

Therefore since λ_0 is a simple eigenvalue, we must necessarily have $g = \alpha g_0$ which is not possible from (8.43). Therefore the hypothesis is false and $< \tilde{g}, g_0 > \neq 0$. $\square$

Lemma 8.2.3 *The mapping $\Phi(\hat{\epsilon}, w_0)$ is a bijection :$R^7 \to R^7$.*

Proof :

To show injection it suffices to show that if

$$(A - \lambda_0 I) g - \lambda g_0 = 0 \tag{8.44}$$

then $\lambda = 0$ and $g = 0$. Taking the inner product of the above equation with $\tilde{g}$ which is defined as in the Lemma 8.2.2 above we have,

$$< (A - \lambda_0 I) g - \lambda g_0, \tilde{g} >= 0, \ < (A - \lambda_0 I) g, \tilde{g} >= \lambda < g_0, \tilde{g} >$$

$$\Rightarrow < g, (A^{\dagger} - \lambda_0 I)\tilde{g} > = < g, 0 > = 0 = \lambda < g_0, \tilde{g} > .$$

From Lemma 8.2.2, since $< g_0, \tilde{g} > \neq 0$, therefore $\lambda = 0$. Putting this back in the equation (8.44) gives us

$$(A - \lambda_0 I)g = 0 \Rightarrow g = 0.$$

This follows from the fact that g cannot be an eigenvector of A since it is orthogonal to g_0. Finally, setting $\lambda = 0$ and $g = 0$ in

$$\xi + K^{-1}[\lambda_0 C g + \lambda C g_0 - m_e g] = 0 \Rightarrow \xi = 0.$$

Therefore we have injection for the map $\Psi_w(0, w_0)$. To show surjection we need that for every $\mathbf{y} \in R^7$, there exists an $\mathbf{x} \in R^7$ such that $\Phi_w(0, w_0; x) = y$. To this end we define $g = G + < g, g_0 > g_0$ from which it follows that $< G, g_0 > = 0$. Then we can write

$$Ag - \lambda_0 g - \lambda g_0 = f_2$$

as

$$\begin{aligned} Ag - \lambda_0 g + \lambda_0[< g, g_0 > g_0] - A[< g, g_0 > g_0] &= f_2 + \lambda g_0 = \mathcal{F} \\ \Rightarrow (A - \lambda_0 I)G &= \mathcal{F} \end{aligned} \tag{8.45}$$

If we now define

$$\lambda = -\frac{< f_2, \tilde{g} >}{< g_0, \tilde{g} >} \tag{8.46}$$

then $< \mathcal{F}, \tilde{g} > = 0$. Therefore again applying the Fredholm alternative we have that equation (8.45) is solvable with G given by

$$G = (A - \lambda_0 I)_{\perp}^{-1} \mathcal{F} \tag{8.47}$$

where the $\perp$ symbol indicates that G is defined in the space perpendicular to g_0. Therefore substituting for G, we have

$$g = \frac{f_3}{2} g_0 + (A - \lambda_0 I)^{-1}_{\perp} \mathcal{F} \tag{8.48}$$

where λ is defined by equation (8.46). The final step in the argument follows trivially. We then have that

$$\xi = f_1 - K^{-1}[\lambda_0 C g + \lambda C g_0 - m_e g]$$

where g and λ are given by equations (8.48) and (8.46). Hence in conclusion, we have for each $y = \{f_1, f_2, f_3\} \in R^7$ there exists a vector $x = \{\lambda, g, \xi\} \in R^7$ such that $\Phi_w(0, w_0; x) = y$.

The above two cases suggest therefore that $\Phi_w(0, w_0)$ is a bijection. $\square$

Theorem 8.2.1 (Existence Theorem 2) *Let $\mathcal{B}$ be a body of class $\mathcal{C}^3$. Also let (g_0, λ_0) be the eigenvectors and corresponding eigenvalue solving*

$$A \cdot g_0 = \lambda_0 g_0.$$

Then, the steady fall problem (8.8)-(8.10) has at least one solution $\{\xi, \lambda, g\}$, provided λ_0 is a simple eigenvalue. Furthermore, this suggests that the equation (8.39) is solvable and the solution is analytic in $\hat{\epsilon}$.

Proof:
For the proof of the theorem we invoke the Lemmas 8.2.2 and 8.2.3 and the Implicit Function theorem. $\square$

The above proof has been furnished with the restriction that λ_0 be simple. For instance if we assume that the multiplicity of the eigenvalue is 1 with the corresponding eigenvector g_1 with $|g_1| = 1$, then this means the sedimenting body in the Second order fluid will rotate about the direction g_1 with magnitude $|\lambda_0|$ (while also translating). The assumption of

multiplicity 1, says here that there is only one direction about which rotation of the falling body will occur.

8.3 Existence Theorem for Arbitrary $\alpha_1 + \alpha_2$

In this section, we prove the existence of solutions to the full problem of freefall of a rigid body in a Second order fluid with no restrictions on $\alpha_1 + \alpha_2$ (i.e. ϵ), but with $\mathrm{Re} = 0$. Therefore the governing equations for our problem, as in the earlier Section 8.1, can be given in two parts, the first will involve the equations for the liquid which is modeled by the Second order fluid. Based on the work of Novotny et. al.[59,60] we may write the Second order fluid equations as

$$-\Delta v + \mathrm{We}\, v \cdot \mathrm{grad}\ \Delta v + \mathrm{grad}\ p = -\mathrm{We}\, \mathrm{div}\ N(v) \tag{8.49}$$

$$\left.\begin{array}{c} \mathrm{div}\ v = 0 \\ v = 0 \text{ on } \partial\Omega \\ \lim_{|x|\to\infty}[v(x) + v_\infty(x)] = 0. \end{array}\right\} \tag{8.50}$$

where $p = \tilde{p} + x \cdot g$ and

$$N(v) = (\mathrm{grad}\ v)^T A(v) + (1+\epsilon) A(v)^2.$$

Recall that v_∞ here represents the rigid body motion given by $\xi + \omega \times x$. We rewrite, for convenience, the additional equations for the body which can be given in terms of the net force and torque imposed on $\mathcal{B}$ due to the liquid, namely

$$\left.\begin{array}{c} \displaystyle\int_\Sigma T(\omega,\pi)\cdot n = m_e g \\ \displaystyle\int_\Sigma y \times T(\omega,\pi)\cdot n = R \times g \\ \omega \times g = 0 \end{array}\right\} \tag{8.51}$$

where $m_e = (m - |\mathcal{B}|g)$ is the effective mass. The objective is to establish the existence of

solutions, (v, p), to the coupled system of equations (8.49), (8.50) and (8.51). The complex nature of the problem requires us to treat the existence problem in two stages. In the first, we prescribe ξ and ω and establish the existence of (v, p).

8.3.1 Existence and Uniqueness with Prescribed (ξ,ω).

The specific objective of this section is to show the existence of solutions to the equations (8.49)and (8.50) for arbitrary ϵ and sufficiently small We. The motion of the body, i.e. ξ and ω are now prescribed. This is an important intermediate step that will find use in our final existence arguments. The strategy that we employ involves splitting this problem into a Stokes Problem and a Transport problem by a map $\mathcal{A}$, such that (see[30,59,60])

$$\mathcal{A} : \psi \to (v, \pi) \to z \tag{8.52}$$

Here, (v, π) solve the Stokes problem

$$\left.\begin{array}{c} -\Delta v + \text{grad } \pi = \text{div } \psi \\ \text{div } v = 0 \\ v = 0 \text{ on } \partial\Omega \\ \lim_{|x|\to\infty}[v(x) + v_\infty(x)] = 0 \end{array}\right\} \tag{8.53}$$

where the modified pressure π is related to the original pressure by $p = \pi - \text{We} v \cdot \text{grad } \pi$. Furthermore, z solves the equation

$$\left.\begin{array}{rcl} z - \text{We}(v \cdot \text{grad } z - z \cdot \text{grad }^T v) & = & -\text{We} N(v, \pi) \\ N(v, \pi) = N(v) - \pi \text{grad } v. & & \end{array}\right\} \tag{8.54}$$

Therefore, if we replace ψ by z in the above problem we get back the equations for the second order fluid (see[59,60]). Existence of solutions for the equations (8.49) is then proved by showing that $\mathcal{A}$ is a contraction in space X(defined in Chapter 3), for small We.

Another way of writing the equations for the body is based upon the argument outlined in Section 8.1. Using the auxiliary fields introduced in equations (3.3) and (3.4) and upon performing a similar calculation, we obtain

$$K \cdot \xi + C \cdot \omega = m_e g + \mathrm{We}\mathcal{F}(v) \tag{8.55}$$

$$C^{\dagger} \cdot \xi + \Omega \cdot \omega = R \times g + \mathrm{We}\mathcal{M}(v) \tag{8.56}$$

$$\omega \times g = 0. \tag{8.57}$$

where the tensors K, C and Ω are defined in equations (3.7-3.9).

We subdivide the following subsection into two parts. In the first part we shall obtain preliminary estimates for the Stokes and Transport equations in appropriate Sobolev spaces. In the second part, we establish the existence of solutions to the steady freefall problem with prescribed ξ and ω.

8.3.1.1 Preliminary Results .

Lemma 8.3.1 *Let $\Omega \subset C^{k+4}(\Omega)$ be an exterior domain in $\mathbf{R}^n$ with $k \geq 0$ and $f \in W^{k,q}(\Omega)$, then there exists a solution $F \in W^{k+1,q}(\Omega)$ to the problem*

$$div\ F = f$$

in Ω satisfying the estimate

$$||F||_{k+1,q} \leq c||f||_{k,q}$$

where c is a constant depending only upon k and q.

Proof:

See.[59,60,70] □

Lemma 8.3.2 *Let Ω be an exterior domain of class $C^{k+2}(\Omega)$, $k \geq 0$. Let us also consider $\psi \in W^{k+1,q}$, $u_* \in W^{k+2-1/q,q}(\partial\Omega)$, div $\psi \in L^t(\Omega)$ and $u_* \in W^{2-1/t,t}(\partial\Omega)$ for $1 < t < 3/2$ and $3 < q < \infty$. Then, there exists a unique solution, (u, π) to the Stokes problem (8.53) such that*

$$u \in \tilde{D}^{2,t}(\Omega) \cap [\cap_{m=0}^{k} D^{m+2,q}(\Omega)]$$

$$\pi \in D^{1,t}(\Omega) \cap [\cap_{m=0}^{k} D^{m+1,q}(\Omega)].$$

Also, (u, π) satisfies the estimate

$$\begin{aligned} ||grad\ u||_{C^k} + ||u||_s \quad &+ \quad |u|_{1,r} + |u|_{2,t} + ||\pi||_r + |\pi|_{1,t} \\ + \sum_{m=0}^{k} (|u|_{m+2,q} + |\pi|_{m+1,q}) \quad &\leq \quad c(||div\ \psi||_t + ||\psi||_{k+1,q} + |\xi| + |\omega|) \end{aligned} \tag{8.58}$$

with $r = \frac{3t}{3-t}$, $s = \frac{3t}{3-2t}$, $v = u + v_\infty$ and $c = c(q, t, k)$.

Proof:

See [25, Theorem V.4.3]. □

Lemma 8.3.3 *Let Ω be an exterior domain of class C^{k+5}, $k \geq 0$. Moreover, let v be such that grad $v \in C^k$ with $v \cdot n = 0$ and $\hat{F} \in W^{k+1,q}(\Omega)$, $1 < q < \infty$. Then there exists a $\delta > 0$ such that if $We||grad\ v||_{C^k(\Omega)} < \delta$, then the transport problem*

$$z - We(v \cdot grad\ z - z \cdot grad^{\ T} v) = \hat{F}$$

has a unique solution $z \in W^{k+1,q}(\Omega)$*, such that*

$$||z||_{k+1,q} \leq c||||_{k+1,q}$$

where c *is a constant depending only upon* k, q, t *and* Ω*.*

Proof:

It is sufficient to find suitable *a priori* estimates for the transport equation (8.54). Firstly, multiplying equation $(8.54)_1$ by $z|z|^{q-2}$ and integrating over Ω, we obtain

$$\begin{aligned} ||z||_q^q &\leq \text{We}||\text{grad } v||_{C^0(\Omega)}||z||_q^q + ||||_q||z||_q^{q-1} \\ \Rightarrow ||z||_q &\leq \frac{1}{(1 - \text{We}||\text{grad } v||_{C^0(\Omega)})}||||_q. \end{aligned} \tag{8.59}$$

Next, we take the gradient of transport equation, multiply through by grad $z|\text{grad } z|^{q-2}$ and integrate over Ω to get

$$||\text{grad } z||_q \leq \frac{1}{(1 - \text{We}||\text{grad } v||_{C^1(\Omega)})}||\text{grad } ||_q. \tag{8.60}$$

To show this estimate in general for arbitrary n, we take the $(n+1)^{th}$ derivative of the transport equation. Therefore, we get

$$\begin{aligned} \text{grad }^{n+1}z &+ \text{We}\sum_{r=0}^{n+1}\begin{pmatrix} n+1 \\ r \end{pmatrix}(\text{grad }^{n+1-r}v)(\text{grad }^{r}\text{grad } z) \\ &- We\sum_{r=0}^{n+1}\begin{pmatrix} n+1 \\ r \end{pmatrix}(\text{grad }^{n+1-r}z)(\text{grad }^{r}\text{grad } v) = \text{grad }^{n+1}. \end{aligned} \tag{8.61}$$

As earlier, multiply by grad $^{n+1}z|\text{grad }^{n+1}z|^{q-2}$ and integrate over Ω to get

$$||\text{grad }^{n+1}z||_q \leq \frac{1}{(1 - \text{We}||\text{grad } v||_{C^{n+1}(\Omega)})}||\text{grad }^{n+1}||_q. \tag{8.62}$$

We obtain the desired estimate by an induction argument. To this end, we consider the case of $k = 0$ and $k = 1$, which upon addition yields

$$(1 - c_1 \mathrm{We}||\text{grad } v||_{C^1(\Omega)})||z||_{1,q} \leq ||||_{1,q}. \tag{8.63}$$

Also assume that the result holds for $k = n$. Hence

$$(1 - c_n \mathrm{We}||\text{grad } v||_{C^n(\Omega)})||z||_{n,q} \leq ||||_{n,q}. \tag{8.64}$$

Then adding the two estimates above corresponding to cases $k = 1$ and $k = n$, we obtain the estimate

$$(1 - c_{n+1} \mathrm{We}||\text{grad } v||_{C^{n+1}(\Omega)})||z||_{n+1,q} \leq ||||_{n+1,q}. \tag{8.65}$$

Once we have obtained the *a priori* estimates, the existence of such a z can be shown by an argument similar to Galdi and Rajagopal[30] (also see[63]). □

Additionally, we also have similar estimates for div z. It is easily verified from the transport equation that

$$\text{div } z - \mathrm{We} v \cdot \text{grad div } z = \text{div} \tag{8.66}$$

Lemma 8.3.4 *Let Ω be an exterior domain of class C^{k+3}, $k \geq 1$ and let v satisfy grad $v \in C^{k-1}$ and $v \cdot n = 0$. Also, let $q > 3$ and $1 < r < \infty$. Then there exists a $\delta > 0$ such that if $We||grad\ v||_{C^{k-1}} < \delta$ then there exists a solution to the equation (8.66) satisfying the following estimates:*

$$||div\ z||_{k,q} \;\leq\; c_1||div\ ||_{k,q}, \quad for \;\; k \geq 1 \tag{8.67}$$

and

$$||div\ z||_r \leq c_2||div\ ||_r \tag{8.68}$$

where c_1, c_2 depend on k, q, t and c_1 additionally depends also on We.

Proof:

Proof of this Lemma is similar to that of Lemma 3. Also see.[30,63] $\square$

The next Lemma concerns the property of the extra stress tensor, $S(v)$ for the Second order fluid model which is written as

$$S(v) = v \cdot \text{grad } A(v) + \epsilon A(v) \cdot A(v) + (\text{grad } v)^T \cdot A(v) + A(v) \cdot \text{grad } v$$

We make the following observation.

Lemma 8.3.5 *If we write $u = v + v_\infty$, then*

$$S(v) = v_\infty \cdot grad\ A(u) + \tilde{S}(u)$$

where

$$\tilde{S}(u) = u \cdot grad\ A(u) + \epsilon A(u) \cdot A(u) + (grad\ u)^T \cdot A(u) + A(u) \cdot grad\ u.$$

Proof:

It is easy to see that $A(v) = A(u)$. Therefore the only thing that remains to be shown is that the final two terms of $S(v)$ are invariant under the transformation of $v \to u$. We have that

$$\begin{aligned}
(\text{grad } u)^T \cdot A(u) \ &+ \ A(u) \cdot \text{grad } u = (\text{grad } u)^T \cdot A(v) + A(v) \cdot \text{grad } u \\
&= (\text{grad } v)^T \cdot A(v) + A(v) \cdot \text{grad } v + (\text{grad } v_\infty)^T \cdot A(v) + A(v) \cdot \text{grad } v_\infty \\
&= (\text{grad } v)^T \cdot A(v) + A(v) \cdot \text{grad } v + (\text{grad } \omega \times x)^T \cdot A(v) + A(v) \cdot (\text{grad } \omega \times x)
\end{aligned}$$

However

$$\begin{aligned}(\text{grad } \omega \times x)^T \cdot A(v) &+ A(v) \cdot (\text{grad } \omega \times x) \\ &= (\epsilon_{ikm} + \epsilon_{imk})\omega_i \partial_k v_j + (\epsilon_{ikm} + \epsilon_{imk})\omega_i \partial_j v_k \\ &= 0\end{aligned}$$

Therefore it follows that $S(v) = v_\infty \cdot \text{grad } A(u) + \tilde{S}(u)$ $\square$

8.3.1.2 Existence Results.

In this section, we establish the existence of solutions to the equation (8.49) using the Banach fixed point theorem. We define the Banach space $B = \{\psi : ||\psi||_{k+1,q} + ||\text{div } \psi||_t < \infty\}$ and also the subspace G_D of B, such that

$$G_D := \{\psi : ||\psi||_{k+1,q} + ||\text{div } \psi||_t \leq D\}.$$

Lemma 8.3.6 *Let Ω be an exterior domain of class C^{k+5}, $k \geq 0$ and q, t be as defined in Lemma 8.3.2. Also, let the map $\mathcal{A}$ be as defined in equation (8.52). Then, $\mathcal{A}$ maps G_D to G_D.*

Proof:

We define G_D as above and recall that $v = u + v_\infty$. Then it follows from Lemma 8.3.2 that

$$\begin{aligned}||u||_s &+ |u|_{1,r} + |u|_{2,t} + ||\pi||_r + |\pi|_{1,t} \\ + \sum_{m=0}^{k} (|u|_{m+2,q} + |\pi|_{m+1,q}) &\leq c(D + |\xi| + |\omega|) \end{aligned} \tag{8.69}$$

with $r = \frac{3t}{3-t}$, $s = \frac{3t}{3-2t}$ and $c = c(q, t, k, \Omega)$. We can also show without difficulty and using

the estimate (8.69), that

$$||\text{div } N(v,\pi)||_t \leq c_1(||Dv||_{C^0} + ||\pi||_\infty)(||D^2v||_t + ||\text{grad } \pi||_t)$$

$$\leq c_2(D + |\xi| + |\omega|)^2.$$

where we use the fact that $||Dv||_{C^0} \leq ||Du||_{C^0} + |\omega|$. Similarly, using the Sobolev inequality [25, Equation (2.7), p.32] and equation (8.69),

$$\begin{aligned} ||N(v,\pi)||_q &\leq c_3||\text{grad } v||_{C^0}(||A(v)||_q + ||\pi||_q) \\ &\leq c_4||\text{grad } v||_{C^0}(||D^2v||_p + ||\text{grad } \pi||_p), \end{aligned} \tag{8.70}$$

where $\frac{3}{2} < p = \frac{3q}{3+q} < 3$. Furthermore, it is easily verified that

$$||\text{grad } N(v,\pi)||_{k,q} \leq c_5(||Dv||_{C^0(\Omega)} + ||\pi||_\infty)(||D^2v||_{k,q} + ||\text{grad } \pi||_{k,q}). \tag{8.71}$$

Hence, combining equations (8.70), (8.71) and (8.69), we have

$$\begin{aligned} ||N(v,\pi)||_{k+1,q} &\leq c_6(||Dv||_{C^0(\Omega)} + ||\pi||_\infty)(||D^2v||_{\frac{3q}{3+q}} + ||\text{grad } \pi||_{\frac{3q}{3+q}} \\ &+ ||D^2v||_{k,q} + ||\text{grad } \pi||_{k,q}) \\ &\leq c_7(D + |\xi| + |\omega|)^2. \end{aligned} \tag{8.72}$$

In order to fulfill the assumptions of Lemmas 8.3.3 and 8.3.4, we require that

$$\text{We}||\text{grad } v||_{C^k} \leq \delta$$

and also that

$$\text{We}(||\text{div } z||_t + ||z||_{k+1,q}) \leq D$$

which follow from the observations that

$$\begin{aligned} \mathrm{We}||\text{grad } v||_{C^k} &\leq \mathrm{We}(||\text{grad } u||_{C^k} + |\omega|) \\ &\leq \mathrm{We}(D + |\xi| + |\omega|) \leq \delta, \end{aligned} \tag{8.73}$$

and

$$\mathrm{We}(||\text{div } z||_t + ||z||_{k+1,q}) \leq \tilde{c}\mathrm{We}(D + |\xi| + |\omega|)^2 \leq D, \tag{8.74}$$

respectively. Hence, for the choice, $D = \beta(|\xi| + |\omega|)$, for $\beta > 0$, the two conditions are satisfied if $\mathrm{We}(|\xi| + |\omega|) < \frac{\delta}{\beta+1}$ and $\mathrm{We}(|\xi| + |\omega|) < \frac{\beta}{(\beta+1)^2}$, respectively. Consequently, for $\mathrm{We}(|\xi| + |\omega|) < \min(\frac{\delta}{\beta+1}, \frac{\beta}{(\beta+1)^2})$, we have that $z \in G_D$ and hence $\mathcal{A}$ maps G_D to G_D. $\square$

Lemma 8.3.7 *The mapping $\mathcal{A}$ is a contraction in G_D.*

Proof:

Let z_1 and z_2 be two different solutions to the transport equation (8.54) and let the pairs (v_1, π_1) and (v_2, π_2) be two different solutions to the Stokes problem with corresponding translational and rotation components (ξ, ω). Let us also define

$$\psi := \psi_1 - \psi_2, \ v := v_1 - v_2, \ \pi := \pi_1 - \pi_2, \ z := z_1 - z_2.$$

Then subtracting the equations (8.53) corresponding to the pairs (v_1, π_1) and (v_2, π_2), we have

$$
\begin{aligned}
-\Delta v + \text{grad } \pi &= \text{div } \psi \qquad (8.75)\\
\text{div } v &= 0\\
v &= 0 \text{ on } \partial\Omega\\
\lim_{|x|\to\infty} v(x) &= 0,
\end{aligned}
$$

with corresponding estimate,

$$
\begin{aligned}
||v||_s \;+\; & |v|_{1,r} + |v|_{2,t} + ||\pi||_r + |\pi|_{1,t} + \sum_{m=0}^{k} (|v|_{m+2,q} + |\pi|_{m+1,q})\\
\leq\; & c(||\text{div } \psi||_t + ||\psi||_{k+1,q}) \qquad (8.76)
\end{aligned}
$$

where $r = \frac{3t}{3-t}$, $s = \frac{3t}{3-2t}$ and $c = c(q,t,k)$. Similarly, subtracting the transport equation (8.54) and its divergence, equation (8.66), corresponding to z_1 and z_2, we get upon simplification,

$$
\begin{aligned}
z - \text{We}(v_1 \text{grad } z \;-\; & z(\text{grad } v_1)^T) + \text{We}(z_2(\text{grad } v)^T - v\text{grad } z_2)\\
=\; & \text{We}(N(v_1,\pi_1) - N(v_2,\pi_2)) \qquad (8.77)
\end{aligned}
$$

and

$$
\begin{aligned}
\text{div } z - \text{We } v \cdot \text{grad } (\text{div } z_1) \;+\; & \text{We } v_2 \cdot \text{grad } (\text{div } z)\\
=\; & -\text{Wediv } (N(v_1,\pi_1) - N(v_2,\pi_2)) \qquad (8.78)
\end{aligned}
$$

respectively, where

$$\begin{aligned} N(v_1,\pi_1)-N(v_2,\pi_2) &= (\text{grad } v)^T A(v_1)+(\text{grad } v_2)^T A(v)+(1+\epsilon)A(v)A(v_1) \\ &+ (1+\epsilon)A(v_2)A(v)-\pi\text{grad } v_1-\pi_2\text{grad } v. \end{aligned} \tag{8.79}$$

Then we have the estimates

$$\begin{aligned} ||\text{div } [N(v_1,\pi_1) &- N(v_2,\pi_2)]||_t \leq c(||\text{grad } v_1||_{C^0}+||\pi_2||_\infty+||\text{grad } v_2||_{C^0}+||D^2v_1||_t+||D^2v_2||_t \\ &+ |||\text{grad } \pi_2||_t)(||\text{grad } v||_{C^0}+||\pi||_\infty+|D^2v||_t+||\text{grad } \pi||_t) \end{aligned}$$

and

$$\begin{aligned} |||[N(v_1,\pi_1)-N(v_2,\pi_2)]||_{k+1,q} &\leq c(||\text{grad } v_1||_{C^0}+||\text{grad } v_2||_{C^0}+||\pi_2||_\infty+||D^2v_1||_{k,q} \\ +||D^2v_2||_{k,q}+||\text{grad } \pi_2||_{k,q} &+ ||D^2v_1||_{\frac{3q}{3+q}}+||D^2v_2||_{\frac{3q}{3+q}}+||\text{grad } \pi_2||_{\frac{3q}{3+q}})(||\text{grad } v||_{C^0} \\ +||\pi||_\infty+||D^2v||_{k,q} &+ ||D^2v||_{\frac{3q}{3+q}}+||\text{grad } \pi||_{k,q}+||\text{grad } \pi||_{\frac{3q}{3+q}}) \end{aligned} \tag{8.80}$$

upon suitable application of the Sobolev inequality.[25]

The estimates for the transport equation (8.77), employing also equation (8.80) is then

given by

$$
\begin{aligned}
||\text{div } z||_t \;+\; & ||z||_{k+1,q} \leq c\text{We}(||\text{grad } v_1||_{C^0} + ||\text{grad } v_2||_{C^0} + ||\pi_2||_\infty + ||D^2 v_1||_{k,q} + ||D^2 v_2||_{k,q} \\
+\; & ||\text{grad } v_2||_{k,q} + ||\pi_2||_\infty + ||D^2 v_1||_t + ||D^2 v_2||_t + |||\text{grad } \pi_2||_t + ||D^2 v_1||_{\frac{3q}{3+q}} \\
+\; & ||D^2 v_2||_{\frac{3q}{3+q}} + ||\text{grad } \pi_2||_{\frac{3q}{3+q}})(||\text{grad } v||_{C^0} + ||\pi||_\infty + |D^2 v||_t + ||\text{grad } \pi||_t \\
+\; & ||\text{grad } v||_{C^0} + ||\pi||_\infty + ||D^2 v||_{k,q} + ||\text{grad } \pi||_{k,q} + ||D^2 v||_{\frac{3q}{3+q}} + ||\text{grad } \pi||_{\frac{3q}{3+q}}) \\
\leq\; & c\text{We}(||\text{grad } v_1||_{C^0} + ||\text{grad } v_2||_{C^0} + ||\pi_2||_\infty + ||D^2 v_1||_{k,q} + ||D^2 v_2||_{k,q} \\
+\; & ||\text{grad } \pi_2||_{k,q} + ||\pi_2||_\infty + ||D^2 v_1||_t + ||D^2 v_2||_t + |||\text{grad } \pi_2||_t + ||D^2 v_1||_{\frac{3q}{3+q}} \\
+\; & ||D^2 v_2||_{\frac{3q}{3+q}} + ||\text{grad } \pi_2||_{\frac{3q}{3+q}})(||\text{div } \psi||_t + ||\psi||_{k+1,q}) \\
\leq\; & c\text{We}(||\text{div } \psi_1||_t + ||\psi_1||_{k+1,q} + ||\text{div } \psi_2||_t + ||\psi_2||_{k+1,q} + 2|\xi| \\
+\; & 2|\omega|)(||\text{div } \psi||_t + ||\psi||_{k+1,q}) \\
\leq\; & \hat{c}\text{We}(D + |\xi| + |\omega|)(||\text{div } \psi||_t + ||\psi||_{k+1,q}). \qquad (8.81)
\end{aligned}
$$

Therefore, combining the results of equations (8.82) and (8.81), and recognizing that $\hat{c}\text{We}(D+|\xi|+|\omega|) < 1$, from the results of Lemma 8.3.6, we have that $\mathcal{A}$ is a contraction. $\square$

We are now in a position to prove the main result of this section.

Theorem 8.3.1 *Let Ω be an exterior domain of class C^{k+5}, $k \geq 0$ and ξ, $\omega \in R^3$. Also, let $q > 3$ and $1 < t < \frac{3}{2}$. Then, there is a $c > 0$, such that if $We(|\xi| + |\omega|) < c$, the problem (8.49) has a unique solution (v, π) where*

$$u \in \tilde{D}^{2,t}(\Omega) \cap [\cap_{m=0}^{k} D^{m+2,q}(\Omega)]$$

$$\pi \in D^{1,t}(\Omega) \cap [\cap_{m=0}^{k} D^{m+1,q}(\Omega)]$$

satisfying the estimate,

$$\begin{aligned} ||u||_s &+ |u|_{1,r} + |u|_{2,t} + ||\pi||_r + |\pi|_{1,t} + \sum_{m=0}^{k}(|u|_{m+2,q} + |\pi|_{m+1,q}) \\ &\leq C(|\xi| + |\omega|) \end{aligned} \tag{8.82}$$

where $r = \frac{3t}{3-t}$, $s = \frac{3t}{3-2t}$, $C = C(q,t,k)$ *and* $v = u + \xi + \omega \times x$.

Proof:

The proof of this theorem follows from the above Lemmas 8.3.2, 8.3.3 and 8.3.7 and the Banach Fixed Point theorem. □

8.4 Application to Particle Sedimentation

8.4.1 Formulation of Problem to First Order in We.

In the previous parts of this paper, we have established the existence of solutions (u, π, ξ, ω, g) to the problem (8.49) corresponding to the freefall of a rigid body of arbitrary shape in a Second order liquid. In this section, we shall specialize the relevant equations (8.55)-(8.57) to study the terminal orientation of rigid bodies in the Second order fluid. We shall follow the argument outlined in[31,79] and consider, for our rigid body, several different symmetries. We employ the heuristic idea proposed by Joseph & Feng[39] that the terminal orientation of elongated bodies in liquids are a result of competing inertial and viscoelastic torques acting on the body. Since our analysis assumes a zero Reynolds number flow, we need to obtain our equations upto first order in We. We therefore write

$$v = v_s + \tilde{v},\ \pi = \pi_s + \tilde{\pi}$$

where (v_s, π_s) are the solutions to the Stokes problem and which asymptotically approaches a rigid body motion. Additionally we also define $u = u_s + \tilde{u}$ where $v_s = u_s + v_\infty$. Hence

substituting this formulation in equation (8.49) we have that $(\tilde{v}, \tilde{\pi})$ satisfies

$$\left.\begin{aligned} -\Delta\tilde{v} + \text{grad } \tilde{\pi} &= We\text{div } S(v,\epsilon) \\ \tilde{v}|_{\Sigma} &= 0, \\ \text{div } \tilde{v} &= 0, \\ \lim_{|x|\to\infty}\tilde{v} &= 0. \end{aligned}\right\} \tag{8.83}$$

So, in order to obtain the relevant equation at first order in We, we evaluate the freefall equations at v_s and establish that there are several remnant terms which are of $O(We^2)$ and hence can be ignored in our analysis. More specifically, we must show the following properties:

Lemma 8.4.1 *Let $\mathcal{B}$ be a body of class C^3. Then there exist positive numbers $We_0 = We_0(\mathcal{B}, \epsilon)$, $C_i = C_i(\mathcal{B}, D, k, q, t)$ $(i = 1, 2, 3)$, such that for any $0 < We < We_0$, $\frac{3}{2} < q_1 < \infty$, $k \geq 0$, $1 < t < 3/2$ and $q > 3$, we have*

1. $||v - v_s||_X \leq C_1 We$,
2. $||\tilde{S}(u) - \tilde{S}(u_s)||_{q_1} \leq C_2 We$,
3. $|\mathcal{N}_1 + \mathcal{N}_2| \leq C_3 We$.

where $\mathcal{N}_1 = \mathcal{F}(v) - \mathcal{F}(v_s)$ and $\mathcal{N}_2 = \mathcal{M}(v) - \mathcal{M}(v_s)$.

Proof of Property 1:

From the Stokes estimates that we had earlier, we have

$$\begin{aligned} ||\tilde{v}||_s \;+\; & ||\tilde{\pi}||_m + ||\text{grad } \tilde{v}||_m + ||\text{grad } \tilde{\pi}||_t + ||D^2\tilde{v}||_t \\ +\; & ||D^2\tilde{v}||_{k,q} + ||\text{grad } \tilde{\pi}||_{k,q} \leq cWe(||\text{div } S(v)||_t + ||\text{div } S(v)||_{k,q}) \end{aligned} \tag{8.84}$$

The final estimates on $S(v)$ follows from our arguments earlier in this paper regarding estimates of the transport equation. Based on the results of Lemma 8.3.4 and Theorem 8.3.1,

it is therefore easily verified that

$$\begin{aligned} ||\text{div } S(v)||_t \;+\; ||\text{div } S(v)||_{k+1,q} &\leq c_1(||\text{grad } v||_{C^0} + ||\pi||_\infty + ||D^2 v||_{k,q} + ||D^2 v||_t \\ &+ ||D^2 v||_{\frac{3q}{3+q}})(||\text{grad } v||_{C^0} + ||\pi||_\infty + |D^2 v||_t + ||\text{grad } \pi||_t \\ &+ ||\pi||_\infty + ||D^2 v||_{k,q} + ||\text{grad } \pi||_{k,q} + ||D^2 v||_{\frac{3q}{3+q}} + ||\text{grad } \pi||_{\frac{3q}{3+q}}) \\ &\leq c_2(||u||_X + ||\pi||_X + |\omega|)^2 \leq c_3(|\xi| + |\omega|)^2 \leq C_1(\mathcal{B}, D, k, q, t). \end{aligned} \tag{8.85}$$

Proof of Property 1 of Lemma 8.4.1 follows. □

Proof of Property 2:

Let us write $\tilde{S}(u) = \tilde{S}_0(u) + \tilde{S}_1(u)$ where $\tilde{S}_0(u) = u \cdot \text{grad } A(u)$ and $\tilde{S}_1(u)$ is the remaining term. Similarly, we may write $\tilde{S}(u_s) = \tilde{S}_0(u_s) + \tilde{S}_1(u_s)$. Then,

$$\begin{aligned} \tilde{S}_0(u) - \tilde{S}_0(u_s) &= \tilde{u} \cdot \text{grad } A(u) + u_s \cdot \text{grad } A(\tilde{u}) \\ \Rightarrow ||S_0(u) - S_0(u_s)||_q &\leq ||\tilde{u} \cdot \text{grad } A(u)||_q + ||u_s \cdot \text{grad } A(\tilde{u})||_q \\ &\leq ||D^2 u||_q ||\tilde{u}||_\infty + ||D^2 \tilde{u}||_q ||u_s||_\infty. \end{aligned}$$

Similarly, we can obtain estimates for the remaining terms. Hence,

$$\begin{aligned} ||\tilde{S}_1(u) - \tilde{S}_1(u_s)||_q &\leq ||\epsilon A(u)A(\tilde{u}) + \epsilon A(\tilde{u})A(u) + (\text{grad } \tilde{u})^T A(u) \\ &+ (\text{grad } u)^T A(\tilde{u}) + \text{grad } u\, A(\tilde{u}) + \text{grad } \tilde{u}\, A(u)||_q \\ &\leq c_3(||Du||_{C^0} + ||D^2 u||_{\frac{3q}{3+q}})(||D\tilde{u}||_{C^0} + ||D^2 \tilde{u}||_{\frac{3q}{3+q}}). \end{aligned}$$

Finally combining the above estimates, we have

$$||\tilde{S}(u) - \tilde{S}(u_s)||_q \leq c_4 ||\tilde{u}||_X \leq C_2(\mathcal{B}, D, k, q, t) We$$

with $q > 3/2$, upon using the results of Property 1. $\Box$

Proof of Property 3:

For proof of the final property, we need to make some preliminary definitions. We define

$$\mathcal{N}_1 = \mathcal{F}(v) - \mathcal{F}(v_s) = -\int_\Omega [S(v) - S(v_s)] : D(h^{(i)})$$

and

$$\mathcal{N}_2 = \mathcal{M}(v) - \mathcal{M}(v_s) = -\int_\Omega [S(v) - S(v_s)] : D(H^{(i)})$$

where $i = 1, 2, 3$. Let us also define

$$\tilde{H}^{(i)} = \begin{cases} h^{(i)} & , \, i = 1, 2, 3 \\ H^{(i)} & , \, i = 4, 5, 6. \end{cases} \tag{8.86}$$

It then follows that

$$\begin{aligned} |\mathcal{N}_1 + \mathcal{N}_2| &\leq \int_\Omega |S(v) - S(v_s)||D(\tilde{H}^{(i)})| \\ &\leq \int_\Omega |\tilde{S}(u) - \tilde{S}(u_s)||D(\tilde{H}^{(i)})| + \int_\Omega |v_\infty \cdot \text{grad } A_1(\tilde{u})||D(\tilde{H}^{(i)})| \\ &\leq (1 + |\xi|)||\tilde{S}(u) - \tilde{S}(u_s)||_2||D(\tilde{H}^{(i)})||_2 + c_1|\omega|||\frac{1}{x}||_3||D^2\tilde{u}||_{\frac{3}{2}} \\ &\leq c_2||\tilde{u}||_X \leq C_3(\mathcal{B}, D, k, q, t)We \end{aligned} \tag{8.87}$$

where we use the fact that $||\text{grad } \tilde{H}^{(i)}||_s < \infty$ for $s > \frac{3}{2}$ from the Stokes estimates and also Property 2. Therefore, we have our desired result. $\Box$

In light of these above results, we note that the equations for force and torque are given by

$$K \cdot \xi + C \cdot \omega = m_e g + We\mathcal{F}(v_s) + O(We^2) \tag{8.88}$$

$$C^\dagger \cdot \xi + \Omega \cdot \omega = R \times g + We[\mathcal{M}(v_s)] + O(We^2). \tag{8.89}$$

where the higher order terms in We can be ignored. Also, note that we can write

$$\begin{aligned} \mathcal{F}(v_s) &= \int_\Omega \{v_s \cdot \text{grad } \Delta v_s + \text{div } [(\text{grad } v_s)^T A(v_s)] + (1+\epsilon)\text{div } [A(v_s)A(v_s)]\} \cdot h^{(i)} \\ &= \mathcal{F}_1(v_s) + (1+\epsilon)\mathcal{F}_2(v_s) \end{aligned} \tag{8.90}$$

$$\begin{aligned} \mathcal{M}(v_s) &= \int_\Omega \{v_s \cdot \text{grad } \Delta v_s + \text{div } [(\text{grad } v_s)^T A(v_s)] + (1+\epsilon)\text{div } [A(v_s)A(v_s)]\} \cdot H^{(i)} \\ &= \mathcal{M}_1(v_s) + (1+\epsilon)\mathcal{M}_2(v_s). \end{aligned} \tag{8.91}$$

We have managed to separate out the two cases dealt in Sections 8.1 and 8.3. Therefore, when $\epsilon = -1$, we obtain $\mathcal{F}(v_s) = \mathcal{F}_1(v_s)$ and $\mathcal{M}(v_s) = \mathcal{M}_1(v_s)$ which have the explicit forms given in equations (8.28) and (8.29), respectively. However, when ϵ is arbitrary, then $\mathcal{F}(v_s)$ and $\mathcal{M}(v_s)$ assume the form given above. In the latter case, it may not be possible to simplify these terms any further.

Writing $v_s = \xi_i h^{(i)} + \omega_i H^{(i)}$, we can express the viscoelastic terms in the simple form

$$\begin{aligned} \mathcal{F}(v_s) &= \xi_i\xi_j(A_{Tk}^{(i,j)} + (1+\epsilon)U_{Tk}^{(i,j)}) + \omega_i\omega_j(B_{Tk}^{(i,j)} + (1+\epsilon)V_{Tk}^{(i,j)}) \\ &+ \xi_i\omega_j(C_{Tk}^{(i,j)} + (1+\epsilon)W_{Tk}^{(i,j)}) \end{aligned} \tag{8.92}$$

$$\begin{aligned} \mathcal{M}(v_s) &= \xi_i\xi_j(A_{Rk}^{(i,j)} + (1+\epsilon)U_{Rk}^{(i,j)}) + \omega_i\omega_j(B_{Rk}^{(i,j)} + (1+\epsilon)V_{Rk}^{(i,j)}) \\ &+ \xi_i\omega_j(C_{Rk}^{(i,j)} + (1+\epsilon)W_{Rk}^{(i,j)}) \end{aligned} \tag{8.93}$$

so when $\epsilon = -1$, we revert back to the case studied in Section 8.1. Here, $A^{(i,j)}_{Rk}$, $A^{(i,j)}_{Tk}$, $B^{(i,j)}_{Rk}$, $B^{(i,j)}_{Tk}$, $C^{(i,j)}_{Rk}$ and $C^{(i,j)}_{Tk}$ are as defined in equations (8.27). Additionally, we also define

$$\begin{aligned}
\mathbf{U}^{(i,j)}_T &= \int_\Omega h^{(k)} \cdot \text{div } [A(h^{(i)})A(h^{(j)})] \\
\mathbf{V}^{(i,j)}_T &= \int_\Omega h^{(k)} \cdot \text{div } [A(H^{(i)})A(H^{(j)})] \\
\mathbf{W}^{(i,j)}_T &= \int_\Omega h^{(k)} \cdot \text{div } [A(h^{(i)})A(H^{(j)}) + A(H^{(i)})A(h^{(j)})] \\
\mathbf{U}^{(i,j)}_R &= \int_\Omega H^{(k)} \cdot \text{div } [A(h^{(i)})A(h^{(j)})] \\
\mathbf{V}^{(i,j)}_R &= \int_\Omega H^{(k)} \cdot \text{div } [A(H^{(i)})A(H^{(j)})] \\
\mathbf{W}^{(i,j)}_R &= \int_\Omega H^{(k)} \cdot \text{div } [A(h^{(i)})A(H^{(j)}) + A(H^{(i)})A(h^{(j)})].
\end{aligned} \tag{8.94}$$

8.4.2 Viscoelastic Contribution to Torque under Different Symmetries

In this section we shall follow the argument in[36] to study the possible steady falls of $\mathcal{B}$ under different symmetry conditions. The motion of bodies of arbitrary shape has been well studied in the Stokes approximation. A thorough account of this phenomenon is given in.[36] Experiments on fall of isometric bodies, such as tetrahedra, cubes, octahedra etc., in the Stokes case, have also been performed by Pettyjohn and Christiansen.[62] They observe that the bodies freefalling in the Stokes regime keep their initial orientation.

In this section we shall focus on how the viscoelastic force and torque coefficients simplify under different geometric symmetry conditions. We note that the terms $\mathcal{F}$ and $\mathcal{M}$ as defined in equations (8.92) and (8.93) can be treated as third order tensors in the indices i, j and k. Let us now define two classes of tensors

$$\mathcal{U} = \{\mathbf{A}^{(i,j)}_T, \mathbf{B}^{(i,j)}_T, \mathbf{C}^{(i,j)}_R, \mathbf{U}^{(i,j)}_T, \mathbf{V}^{(i,j)}_T, \mathbf{W}^{(i,j)}_R\}$$

and

$$\mathcal{V} = \{\mathbf{A}_R^{(i,j)}, \mathbf{B}_R^{(i,j)}, \mathbf{C}_T^{(i,j)}, \mathbf{U}_R^{(i,j)}, \mathbf{V}_R^{(i,j)}, \mathbf{W}_T^{(i,j)}\}.$$

We shall show that elements of $\mathcal{U}$ transform like tensors while elements of $\mathcal{V}$ transform like pseudo-tensors.

Lemma 8.4.2 *Let Q be a third order tensor. Then $Q \in \mathcal{U}$ transforms as a tensor according to the rule*

$$Q_{ijk} = a_{il}a_{jm}a_{kn}Q_{lmn}$$

whereas $Q \in \mathcal{V}$ transform as a pseudo-tensor which is given by

$$Q_{ijk} = |a|a_{il}a_{jm}a_{kn}Q_{lmn}$$

Proof:

We must begin with the observation that the translational and rotational fields (ξ, $h^{(i)}$) and (ω, $H^{(i)}$) behave as vectors and pseudo-vectors respectively. It then follows from equations (8.92) and (8.93) that in order for the *energy* defined by[36]

$$\xi \cdot K \cdot \xi + \omega \cdot \Omega \cdot \omega + 2\xi \cdot C \cdot \omega - m_e g \cdot \xi - \mathrm{We}\xi \cdot \mathcal{F}(v) - \mathrm{We}\omega \cdot \mathcal{M}(v) \tag{8.95}$$

to be a scalar, elements of $\mathcal{U}$ must transform as tensors while those of $\mathcal{V}$ must transform as pseudo-tensors. □

Note that, in addition to the symmetries mentioned above, the terms $A_{Tk}^{(i,j)}$ and $A_{Rk}^{(i,j)}$ are symmetrical under exchange of indices i and j. We shall now consider the different symmetry conditions and their effect upon these terms.

8.4.2.1 Reflection Symmetry. Let us consider, for definiteness, reflection symmetry in

the x_2x_3 plane. The corresponding transformation can be represented by the matrix, $[a]$ given as

$$[a] = \begin{pmatrix} -1 & 0 & 0 \\ 0 & 1 & 0 \\ 0 & 0 & 1 \end{pmatrix}$$

Under this transformation $I \in \mathcal{U}$ and $J \in \mathcal{V}$ have the following symmetries

$$\begin{aligned} I_1^{(1,1)} &= I_1^{(2,2)} = I_1^{(3,3)} = I_1^{(2,3)} = I_1^{(3,2)} = I_2^{(1,2)} = I_2^{(2,1)} = I_2^{(1,3)} \\ &= I_2^{(3,1)} = I_3^{(1,2)} = I_3^{(2,1)} = I_3^{(1,3)} = I_3^{(3,1)} = 0. \end{aligned} \tag{8.96}$$

$$\begin{aligned} J_1^{(1,2)} &= J_1^{(2,1)} = J_1^{(1,3)} = J_1^{(3,1)} = J_2^{(1,1)} = J_2^{(2,2)} = J_2^{(3,3)} = J_2^{(2,3)} \\ &= J_2^{(3,2)} = J_3^{(1,1)} = J_3^{(2,2)} = J_3^{(3,3)} = J_3^{(2,3)} = J_3^{(3,2)} = 0 \end{aligned}$$

Similarly, reflection symmetry about the remaining two planes can be obtained by a simple permutation of the above results. For an orthotropic body which has three symmetry planes about each axis such as a rectangular block,[36] the symmetries simplify tremendously to give us the following result

Lemma 8.4.3 *For orthotropic bodies the viscoelastic force and torque coefficients must obey the following conditions*

$$\begin{aligned} A_{Tk}^{(i,j)} = B_{Tk}^{(i,j)} &= C_{Rk}^{(i,j)} = 0 \\ U_{Tk}^{(i,j)} = V_{Tk}^{(i,j)} &= W_{Rk}^{(i,j)} = 0 \end{aligned}$$

for all i, j, k *and*

$$A^{(i,j)}_{Rk} = B^{(i,j)}_{Rk} = C^{(i,j)}_{Tk} = 0$$
$$U^{(i,j)}_{Rk} = V^{(i,j)}_{Rk} = W^{(i,j)}_{Tk} = 0$$

for any two i, j *or* k *equal.*

8.4.2.2 Skew Symmetry. Skew-Symmetry refers to invariance under rotation by $\theta = \pi$ without reflection symmetry.[36] The corresponding transformation about the x_1 axis may be represented by the matrix

$$[a] = \begin{pmatrix} 1 & 0 & 0 \\ 0 & -1 & 0 \\ 0 & 0 & -1 \end{pmatrix}$$

giving rise to the same symmetries (since for bodies with skew symmetry, $det(a) = 1$) as equation $(8.96)_2$ for $Q \in \mathcal{U}, \mathcal{V}$. Symmetries about the other axes can be obtained by a straightforward permutation of the above results.

8.4.2.3 Rotational Symmetry. By Rotational Symmetry, we refer to invariance under rotation by any angle θ.[36] For convenience, we choose $\theta = \pi/2$. The corresponding rotation matrix for invariance about the x_1 axis is given by

$$[a] = \begin{pmatrix} 1 & 0 & 0 \\ 0 & 0 & -1 \\ 0 & 1 & 0 \end{pmatrix}$$

This transformations yields the same relations as for the case of skew symmetry. In

addition, it also gives

$$\begin{aligned} Q_1^{(2,3)} + Q_1^{(3,2)} &= 0, \quad Q_2^{(3,1)} + Q_3^{(2,1)} = 0, \quad Q_3^{(1,2)} + Q_2^{(1,3)} = 0 \\ Q_2^{(1,2)} - Q_3^{(1,3)} &= 0, \quad Q_2^{(2,1)} - Q_3^{(3,1)} = 0, \quad Q_1^{(2,2)} - Q_1^{(3,3)} = 0 \end{aligned} \tag{8.97}$$

for $Q \in \mathcal{U}, \mathcal{V}$. Since the terms $A_{Tk}^{(i,j)}$ and $A_{Rk}^{(i,j)}$ also have additional symmetries in i and j, we have in addition to equation (8.97),

$$A_{M1}^{(2,3)} = A_{M1}^{(3,2)} = 0,$$

where $M = T, R$. We shall employ the above symmetries to find simplifications for geometries with *fore-aft symmetry* (that is, orthotropic with rotational symmetry about a single axis[36]), *spherical isotropy* (orthotropic with rotational symmetry about all three axes[36]), helicoidal symmetry and helicoidal isotropy.

Lemma 8.4.4 *If $\mathcal{B}$ is a body with fore-aft symmetry, then the following conditions hold:*

$$\begin{aligned} A_{Tk}^{(i,j)} = B_{Tk}^{(i,j)} &= C_{Rk}^{(i,j)} = 0 \\ U_{Tk}^{(i,j)} = V_{Tk}^{(i,j)} &= W_{Rk}^{(i,j)} = 0 \end{aligned}$$

for all i, j and k and

$$\left.\begin{aligned} A_{R1}^{(2,3)} = A_{R1}^{(3,2)} &= 0, \quad A_{R2}^{(3,1)} + A_{R3}^{(2,1)} = 0, \quad A_{R3}^{(1,2)} + A_{R3}^{(1,3)} = 0 \\ B_{R1}^{(2,3)} + B_{R1}^{(3,2)} &= 0, \quad B_{R2}^{(3,1)} + B_{R3}^{(2,1)} = 0, \quad B_{R3}^{(1,2)} + B_{R2}^{(1,3)} = 0 \\ C_{T1}^{(2,3)} + C_{T1}^{(3,2)} &= 0, \quad C_{T2}^{(3,1)} + C_{T3}^{(2,1)} = 0, \quad C_{T3}^{(1,2)} + C_{T2}^{(1,3)} = 0 \\ U_{R1}^{(2,3)} + U_{R1}^{(3,2)} &= 0, \quad U_{R2}^{(3,1)} + U_{R3}^{(2,1)} = 0, \quad U_{R3}^{(1,2)} + U_{R2}^{(1,3)} = 0 \\ V_{R1}^{(2,3)} + V_{R1}^{(3,2)} &= 0, \quad V_{R2}^{(3,1)} + V_{R3}^{(2,1)} = 0, \quad V_{R3}^{(1,2)} + V_{R2}^{(1,3)} = 0 \\ W_{T1}^{(2,3)} + W_{T1}^{(3,2)} &= 0, \quad W_{T2}^{(3,1)} + W_{T3}^{(2,1)} = 0, \quad W_{T3}^{(1,2)} + W_{T2}^{(1,3)} = 0 \end{aligned}\right\} \tag{8.98}$$

Lemma 8.4.5 *If $\mathcal{B}$ is a body with spherical isotropy, then in addition to the symmetries of a fore-aft body, we have*

$$A_{Rk}^{(i,j)} = 0$$

and

$$\left.\begin{aligned} B_{R1}^{(2,3)} = -B_{R1}^{(3,2)} = B_{R2}^{(3,1)} = -B_{R3}^{(2,1)} = B_{R3}^{(1,2)} = -B_{R2}^{(1,3)} \\ C_{T1}^{(2,3)} = -C_{T1}^{(3,2)} = C_{T2}^{(3,1)} = -C_{T3}^{(2,1)} = C_{T3}^{(1,2)} = -C_{T2}^{(1,3)} \\ U_{R1}^{(2,3)} = -U_{R1}^{(3,2)} = U_{R2}^{(3,1)} = -U_{R3}^{(2,1)} = U_{R3}^{(1,2)} = -U_{R2}^{(1,3)} \\ V_{R1}^{(2,3)} = -V_{R1}^{(3,2)} = V_{R2}^{(3,1)} = -V_{R3}^{(2,1)} = V_{R3}^{(1,2)} = -V_{R2}^{(1,3)} \\ W_{T1}^{(2,3)} = -W_{T1}^{(3,2)} = W_{T2}^{(3,1)} = -W_{T3}^{(2,1)} = W_{T3}^{(1,2)} = -W_{T2}^{(1,3)} \end{aligned}\right\} \tag{8.99}$$

8.4.2.4 Helicoidal Symmetry. We define a body with helicoidal symmetry to be one which is invariant under rotation by $\theta = \pi/2$ but without reflection symmetry.[36] In this subsection we shall consider a special object called the *Isotropic Helicoid*, referring to bodies which possesses helicoidal symmetry about two mutually perpendicular axes. Specific means of constructing objects with this geometry are mentioned in [36, p.152]. For such a body, translational and rotational motions are coupled and it cannot perform one without the other.

Lemma 8.4.6 *Consider a body $\mathcal{B}$ with helicoidal isotropic symmetry and with x_1 and x_2 as the rotational axes, then the members of $\mathcal{U}$ and $\mathcal{V}$ must satisfy*

$$A_{Tk}^{(i,j)} = 0, \quad A_{Rk}^{(i,j)} = 0$$

and all other coefficients must satisfy

$$Q_1^{(2,3)} = Q_3^{(1,2)} = Q_2^{(3,1)} = -Q_1^{(3,2)} = -Q_3^{(2,1)} = -Q_2^{(1,3)}$$

and

$$\begin{aligned} Q_2^{(1,2)} - Q_3^{(1,3)} &= Q_2^{(2,1)} - Q_3^{(3,1)} = Q_1^{(2,2)} - Q_1^{(3,3)} = 0 \\ Q_3^{(2,3)} - Q_1^{(2,1)} &= Q_3^{(3,2)} - Q_1^{(1,2)} = Q_2^{(3,3)} - Q_2^{(1,1)} = 0 \end{aligned}$$

for $Q \in \mathcal{U}, \mathcal{V}$.

8.4.3 Spin-Free Terminal States of $\mathcal{B}$

The difficulty in obtaining flows past bodies of different geometries further makes it difficult, if at all possible, to explicitly calculate the integrals in equations (8.27) and (8.94) for our problem. The only calculation that we can perform is for a sphere or an ellipsoid. However, a simpler method to explicit calculation, lies in studying the motion without rotation, which is referred to in[36] as the *spin-free* state. In this section we shall analyze the conditions for which bodies, with different symmetries, sedimenting in a Second order fluid can have only translational motions, that is, for which $\omega = 0$. A similar problem, in the Newtonian case, has been studied in[36] and a sufficient condition is provided for pure translational motion.

It is shown in[36] that every body, intrinsically possesses a point called the *center of hydrodynamic reaction* at which $C = C^{\dagger}$. For some of the geometries that we consider in this paper such as the sphere, orthotropic bodies and bodies with fore-aft symmetry, the origin of $\mathcal{B}$ coincides with the center of reaction. The reason for introducing this *center of hydrodynamic reaction* point is to make the coupling tensor symmetric while the translation and rotation tensors are inherently symmetric at all points.

Theorem 8.4.1 *A sufficient condition for a body* $\mathcal{B}$*, of class* $\mathcal{C}^3$*, of arbitrary shape under-*

going slow, steady, spin-free fall in a Second order fluid is given by

$$\begin{aligned} m_e C^\dagger \cdot K^{-1} \cdot g &- R \times g + We\xi_i\xi_j\{C \cdot K^{-1}(A_{Tk}^{(i,j)} + (1+\epsilon)U_{Tk}^{(i,j)}) \\ &- (A_{Rk}^{(i,j)} + (1+\epsilon)U_{Rk}^{(i,j)})\} = 0. \end{aligned} \tag{8.100}$$

Proof:

We employ the fact that the tensor K is invertible to solve equation (8.55) for ξ. Thus,

$$\xi = m_e K^{-1} \cdot g - K^{-1} \cdot C \cdot \omega + We K^{-1} \cdot \mathcal{F} \tag{8.101}$$

Substituting this in equation (8.57), setting $\omega = 0$ and upon some rearrangement, we obtain equation (8.100). □

This theorem can be exploited to study the steady freefalls of $\mathcal{B}$ under different symmetry conditions. In particular, the theorem reveals the orientation of $\mathcal{B}$ in its steady state. In the Stokes case, as discussed earlier, it has been experimentally observed that the body tends to retain its initial orientation for all times. However, we shall see that this is not always the case for a Second order liquid. Using the symmetry properties of $\mathcal{B}$, from the earlier section, we analyze bodies for which this difference from the Stokes problem becomes apparent.

8.4.3.1 Sphere. The equation (8.100) is non-trivially satisfied if $A_{Tk}^{(i,j)}$, $U_{Tk}^{(i,j)}$, $A_{Rk}^{(i,j)}$ and $U_{Rk}^{(i,j)}$ are zero for each i. We observe from Lemma 8.4.5 that this occurs for homogeneous bodies with spherical symmetry (for which $C = 0$). In the inhomogeneous case, the condition tells us that $R \times g = 0$, which suggests that the body will translate with R either parallel or anti-parallel to the direction of gravity, as is intuitively expected. The former position is stable while the latter is unstable. Therefore we see that for these bodies condition (8.100) for purely translational motion is the same as for the Stokes flow.

8.4.3.2 Orthotropic Bodies.

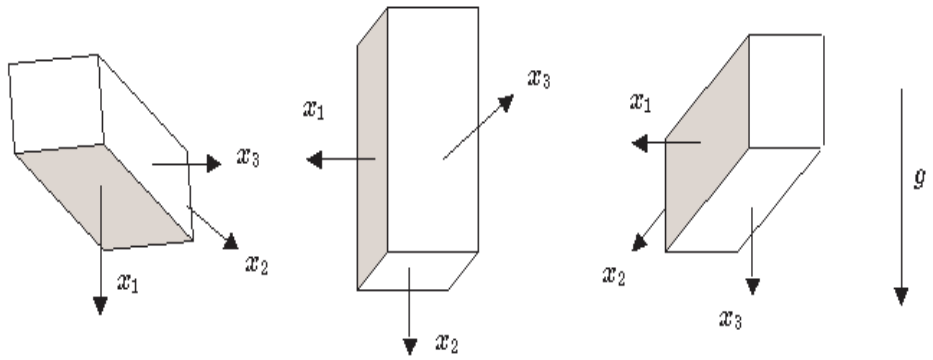

Figure 8.1. Orientation of Orthotropic bodies.

For an orthotropic body we have that $A_{Tk}^{(i,j)} = 0$ and also $C = 0$. Then from [79, Lemma 5], the condition (8.100) reduces to

$$\begin{aligned} R \times g &+ We(\xi_2\xi_3(A_{R1}^{(2,3)} + (1+\epsilon)U_{R1}^{(2,3)}) + \xi_2\xi_3(A_{R1}^{(2,3)} + (1+\epsilon)U_{R1}^{(3,2)}))\hat{\mathbf{e}}_1 \\ (\xi_1\xi_3(A_{R1}^{(1,3)} &+ (1+\epsilon)U_{R1}^{(1,3)}) + \xi_1\xi_3(A_{R1}^{(1,3)} + (1+\epsilon)U_{R1}^{(3,1)}))\hat{\mathbf{e}}_2 \\ (\xi_2\xi_1(A_{R1}^{(2,1)} &+ (1+\epsilon)U_{R1}^{(2,1)}) + \xi_2\xi_1(A_{R1}^{(2,1)} + (1+\epsilon)U_{R1}^{(1,2)}))\hat{\mathbf{e}}_3 = 0. \end{aligned} \tag{8.102}$$

So when the body is homogeneous, equation (8.102) is satisfied if either (a) $A_{R1}^{(2,3)} = A_{R3}^{(1,2)} = A_{R2}^{(1,3)} = \mathrm{U}_{R1}^{(2,3)} = U_{R3}^{(1,2)} = U_{R2}^{(1,3)} = 0$, (b) $\xi_2 = \xi_3 = 0$, (c) $\xi_1 = \xi_3 = 0$, or (d) $\xi_1 = \xi_2 = 0$. Cases (b), (c) and (d) imply that motion must occur only along the x_1, x_2 or x_3 directions respectively

(Figure 8.1). When $\mathcal{B}$ is inhomogeneous, the body can sediment with orientations other than along the three basis directions. The possible cases are more complicated and the reader is referred to[79] for a detailed discussion.

8.4.3.3 Bodies with Fore-Aft Symmetry.

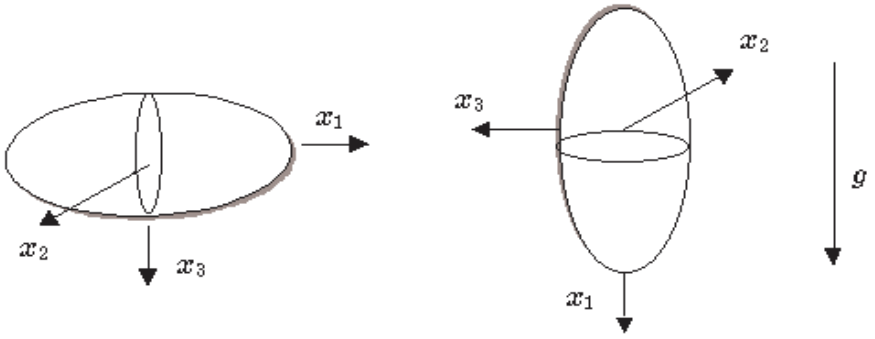

Figure 8.2. Orienation of bodies with fore-aft symmetry.

Bodies with fore-aft symmetry have *three symmetry planes and ones axis of rotational symmetry.* For such bodies, $C \equiv 0$, therefore on using [79, Lemma 6], the condition (8.100) becomes

$$\begin{aligned} R \times g \quad &+ \quad We(\xi_1\xi_3(A_{R1}^{(1,3)} + (1+\epsilon)U_{R1}^{(1,3)}) + \xi_1\xi_3(A_{R1}^{(1,3)} + (1+\epsilon)U_{R1}^{(3,1)}))\hat{\mathbf{e}}_2 \\ (\xi_2\xi_1(A_{R1}^{(2,1)} \quad &+ \quad (1+\epsilon)U_{R1}^{(2,1)}) + \xi_2\xi_1(A_{R1}^{(2,1)} + (1+\epsilon)U_{R1}^{(1,2)}))\hat{\mathbf{e}}_3 = 0. \end{aligned} \tag{8.103}$$

Note that we have chosen the axis of symmetry to lie along x_1, without any loss of generality. When $\mathcal{B}$ is homogeneous, equation (8.103) holds if (a) $A_{R2}^{(1,3)} = A_{R2}^{(1,3)} = \mathrm{U}_{R2}^{(1,3)} = U_{R2}^{(1,3)} = 0$, (b) $\xi_1 = 0$ or (c) $\xi_2 = \xi_3 = 0$. Condition (b) suggests that the body is moving along the x_2x_3 plane and (c) says that the body moves along the x_1 direction. Once again the case when the body is inhomogeneous, will not be dealt with here. The reader is referred to[79] for details regarding the inhomogeneous case.

A more powerful tool for analyzing the terminal orientations of sedimenting bodies will be discussed in the next chapter. The arguments of this chapter reveal the complex nature of the problem. However, we are still able to obtain some preliminary information regarding the orientations of rigid bodies, by elegant geomertic arguments alone.

8.4.4 Stability

This section discusses the stability for bodies with orthotropic symmetries(with $R = 0$). This body has been, by far the most interesting case examined in this paper. A simple argument based on the perturbation of the torque acting on the body due to the purely viscoelastic part of the fluid is used to obtain some qualitative information about stability and instability of the terminal motion.

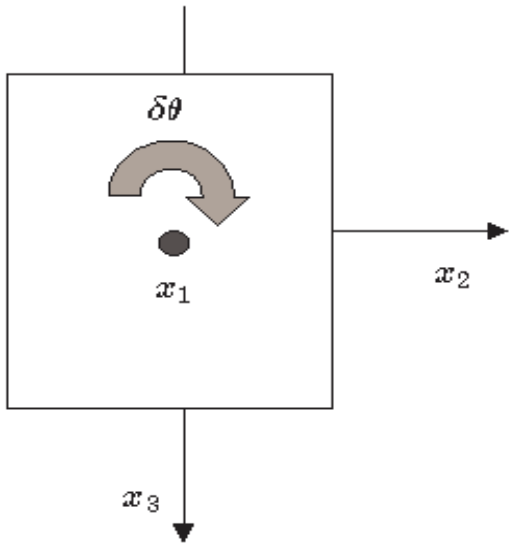

Figure 8.3. Perturbation of an orthotropic body about its equilibrium configuration ($\theta = 0$).

It can be seen easily that the components of the velocity field (with $|\xi| = 1$) are given by

$$\xi_1 = \text{Cos}\phi\ \text{Sin}\theta, \quad \xi_2 = \text{Sin}\phi\ \text{Sin}\theta, \quad \xi_3 = \text{Cos}\theta \tag{8.104}$$

in the spherical coordinate system. Putting these in the equation (8.102) we get the components of the torque on the body due to the viscoelastic part of the fluid $\mathcal{F}$, namely,

$$\mathbf{M} = \gamma_1 \text{Sin}2\theta\ \text{Sin}\phi\mathbf{e}_1 + \gamma_2 \text{Sin}2\theta\ \text{Cos}\phi\mathbf{e}_2 + \gamma_3 \text{Sin}\theta^2\ \text{Sin}2\phi\mathbf{e}_3 \tag{8.105}$$

where

$$\gamma_k = \frac{1}{2}(A^{(i,j)}_{Rk} + (1+\epsilon)U^{(i,j)}_{Rk})$$

with $k = 1, 2, 3$. Holding ϕ fixed such that Sinϕ and Cosϕ are both positive, we can consider three different cases of orientations of the body. The first case is when the body is restricted to move in the x_2 and x_3 directions only. Therefore $\xi_1 = 0$ (Figure 8.3) and

$$\mathbf{M} = \gamma_1 \text{Sin}2\theta \ \text{Sin}\phi \mathbf{e}_1.$$

Hence the equilibrium position, i.e. where the torque is zero occurs when $\theta = 0$ or $\frac{\pi}{2}$. The only meaningful perturbation here is one of the form $\delta\theta \ \mathbf{e}_1$ since we are now restricted to the x_2x_3 plane. Therefore,

$$\mathbf{M} \cdot \delta\theta \mathbf{e}_1 = \gamma_1 \text{Sin}2\theta \ \text{Sin}\phi \delta\theta. \tag{8.106}$$

If $\delta\theta > 0$ then we say that the body is in a stable position, if the resulting work done is negative, i.e. in the opposite direction to the perturbation. Thus in the above equation, since Sin2θ is positive for small enough perturbations, the condition for stability is $\gamma_1 < 0$. If, however $\gamma_1 > 0$, then the position of the body is unstable and the torque will force the body out of this equilibrium state.

Secondly, if the motion is restricted to the x_1 and x_3 directions ($\xi_2 = 0$), and if the pertubation is of the form $\delta\theta \ \mathbf{e}_2$, then again for a small positive perturbation, the condition for stability reduces to $\gamma_2 < 0$. Using a similar argument to the final case when the motion is along the x_1x_2 plane only ($\xi_3 = 0$), we obtain the restriction $\gamma_3 < 0$ for stability. Note that the equilibruim states in the second and third cases also occurs when $\theta = 0$ or $\frac{\pi}{2}$. Since stability for this problem seems to be linked to the sign of the terms γ_k, it must be noted that it is not physically viable for all of these terms to be positive, since, then each of the equilibrium positions will be unstable.

The argument made above can also be specialized to bodies with fore-aft symmetry. For such bodies, the equilibrium configurations at $\theta = 0$ and $\frac{\pi}{2}$ are consistent with the results of Galdi[28] and stability of the configuration, as in the case of orthotropic bodies, depends upon the sign of the coefficients γ_2 and γ_3.

9.0 FREEFALL IN A SECOND ORDER FLUID AT FIRST ORDER IN RE AND WE

In this chapter we test the heuristic explanation of Joseph and Feng[39] to examine the orientation phenomenon. Already, in the previous chapter we have seen that even upon ignoring the inertial effects, we are able to correctly predict the terminal orientation behavior of rigid bodies in viscoelastic liquids. In this chapter, we consider the effects of inertia, viscoelasticity and shear-thinning in different combinations, by using different liquid models in order to identify the significant cause of the orientation phenomenon. Four different fluid models are studied, Newtonian, Power-Law, Second Order and the Modified Second Order (see Chapter 4 for details). In the previous chapter, we have shown existence and uniques to the problem of freefall in a Second order fluid for $Re = 0$. The existence of solutions (u, p, ξ, g) for small, non-zero Re is also proved in.[28] In this chapter, perform a rigorous analysis of the terminal orientation behavior of freefalling bodies in different liquids. Also, we assume for the rest of this chapter that the sedimenting body is homogeneous ($R = 0$), possesses fore-aft symmetry and that the motion is purely translational ($\omega = 0$).

Since the experiments in literature and our own, in fact, exhibit the orientation phenomenon at very small values of Re and We, it is sufficient to consider the theory at first order in these parameters. Furthermore, to examine the orientation behavior, it is sufficient that we consider simply the translational motion of the body. Therefore, setting $\omega = 0$ in the equations (7.15), the equation of motion in non-dimensional form are given by

$$\left.\begin{array}{c} \text{Re } u \cdot \ \text{grad}(u) = \text{div } T(u,p) + g \\ \text{div } (u) = 0 \\ u = 0 \text{ at } \partial\Omega \\ \lim_{|x|\to\infty}(u(x) + \xi) = 0 \end{array}\right\} \tag{9.1}$$

where, we write the stress tensor as

$$T(u,p) = T_N(u,p) + \lambda T_E(u)$$

where T_N is the Newtonian part of the stress tensor and T_E is the extra stress tensor which can stand for the viscoelastic contribution to the stress, for instance. T_N is given by the well known formula, $-pI + 2\eta D(u)$, while T_E would vary depending on the chosen fluid model. Also, λ here represents the significant material parameter corresponding to the fluid model. Multiplying equation $(9.1)_1$ by $H^(i)$, integrating by parts over Ω and after several rearrangements, we obtain the equation

$$\int_\Sigma (e_i \times x) \cdot T(u) \cdot n = 2\int_\Omega D(u) : D(H^{(i)}) + \mathrm{Re}\ \int_\Omega u \cdot\ \mathrm{grad}(u) \cdot \mathbf{H}^{(i)} + \lambda \int_\Omega T_E(u) : D(H^{(i)}) \tag{9.2}$$

where

$$-e_i \cdot \int_\Sigma x \times T(u,p) \cdot n = \mathcal{M}, \tag{9.3}$$

the net torque, the first term on the right hand side of equation (9.2)

$$2\int_\Omega D(u) : D(H^{(i)}) = \mathcal{M}^S \tag{9.4}$$

is the torque in the Stokes approximation (i.e. with $\mathrm{Re} = 0$ and $\lambda = 0$,

$$-\int_\Sigma u \cdot \mathrm{grad}\ u \cdot H^{(i)} = \mathcal{M}^I, \tag{9.5}$$

is the inertial contribution to the torque and

$$-\int_\Omega T_E(u) : D(H^{(i)}) = \mathcal{M}^E \tag{9.6}$$

is the extra-stress contribution to the torque. Hence, we have now managed to isolate the

net torque into independent contributions due to inertia and additional effects. In order to simplify the argument, motivated by the fact that the motions of the paricle and liquid are in the creeping flow regime, we write field, $u = u_s + w(Re, We)$ where u_s is the stokes velocity field. Hence, the net torque is given as

$$\mathcal{M}(u) = \mathcal{M}^S(u_s) + Re\mathcal{M}^I(u_s) + \lambda\mathcal{M}^E(u_s) + \mathcal{N}(u_s, w).$$

Here $\mathcal{N}(u_s, w)$ depends on higher order terms in Re and We, which we show rigorously for certain models. Therefore, ignoring the term $\mathcal{N}(u_s, w)$, at first order in Re and We, we have

$$\mathcal{M} = \mathcal{M}^{0,S} + Re\mathcal{M}^{0,I}(u_s) + \lambda\mathcal{M}^{0,E}(u_s).$$

In the final part of this analysis, we write without loss of generality,

$$u_s = \xi_1 h^{(1)} + \xi_2 h^{(2)} = |\xi| \left(h^{(1)} \sin\theta + h^{(2)} \cos\theta\right).$$

Hence, the net torque is finally given by

$$\mathcal{M} = \mathcal{M}^{0,S}(\theta) + Re\mathcal{M}^{0,I}(\theta) + \lambda\mathcal{M}^{0,E}(\theta).$$

At equilibrium, the net torque must be zero. Therefore setting $\mathcal{M} = 0$ and analyzing the explicit dependence of the inertial and extra torque terms upon θ reveals the possible steady orientations of the body in different liquid media. We analyze these results and more in following sections for four different fluid models.

9.1 Newtonian Fluid

Recall that the Newtonain stress tensor is given by

$$T(u, p) = T_N(u, p) = -pI + 2\eta D(u). \tag{9.7}$$

As seen from the above discussion, the net torque, at first order in Re, upon a rigid body may be given by

$$\mathcal{M} = \mathcal{M}^{0,S}(u_s) + Re\mathcal{M}^{0,I}(u_s)$$

where

$$\begin{aligned} \mathcal{M}^{0,S}(u_s) &= 2\int_\Omega D(\xi_1 h^{(1)} + \xi_2 h^{(2)}) : D(H^{(i)}) \\ &= 2\int_\Omega D(u_s) : D(H^{(i)}) \end{aligned} \tag{9.8}$$

and

$$\begin{aligned} \mathcal{M}^{0,I}(u_s) &= -\int_\Sigma u_s \cdot \text{grad } u_s \cdot H^{(i)} \\ &= -\int_\Sigma (\xi_1 h^{(1)} + \xi_2 h^{(2)}) \cdot \text{grad } (\xi_1 h^{(1)} + \xi_2 h^{(2)}) \cdot H^{(i)}. \end{aligned} \tag{9.9}$$

The symmetry of the body, allows us to simplify the torque contributions significantly. We make two important observations which are proved in the form of Lemmas below.

Lemma 9.1.1 *Let $\mathcal{B}$ be a homogeneous body with fore-aft symmetry and the fields $(h^{(i)}, p^{(i)})$ and $(H^{(i)}, P^{(i)})$ for $i = 1, 2, 3$ be as defined in equations (3.3) and (3.4). Then we have the following results:*

1. $\mathcal{M}_i^{0,S}(u_s) = 0$ *for* $i = 1, 2, 3$.
2. $\mathcal{M}_j^{0,I}(u_s) = 0$ *for* $j = 1, 2$.
3. $\mathcal{M}_3^{0,I}(u_s) = \int_\Sigma (h^{(1)} \cdot grad\ h^{(2)} + h^{(2)} \cdot grad\ h^{(1)}) \cdot H^{(3)}$.

Proof:

Proof of this Lemma follows from invoking the symmetries introduced in the Lemma 3.4.3.

For the first result, we observe that

$$(\xi_1 D(\mathbf{h}^{(1)}) \quad + \quad \xi_2 D(\mathbf{h}^{(2)})) : D(\mathbf{H}^{(1)}) \in \mathcal{C}_3^s, \tag{9.10}$$

$$(\xi_1 D(\mathbf{h}^{(1)}) \quad + \quad \xi_2 D(\mathbf{h}^{(2)})) : D(\mathbf{H}^{(2)}) \in \mathcal{C}_3^s, \tag{9.11}$$

$$(\xi_1 D(\mathbf{h}^{(1)}) \quad + \quad \xi_2 D(\mathbf{h}^{(2)})) : D(\mathbf{H}^{(3)}) \in \mathcal{C}_2^s. \tag{9.12}$$

Therfore, since the integral of odd functions over a symmetric domain must vanish, we have that $\mathcal{M}^{0,S}(u_s) = 0$. Similarly, in order to prove our second result, we note that

$$(h^{(1)} \cdot \text{grad } h^{(1)} \quad + \quad h^{(1)} \cdot \text{grad } h^{(2)}) \cdot H^{(1)} + (h^{(1)} \cdot \text{grad } h^{(1)} + h^{(1)} \cdot \text{grad } h^{(2)}) \cdot H^{(2)} \in \mathcal{C}_8^s$$

$$(h^{(2)} \cdot \text{grad } h^{(2)} \quad + \quad h^{(2)} \cdot \text{grad } h^{(1)}) \cdot H^{(1)} + (h^{(2)} \cdot \text{grad } h^{(2)} + h^{(2)} \cdot \text{grad } h^{(1)}) \cdot H^{(2)} \in \mathcal{C}_9^s$$

$$(h^{(1)} \cdot \text{grad } h^{(1)} \quad + \quad h^{(2)} \cdot \text{grad } h^{(2)}) \cdot H^{(3)} \in \mathcal{C}_{10}^s$$

Therefore, integrating in the region exterior to the body, we note that the only surviving term is

$$\int_\Sigma (h^{(1)} \cdot \text{grad } h^{(2)} + h^{(2)} \cdot \text{grad } h^{(1)}) \cdot H^{(3)}.$$

□

In light of this Lemma, we write the net torque as

$$\begin{aligned} \mathcal{M}(u) &= -Re\xi_1\xi_2 \int_\Sigma (h^{(1)} \cdot \text{grad } h^{(2)} + h^{(2)} \cdot \text{grad } h^{(1)}) \cdot H^{(3)} \\ &= -Re|\xi|^2 \mathcal{G}_I \sin\theta\cos\theta \end{aligned} \tag{9.13}$$

where

$$\mathcal{G}_I = \int_\Sigma (h^{(1)} \cdot \text{grad } h^{(2)} + h^{(2)} \cdot \text{grad } h^{(1)}) \cdot H^{(3)}. \tag{9.14}$$

Evaluation of the integral was performed using a numerical integration package in the Mathematica software (Wolfram Inc.) for different values of the eccentricity e. It was found that $\mathcal{G}_I$ is always negative except at 0 and 1, where it becomes zero. Table 9.1 summarizes the findings.

Table 9.1. Tabulations of computed torque coefficient $\mathcal{G}_I$versus eccentricity e.

e	$\mathcal{G}_I$
0	0.000
0.05	-0.005
0.10	-0.021
0.20	-0.085
0.30	-0.189
0.40	-0.328
0.50	-0.493
0.60	-0.673
0.70	-0.851
0.80	-0.995
0.90	-1.042
0.95	-0.976
0.98	-0.007

So, since $\mathcal{G}_I(e) \neq 0$ in general,

$$\mathcal{M}(u) \;\; = \;\; -Re|\xi|^2\mathcal{G}_I \sin\theta\cos\theta = 0$$

implies that either, $\theta = 0$ or $\theta = \dfrac{\pi}{2}$. Therefore, the particle can align in two ways only as expected. Further implications of this analysis are summarized in the following Theorem.

Theorem 9.1.1 *Let $\mathcal{B}$ be a body of revolution about the major axis, a, with fore-aft symmetry. Then there is a $Re_0 > 0$ depending only upon the geometric properties of the body such that for all $0 < Re < Re_0$, the only possible translational steady falls are those with 'a' either parallel or perpendicular to the direction of gravity. Furthermore, in both cases, ξ is parallel*

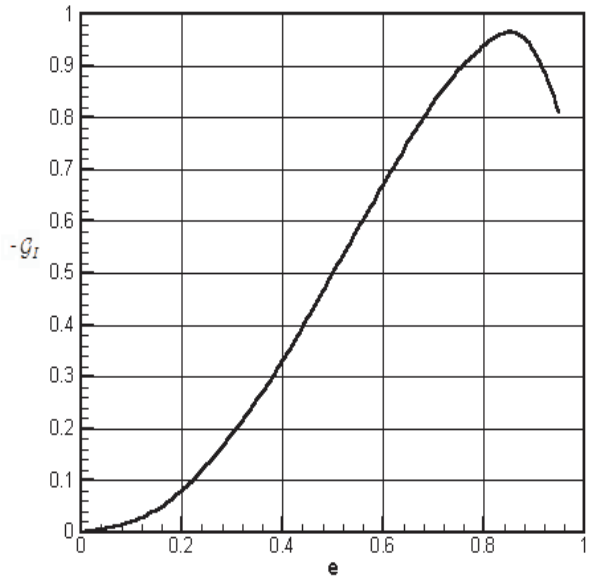

Figure 9.1. Numerical evaluation of $\mathcal{G}_I$ versus eccentricity of the prolate spheroid .

to g with $\xi \cdot g > 0$.

Proof:

The proof of the existence of the two steady falls follows from our earlier arguments and equation (9.15). For the existence of the critical value Re_0 and the relation $\xi \cdot g > 0$, see [27, Theorem 5.1]. □

9.2 Power-Law Fluid

For the Power-law model, T(u,p) is given by

$$\begin{aligned} T(u,p) &= -p\mathbf{I} + \lambda[D(u) : D(u)]^{\frac{n-1}{2}} D(u) \\ &= T_P(p) + \lambda T_{PL}(u) \end{aligned} \tag{9.15}$$

where λ above represents a non-dimensional parameter, related to η, that characterizes the shear-thinning nature of the liquid. Repeating the calculations performed in the earlier section, we obtain Hence, we have, in short

$$\mathcal{M} = \mathcal{M}^S(u) + \mathrm{Re}\mathcal{M}^I(u) + \lambda\mathcal{M}^{PL}(u).$$

where the right hand side contains the Stokes, Inertial and Shear-thinning components of the net torque. In order to represent the torques at first order in Re, we write $u = u_S + w^{(27,28,31)}$ where u_S represents the velocity field corresponding to the Stokes problem (i.e. equation for $Re = 0$). As a result, the net torque $\mathcal{M}$, upon using the result of Lemma (9.1.1), becomes

$$\mathcal{M} = \ \mathrm{Re}\ \mathcal{M}^{0,I}u_S + \lambda\mathcal{M}^{0,PL}(u_S) + \mathcal{N}(w) \tag{9.16}$$

where

$$\mathcal{M}_i^{0I}(u_S) \ = \ -\int_\Sigma (h^{(1)} \cdot \mathrm{grad}\ h^{(2)} + h^{(2)} \cdot \mathrm{grad}\ h^{(1)}) \cdot H^{(3)} \tag{9.17}$$

$$\mathcal{M}_i^{0,PL}(u_S) \ = \ -\int_\Omega [D(u_S) : D(u_S)]^{\frac{n-1}{2}} D(u_S) : D(H^{(i)}). \tag{9.18}$$

Here $\mathcal{N}(w)$ represents higher order terms in Reynolds numbers. Our treatment is restricted to a first order effect in Re. Therefore we effectively ignore the term $\mathcal{N}$.

The components of the shear-thinning torque, employing the symmetries above along with equation (9.18), is

$$\mathcal{M}_i^{PL}(u_S) \ = \ -\int_\Omega [D(\xi_1\mathbf{h}^{(1)} + \xi_2\mathbf{h}^{(2)}) : D(\xi_1\mathbf{h}^{(1)} + \xi_2\mathbf{h}^{(2)})]^{\frac{n-1}{2}} D(\xi_1\mathbf{h}^{(1)} + \xi_2\mathbf{h}^{(2)}) : D(\mathbf{H}^{(i)}) \tag{9.19}$$

for $i = 1, 2, 3$. This expression can be further simplified by using the symmetries of the

auxiliary fields and an argument similar to Lemma (9.1.1).

Lemma 9.2.1 *Let $\mathcal{B}$ be a homogeneous body with fore-aft symmetry and the fields $(h^{(i)}, p^{(i)})$ and $(H^{(i)}, P^{(i)})$ for $i = 1, 2, 3$ be as defined in equations (3.3) and (3.4). Then,*

$$\mathcal{M}_i^{PL} = 0$$

for $i = 1, 2, 3$.

Proof:

The components of the shear-thinning or thickening torque, employing the symmetries above along with equation (9.18), is

$$\begin{aligned}
\mathcal{M}_i^{PL}(u_S) &= -\int_\Omega [D(\xi_1\mathbf{h}^{(1)} + \xi_2\mathbf{h}^{(2)}) : D(\xi_1\mathbf{h}^{(1)} + \xi_2\mathbf{h}^{(2)})]^{\frac{n-1}{2}} D(\xi_1\mathbf{h}^{(1)} + \xi_2\mathbf{h}^{(2)}) : D(\mathbf{H}^{(i)}) \\
&= -\int_\Omega [\xi_1^2 D(\mathbf{h}^{(1)}) : D(\mathbf{h}^{(1)}) + \xi_2^2 D(\mathbf{h}^{(2)}) : D(\mathbf{h}^{(2)}) \\
&+ 2\xi_1\xi_2 D(\mathbf{h}^{(1)}) : D(\mathbf{h}^{(2)})]^{\frac{n-1}{2}} \{\xi_1 D(\mathbf{h}^{(1)}) + \xi_2 D(\mathbf{h}^{(2)})\} : D(\mathbf{H}^{(i)}) \qquad (9.20)
\end{aligned}$$

for $i = 1, 2, 3$. Therefore, using definition 3.4.3, we observe that

$$D(\mathbf{h}^{(1)}) : D(\mathbf{h}^{(1)}) \in \mathcal{C}_5^s \quad , \quad D(\mathbf{h}^{(2)}) : D(\mathbf{h}^{(2)}) \in \mathcal{C}_5^s, \quad D(\mathbf{h}^{(1)}) : D(\mathbf{h}^{(2)}) \in \mathcal{C}_5^s \qquad (9.21)$$

and also,

$$D(\mathbf{h}^{(1)}) : D(\mathbf{H}^{(1)}) \in \mathcal{C}_3^s \quad , \quad D(\mathbf{h}^{(2)}) : D(\mathbf{H}^{(1)}) \in \mathcal{C}_4^s, \qquad (9.22)$$

$$D(\mathbf{h}^{(1)}) : D(\mathbf{H}^{(2)}) \in \mathcal{C}_4^s \quad , \quad D(\mathbf{h}^{(2)}) : D(\mathbf{H}^{(2)}) \in \mathcal{C}_3^s, \qquad (9.23)$$

$$D(\mathbf{h}^{(1)}) : D(\mathbf{H}^{(3)}) \in \mathcal{C}_1^s \quad , \quad D(\mathbf{h}^{(2)}) : D(\mathbf{H}^{(3)}) \in \mathcal{C}_2^s. \qquad (9.24)$$

It can easily be verified that the integrand in equation (9.20), has the following symmetries:

$$\dot{\gamma}^{\frac{n-1}{2}}\{\xi_1 D(\mathbf{h}^{(1)}) \;+\; \xi_2 D(\mathbf{h}^{(2)})\} : D(\mathbf{H}^{(i)}) \in \mathcal{C}_7^s$$
$$\dot{\gamma}^{\frac{n-1}{2}}\{\xi_1 D(\mathbf{h}^{(1)}) \;+\; \xi_2 D(\mathbf{h}^{(2)})\} : D(\mathbf{H}^{(3)}) \in \mathcal{C}_6^s$$

where $i = 1, 2$ and

$$\dot{\gamma} = [D(\xi_1\mathbf{h}^{(1)} + \xi_2\mathbf{h}^{(2)}) : D(\xi_1\mathbf{h}^{(1)} + \xi_2\mathbf{h}^{(2)})].$$

On account of these symmetries in equation (9.20), it follows that

$$\mathcal{M}_i^{PL}(u_S) = 0 \tag{9.25}$$

for each $i = 1, 2, 3$. Therefore, the shear-thinning effects contribute nothing towards the torque, at low Re. Note that the argument stated above is independent of the choice of the power $\frac{n-1}{2}$ and therefore applies equally to shear-thickening liquids. $\square$

Hence, in conclusion, employing the Lemmas 9.1.1 and 9.2.1, the net non-zero torque acting on the body $\mathcal{B}$ is given by

$$\mathcal{M}_3 = \text{ -Re}\xi_1\xi_2\mathcal{G}_I = \text{ -Re}|\xi|^2\mathcal{G}_I \sin(\theta)\cos(\theta). \tag{9.26}$$

where we choose, without loss of generality, $\xi = (\xi_1, \xi_2, 0)$ which we further decompose in polar coordinates, with θ measuring the angle between ξ and the horizontal axis. It is seen from equation (9.26) that for the net torque to vanish, $\theta = 0$ or $\dfrac{\pi}{2}$ degrees, just as in the case of a Newtonian fluid. Our results seem to indicate that pure shear-thinning or thickening effects play no role in causing the tilt-angle , at very low Reynolds numbers. In a power-law fluid, the surviving torque is due to inertial effects alone. Hence an ellipsoid, sedimenting in a power-law liquid will orient itself as in a Newtonian liquid.

9.3 Second Order Fluid

In the case of a Second order fluid, the total stress tensor can be given by

$$\begin{aligned} T(u,p) &= T_N(u,p) - \mathrm{We} T_E(u) \\ &= -pI + A_1(u) - \mathrm{We}\left(A_2(u) + \epsilon A_1(u)\cdot A_1(u)\right). \end{aligned} \tag{9.27}$$

See Section 4.6 for the definitions of the tensors A_1 and A_2. As discussed in the above section, we want to evaluate the net torque, in non-dimensional form, at first order in Re and We. The net torque $\mathcal{M}(u)$ appears to be of the form

$$\mathcal{M}(u) = \mathcal{M}^S + \mathrm{Re}\mathcal{M}^I + \mathrm{We}\mathcal{M}^{NN}$$

which is now the sum of the Stokes, inertial and viscoelastic components. If we write $u = u_s + w$, then the net torque, evaluated at u_s may be given by

$$\mathcal{M}(u_s) = \mathcal{M}^{0,S} + Re\mathcal{M}^{0,I}(u_s) + We\mathcal{M}^{0,NN}(u_s) + \mathcal{N}(u,w) \tag{9.28}$$

and

$$\begin{aligned} \mathcal{N}(u,w) &= Re(\mathcal{M}^I(u) - \mathcal{M}^I(u_s)) + We(\mathcal{M}^{NN}(u) - \mathcal{M}^{NN}(u_s)) \\ &= Re\mathcal{N}_1 + We\mathcal{N}_2. \end{aligned} \tag{9.29}$$

Here, $\mathcal{M}^{0,S}(u_s)$ and $\mathcal{M}^{0,I}(u_s)$ are as defined in equations (9.8) and (9.9) and

$$\mathcal{M}^{NN}(u_s) = -\int_\Sigma T_E(u_s) : D(H^{(i)}). \tag{9.30}$$

$$\tag{9.31}$$

It is shown rigorously[28,31] that the nonlinear term

$$|\mathcal{N}(u_s, w)| \leq C(Re^{1+\beta} + We^{1+\gamma})$$

for some positive constants C, β and γ. Therefore, we may ignore this term at first order in Re and We. So, invoking the results of Lemma 9.1.1, the net first order torque is given by

$$\mathcal{M}(u) \;=\; Re\mathcal{M}^{0,I}(u_s) + We\mathcal{M}^{0,NN}(u_s). \tag{9.32}$$

The quantity $\mathcal{M}^{0,I}(u_s)$ is known from the Section 9.1 for a prolate spheroid of varying eccentricities. Now writing $u_s = \xi_1\mathbf{h}^{(1)} + \xi_2\mathbf{h}^{(2)}$ we have

$$\begin{aligned}
\mathcal{M}^{0,NN}(u_s) &= -\int_\Sigma T_E(\xi_1\mathbf{h}^{(i)} + \xi_2\mathbf{h}^{(2)}) : D(H^{(i)}) \\
= -\int_\Sigma [(\xi_1\mathbf{h}^{(i)} &+ \xi_2\mathbf{h}^{(2)}) \cdot \text{grad } A_1(\xi_1\mathbf{h}^{(i)} + \xi_2\mathbf{h}^{(2)}) + A_1(\xi_1\mathbf{h}^{(i)} + \xi_2\mathbf{h}^{(2)}) \cdot \text{grad }^T(\xi_1\mathbf{h}^{(i)} \\
+\xi_2\mathbf{h}^{(2)}) &+ \text{grad } (\xi_1\mathbf{h}^{(i)} + \xi_2\mathbf{h}^{(2)}) \cdot A_1(\xi_1\mathbf{h}^{(i)} + \xi_2\mathbf{h}^{(2)})] : D(H^{(i)}) \\
-\epsilon\int_\Sigma [A_1(\xi_1\mathbf{h}^{(i)} &+ \xi_2\mathbf{h}^{(2)}) \cdot A_1(\xi_1\mathbf{h}^{(i)} + \xi_2\mathbf{h}^{(2)})] : D(H^{(i)}).
\end{aligned} \tag{9.33}$$

We now employ the Definitions 3.4.3 and 3.4.4 to simplify the non-Newtonian contribution to torque in order to make it more tractable. The result is summarized in following Lemma.

Lemma 9.3.1 *Let $\mathcal{B}$ be a homogeneous body with fore-aft symmetry and the fields $(h^{(i)}, p^{(i)})$ and $(H^{(i)}, P^{(i)})$ for $i = 1, 2, 3$ be as defined in equations (3.3) and (3.4). Then,*

1. $\mathcal{M}_1^{0,NN} = \mathcal{M}_2^{0,NN} = 0$.

2. *The only non-zero component of the non-Newtonian torque is given by*

$$\begin{aligned}
\mathcal{M}_3^{0,NN} &= -\xi_1\xi_2\int_\Sigma (h^{(1)} grad\ A_1(h^{(2)}) + h^{(2)} grad\ A_1(h^{(1)}) + A_1(h^{(1)}) \cdot grad\ ^T h^{(2)} \\
&+ A_1(h^{(2)}) \cdot grad\ ^T h^{(1)} + grad\ h^{(1)} \cdot A_1(h^{(2)}) + grad\ h^{(2)} \cdot A_1(h^{(1)}) \\
&+ \epsilon A_1(h^{(1)}) \cdot A_1(h^{(2)}) + \epsilon A_1(h^{(2)}) \cdot A_1(h^{(1)})) : D(H^{(3)})
\end{aligned}$$

Proof:

The explicit calculations for the above results will not be shown here. It suffices to say that the technique to be used is similar to the one employed in Lemmas 9.1.1 and 9.2.1. Then upon suitable application of definitions 3.4.3 and 3.4.4, we have our results. □

In the pages immediately following, we will calculate the non-Newtonian contribution the torque as seen in Table 9.1. In order to do so we must rewrite the viscoelastic part of the torque in a more convenient form to permit ease in computation. We therefore digress a little from the previous arguments to write

$$\mathcal{M}^{0,NN}(u_s) = \frac{1}{2}\int_{\Omega} \text{div } T_E(u_s) \cdot H^{(i)} - \frac{1}{2}\int_{\Sigma} e_i \cdot x \times n \cdot T_E \cdot n. \tag{9.34}$$

To perform our calculation, it is more convenient to write the extra-stress tensor, $T_E(u)$ in a different form.[21] Therefore, we obtain the following useful expressions

$$\begin{aligned} \text{div } T_E(u_s) &= (\Delta\omega_s \times u_s) + \frac{\partial \Delta u_s}{\partial t} + (1+\epsilon)\left\{A_1 \Delta u_s + 2\text{div } \left(\text{grad } (u_s)\text{grad }^T(u_s)\right)\right\}, \\ T_E \cdot n &= \left(-p + |\omega_s|^2)n + \omega_s \times n + (1+\epsilon)|\omega_s|^2|\right)n \end{aligned}$$

where $\omega_s = \text{curl}(u_s)$. With these simplified equations, upon some manipulation, we can express the net viscoelastic contribution to the torque in the form

$$\mathcal{M}^{0,NN}(u_s) = \xi_1 \xi_2 \mathcal{G}_{NN}$$

where the non-Newtonian torque coefficient is of the form

$$\begin{aligned}
\mathcal{G}_{NN} &= \frac{-1}{2}[\int_{\Sigma} x \times n|\omega_s|^2 - (\epsilon+1)[6\int_{\Omega}(H^{(3)} \cdot \nabla h^{(1)} \cdot \Delta h^{(2)} + H^{(3)} \cdot \nabla h^{(2)} \cdot \Delta h^{(1)}) \\
&\quad +2\int_{\Omega}(H^{(3)} \cdot \nabla^T h^{(1)} \Delta h^{(2)} + H^{(3)} \cdot \nabla^T h^{(2)} \Delta h^{(1)}) - \frac{1}{2}\int_{\Sigma} x \times n|\omega_s|^2]] \\
&= \frac{1}{2}\{(1+\frac{\epsilon+1}{2})\int_{\Sigma} x \times n|\omega|^2 - 2(\epsilon+1)[\int_{\Omega}(3H^{(3)} \cdot \nabla h^{(1)} \Delta h^{(2)} \\
&\quad +3H^{(3)} \cdot \nabla h^{(2)} \Delta h^{(1)} + H^{(3)} \cdot \nabla^T h^{(1)} \Delta h^{(2)} + H^{(3)} \cdot \nabla^T h^{(2)} \Delta h^{(1)})]\}. \qquad (9.35)
\end{aligned}$$

We may simplify the equation further by implementing the fact that $\Delta h^{(i)} = \text{grad } p^{(i)}$, from the Stokes equations. Hence

$$\begin{aligned}
\mathcal{G}_{NN} &= \frac{1}{2}((1+\frac{\epsilon+1}{2})\int_{\Sigma} x \times n|\omega_s|^2 - 2(\epsilon+1)[\int_{\Omega}(3H^{(3)} \cdot \nabla h^{(1)} \nabla p_2 \\
&\quad +3H^{(3)} \cdot \nabla h^{(2)} \nabla p_1 + H^{(3)} \cdot \nabla^T h^{(1)} \nabla p_2 + H^{(3)} \cdot \nabla^T h^{(2)} \nabla p_1)]). \qquad (9.36)
\end{aligned}$$

Graphs of the variation of the torque coefficient with eccentricity are shown in Figures 9.2, 9.3 and 9.4. They depict also the variation of the torque coefficients with the parameter ϵ. In fact, we may divide our observations into two categories, one concerning the case $\epsilon > -1$ and a second case, where $-2 < \epsilon < -1$. The essential profile of the curve seems to stay remarkably consistent for each value of the parameter ϵ (see Figure 9.2), changing slightly when $\epsilon > -1$. The magnitude of the coefficients seems to increase with increasing ϵ. It is also interesting to note in Figure 9.3 that as $\epsilon \geq -1$, the torque coefficient changes sign at larger values of e. Specifically, Figure 9.3 considers $\epsilon = -0.7, -0.8$ since the dramatic turn to negative values is more prominent in these cases. It is also worth noting that the curves achieve their peaks at decreasing values of e as ϵ increases. Our calculations seem to match with the lower bounds for ϵ predicted by experiments since the torque becomes negative for $\epsilon > -1$ which is physically meaningless since there is no physically valid reason to believe that the torque should arbitrarily change sign for any specific value of ϵ.

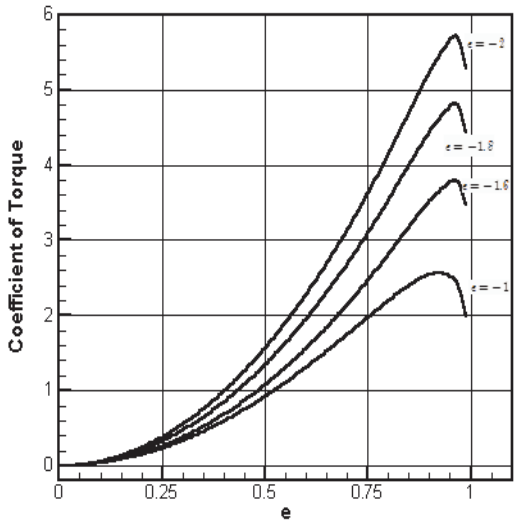

Figure 9.2. Absolute value of torque coefficient versus eccentricity $-2 \leq \epsilon \leq -1$.

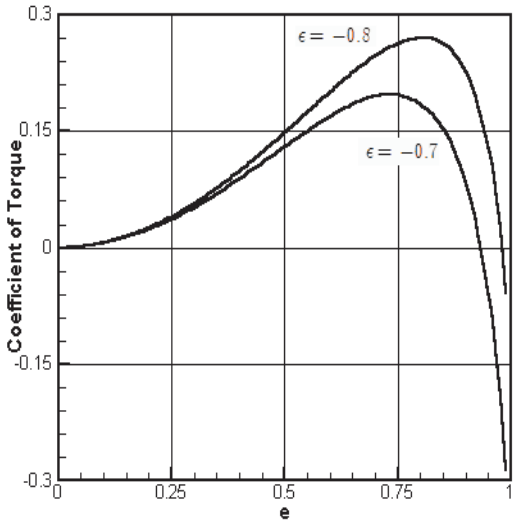

Figure 9.3. Absolute value of torque coefficient versus eccentricity $\epsilon \geq -1$.

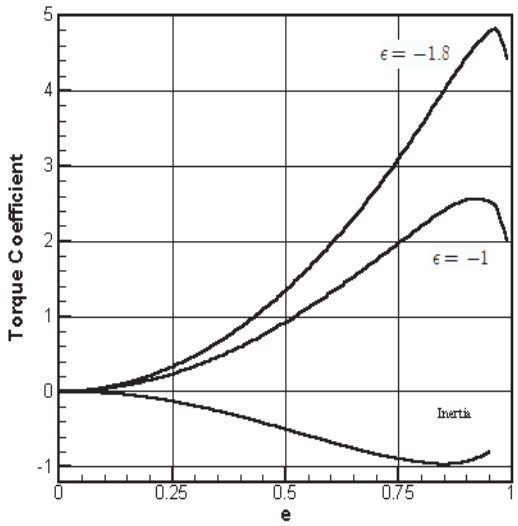

Figure 9.4. Comparison of torques due to Inertial and Viscoelastic effects.

Figure 9.4 compares the inertial effects to the viscoelastic effects for two different values of ϵ. We adopt the recommendation of Joseph and coworkers[37] that $\epsilon = -1.8$. It is obvious that the viscoelastic effects seem to outweigh the inertial ones. This may help explain the experimental observation which we shall discuss in the following section.

Therefore, since in general, $\mathcal{G}_{NN} \neq 0$, the net torque in equilibrium is given by

$$\begin{aligned} Re\mathcal{M}^{0,I} + We\mathcal{M}^{0,NN} &= 0 \\ \Rightarrow |\xi|^2 \left(Re\mathcal{G}_I + We\mathcal{G}_{NN}\right) \sin\theta \cos\theta &= 0. \end{aligned} \tag{9.37}$$

As a result, the equilibrium condition is satisfied if (i) $\theta = 0$, (ii) $\theta = \frac{\pi}{2}$ or (iii) $(Re\mathcal{G}_I + We\mathcal{G}_{NN}) = 0$. The last condition necessarily implies that the first order theory is not sufficient to explain the orientation phenomenon. Therefore, our theory works as long as the condition (iii) is not true. Once again, our argument sufficiently accounts for the steady state orientation of particles in a viscoelastic liquid.

9.4 Stability of Orientation

We have seen from the previous sections, that each of the fluid models allows for more than one steady orientation, while in experiments only one orientation is observed. This demands an analysis of stability of each of the allowed states. With this in mind, we perform a quasi-steady stability analysis. The essential idea is to perturb θ by a small angle, say $\delta\theta$ in the e_3 direction. As a result of this perturbation of this perturbation, if the torque changes sign then we say that the steady orientation is stable. Physically, this change in sign has the implication of returning the body to its original equilibrium position. If however, the torque retains the same sign under the perturbation, then the equilibrium position is unstable and the torque acts away from it to the nearest stable state. Mathematically, we state these conditions as follows:

$$\frac{d(\mathcal{M}\cdot e_3)}{d\theta}|_{\theta=\theta_0} < 0 \qquad \Rightarrow \text{Stability} \tag{9.38}$$

$$\frac{d(\mathcal{M}\cdot e_3)}{d\theta}|_{\theta=\theta_0} > 0 \qquad \Rightarrow \text{Instability} \tag{9.39}$$

We verify the stability of the terminal orientation of bodies in the different fluid models by means of the Figures 9.5 and 9.6 below. The Figure 9.5 indicates the variation of $\mathcal{M}^{0,I}$ with θ while the second Figure 9.6 is a plot of $\mathcal{M}^{0,NN}$ versus θ. The two graphs are shown for a specific value of the eccentricity for the ellipsoid, however the result is true for any choice of e. Also, we choose $|\xi| = 1$ without loss of generality.

The stability analysis indicates the following:

1. In the case of the Newtonian fluid, the figure 9.5 indicates that $\frac{d\mathcal{M}^I}{d\theta} < 0$ when $\theta = 0$. Hence $\theta = 0$ degrees is the stable orientation. Since we have shown that the resulting torque in a Power-Law fluid is the same as in a Newtonian fluid, it follows that the stable orientation for steady fall in a Power-Law fluid is also $\theta = 0$ degrees.

2. In the case of a Second-order fluid, Figure 9.6 indicates that $\frac{d\mathcal{M}^I}{d\theta} < 0$ when $\theta = \frac{\pi}{2}$, hence the stable steady orientation in the case of a viscoelastic liquid is 90 degrees.

Therefore, our results match perfectly with experimental observations.

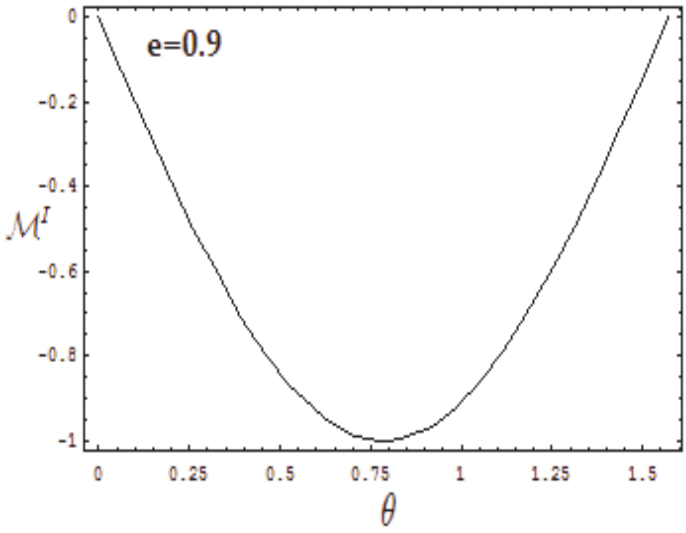

Figure 9.5. Variation of Newtonian torque with θ at $e = 0.9$ and $Re = 1$.

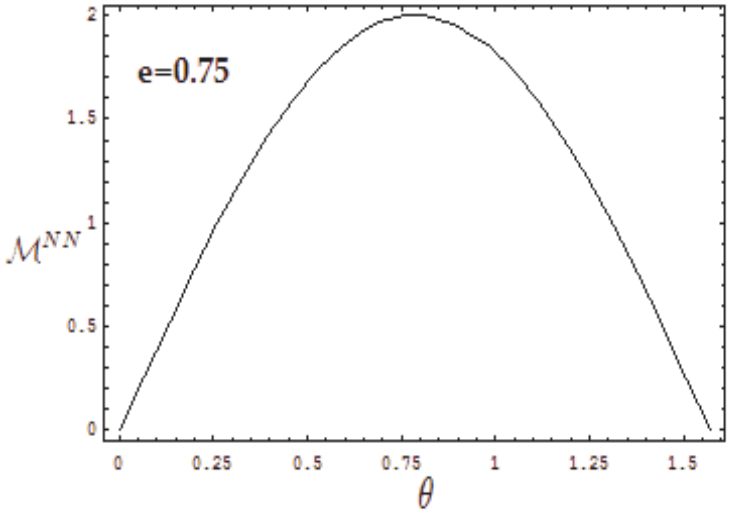

Figure 9.6. Variation of viscoelastic torque with θ at $e = 0.75$ and $We = 1$.

9.5 Comparison with Experiments

We have shown in the previous sections that qualitatively our first order torque argument is sufficient to explain the stable orientations in the different fluid modes considered. However, it would be interesting to see how our theory matches quantitatively with experimental observations. The comparison with experiments are made with the Second order fluid model alone since this is the most interesting case. We recognize that the experimental liquids possess shear-thinning properties while the Second order liquid model would perhaps be more appropriate for modeling a Boger fluid, however the lack of any experimental studies on Boger fluids and numerical calculation of torques with shear-thinning liquids forces us to make comparisons with existing results. This however can still be fruitful in guiding us towards more appropriate treatments in the future.

We define the critical ratio,

$$\gamma_{cr} = \frac{Re|\mathcal{G}_I|}{We\mathcal{G}_{NN}} = 1. \tag{9.40}$$

When the ratio exceeds γ_{cr}, then inertia dominates and the spheroid falls horizontally (i.e. $\theta_{tilt} = 0$), while when the ratio is less than γ_{cr}, Viscoelastic effects dominate and the spheroid falls vertically (i.e. $\theta_{tilt} = 90$). Figure 9.7 shows the critical curves for varying eccentricities. However, when $\gamma_{cr} = 1$, the first order theory fails and we must resort to a second order argument.

The critical curves are seen to be lines of varying slopes for the different e's. Qualitatively, since $\mathcal{G}_{NN}$ is seen to be much larger than $\mathcal{G}_I$ (Figure 9.4), varying the ratio of Re and We would determine the final orientation of the body. For the body to acquire the horizontal state, Re would have to far exceed We.

We shall now make a comparison of our results with experimental observations. This is done in two stages. Firstly we shall make a comparative study with the observations in the

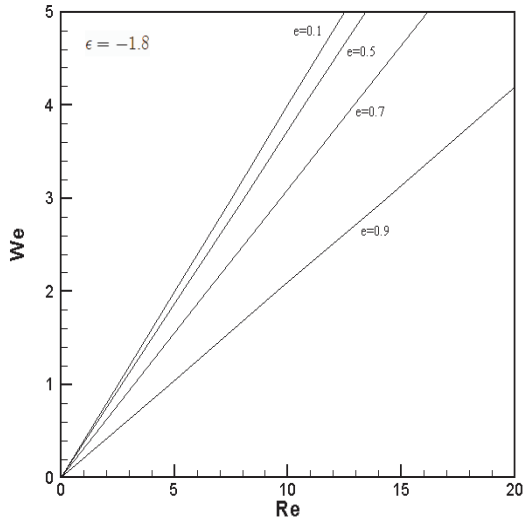

Figure 9.7. Critical ratios of Inertial versus Viscoelastic Torques for varying eccentricities.

literature and secondly we shall test the theory with our experimental data from Chapter 6. Joseph and coworkers have observations of the tilt angle for varying materials, Re and We. It must be mentioned that the experiments were performed using prolate spheroids and cylinders with flat and rounded edges whereas the theoretical calculations were performed for ellipsoidal objects. Therefore, the eccentricities of the cylinders used in the experiments have been approximately evaluated using the formula $e = \sqrt{1 - \frac{D^2}{L^2}}$ where D is the diameter of the cylinder and L, the length.

Figures 9.8, 9.9 and 9.10 show how experimental observations match with our calculations. Comparisons have been shown for three different values of ϵ indicated on the plot. The expect to give an idea of how predictions of the experiment get better with increasing values of ϵ. The observed tilt angles are mentioned besides the plotted points. The dashed line indicates the critical ratio γ_{cr}. If the observations lie above the line then the predicted tilt angle is $\theta_{tilt} = 0$, otherwise $\theta_{tilt} = 90$.

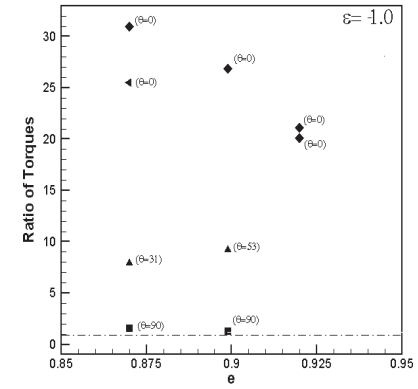

Figure 9.8. Comparison with experimental data for $\epsilon = -1.0$.

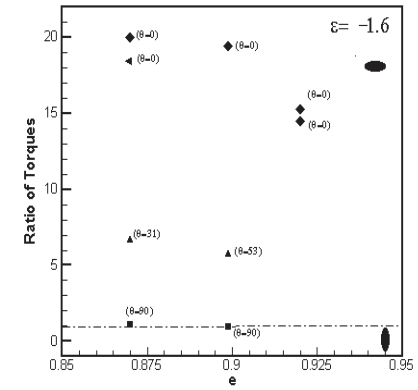

Figure 9.9. Comparison with experimental data for $\epsilon = -1.6$.

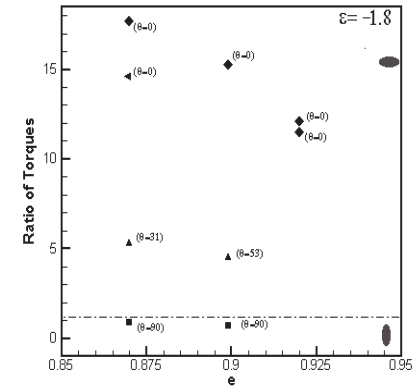

Figure 9.10. Comparison with experimental data for $\epsilon = -1.8$.

It is seen from the figures above that the predictions progressively seem to get better, with increasing ϵ. For the case when $\epsilon = -1$ the ratio of the two torques is not quite large enough. However at $\epsilon = -1.8$ the experimental data all fall in the correct category of the graph. As mentioned earlier, the model fails to account for the tilt angle. The two observed cases of tilt angle (namely of 53^o and 31^o) fall above the critical line for each off the cases. The calculations here seem to suggest that the $\epsilon = -1.8$ model does better to explain the model than the $\epsilon = -1$ model. However as is evident a better model is required to verify and explain the tilt angle phenomenon.

Finally, we make a comparison of the theoretical predictions with our own experiments. The results of this comparison are shown in the Figures 9.11 and 9.12 in the following page and are made for $\epsilon = -1.8$ alone. As in the case of the earlier figures, the plots show the ratio of inertial to viscoelastic torques versus the eccentricity of the body. It must be pointed out that eccentricities of the particles used in this comparison was between 0.85-0.90, with the majority of the particles having $e = 0.87$. Certain particles with e close to 1 were ignored due to difficulty in obtaining the torque coefficients near $e = 1$. As in the earlier graphs, we do not distinguish between the particles with different symbols. Instead we make separate graphs for the different liquid samples used. The angles mentioned besides the points are the observed terminal angles. It is easily seen that from the plots that the data points fall in the correct category, except for a point in the CMC(0.75%) sample whose torque ratio far exceeds 1 but has a terminal angle of 90 degrees contrary to expectation. Also, the tilt angle observations in the same sample cannot be explained. Possible reasons for errors have been discussed in the earlier, experimental chapter and can be attributed to errors in experiments and not to our theory. Besides this case, the other points are well explained by our theory.

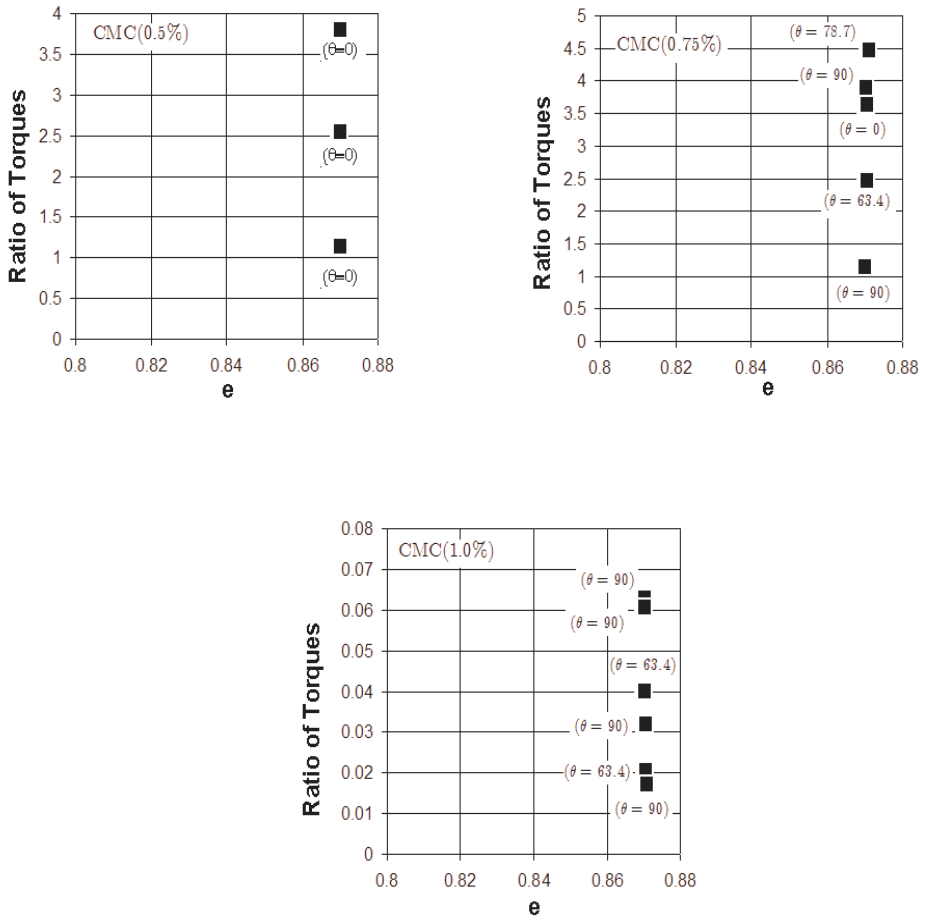

Figure 9.11. Comparison of our experimental data for CMC.

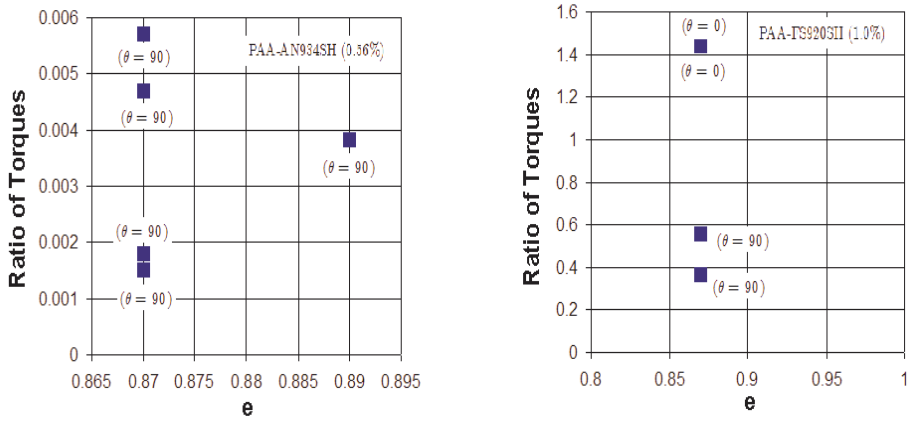

Figure 9.12. Comparison of our experimental data for PAA.

9.6 The Modified Second Order Fluid

So far, with the Newtonian, Power-law and Second order fluid models, we are successful in explaining the horizontal and vertical orientations of particles. The tilt angle still eludes us. Therefore, in this section, we outline the argument used to show the existence of the intermediate angles. We will consider the modified Second order fluid model explained in Section 4.9. The stress tensor for this model is written as

$$T(u,p) = T_N(u,p) + \lambda T_E(u)$$

where

$$T_E(u) = \alpha_1 A_2(u) + \frac{\alpha_2}{1 + k[A_1(u) : A_1(u)]^{\frac{n-1}{2}}} A_1(u)^2.$$

The form of $\hat{\alpha}_2 = \hat{\alpha}_2(\dot{\gamma})$ is chosen in order to ensure convergence. Recall, our reasons for choosing this model are for theoretical convenience and also because this model contains all the relevant terms necessary to establish our result. Repeating the same calculation that we have now performed for the previous models, the torque, at first order in Re and We, becomes

$$\mathcal{M} = Re\mathcal{M}^{0,I}(u_s) + \lambda \mathcal{M}^{0,NN}(u_s) \tag{9.41}$$

where we apply Lemma 9.1.1 and ignore any higher order terms in Re and λ. The viscoelastic contibution to the torque is given by

$$\begin{aligned} \mathcal{M}^{0,NN}(u_s) &= \int_\Omega T_E : D(H^{(i)}) \\ &= \int_\Omega [\alpha_1 A_2(u_s) + \frac{\alpha_2}{1 + k[A_1(u_s) : A_1(u_s)]^{\frac{n-1}{2}}} A_1(u_s)^2] : D(H^{(i)}). \end{aligned} \tag{9.42}$$

Finally, writing $u_s = |\xi|(\cos\theta h^{(1)} + \sin\theta h^{(2)})$, we see that the net torque, in the case of a

prolate spheroid, is of the form

$$\mathcal{M} \;=\; |\xi|^2 \left(Re\mathcal{G}_I(e)\sin\theta\cos\theta + \lambda\mathcal{G}_{NN}(e,k,\theta)\right) \tag{9.43}$$

where $\mathcal{G}_{NN}(e,k,\theta)$ is the torque coefficient corresponding to the non-Newtonian part of the liquid and is given by

$$\begin{aligned}
\mathcal{G}_{NN}(e,\theta) &= \int_\Omega [\alpha_1 A_2(\cos\theta h^{(1)} + \sin\theta h^{(2)}) + \phi(\theta, h^{(i)}) A_1(\cos\theta h^{(1)} + \sin\theta h^{(2)})^2] : D(H^{(i)}) \\
\phi(\theta, h^{(i)}) &= \alpha_2(1 + k[A_1(\cos\theta h^{(1)} + \sin\theta h^{(2)}) : A_1(\cos\theta h^{(1)} + \sin\theta h^{(2)})]^{\frac{n-1}{2}})^{-1}
\end{aligned}$$

The explicit dependence of $\mathcal{G}_{NN}$ upon θ is very complex and cannot be simplified any further. Hence, in equilibrium, we have

$$|\xi|^2(\mathrm{Re}\mathcal{G}_I(e)\sin\theta\cos\theta + \lambda\mathcal{G}_{NN}(e,k,\theta)) \;=\; 0. \tag{9.44}$$

Therefore, as long as the shear-thinning parameter $\mathcal{G}_{NN} \neq 0$, which yet needs to be verified, there is a $\theta = \theta_0$ which satisfies equation (9.44). Symmetry analysis indicates that $\mathcal{G}_{NN} \neq 0$ cannot be simply written as $\chi_i(e,k,\theta)\sin\theta\cos\theta$. This suggests that the equation (9.44) can vanish for θ_0 other than 0 or $\frac{\pi}{2}$, therefore, resulting in the tilt-angle. Observe that when $k = 0$, we revert back to the case of the Second order fluid model, where the results are readily available. Though, we do not have any detailed calculations for this model, we choose to present this section to establish the theoretical existence of the tilt angle. Also, our argument, though heuristic, goes to show that the significant effect that contributes to the terminal orientation of a sedimenting body is the combined competition of inertial, viscoelastic and shear-thinning contributions to the torque. A detailed analysis with such a model is still pending and we hope to carry out as part of future work in this subject.

10.0 CONCLUSION

In this final chapter, we discuss the essential results of the thesis and also suggest possible future work that needs to be done in this area. Our research has been conducted on two essential fronts, experimental and mathematical. We begin with pointing out the significant contributions of this thesis to the problem of orientation of bodies in Newtonian and Non-Newtonian liquids, in particular and to the field of fluid-structure interaction, in general.

Our experimental work has been performed with the aim of reproducing and verifying previous experiments and also to extend the observations to ellipsoidal particles, since most previous work is with cylindrical bodies. Our experiments performed with five different polymeric samples are in agreement with previous experiments and with our own mathematical predictions. One of the sample liquids used in our sedimentation experiment is Polyacryamide(SNF Inc.). We use a very high molecular weight (about 17 Million) of the sample AN934SH to prepare a 0.56% solution of this polymer. This provides us with a highly viscoelastic sample whose rheological properties are ascertained. In fact this liquid has perhaps the highest viscosity and relaxation time of all liquids used in such experiments which provides the advantage of long observation times, upto three hours, in one case while previous experiments have much shorter fall times of the order of a few minutes. With this liquid, we are able to track the transient behavior of a sedimenting particle easily. A second kind of experiment that we perform, namely the flow chamber experiment, is also a novel way of studying the orientation problem, with the unique advantage that the run time of the experiment can be extended to as long as one desires, provided the experiment is made free of leaks. This experiment is completely novel and has not been performed before. Furthermore, we are able to record the orientation behavior of the particles at varying Re where the particle goes from a steady orientation to oscillatory behavior to a final turbulent motion. The flow chamber experiments are still in their preliminary stages and need further tests and verification.

The main contribution of our mathematical study has been to establish the existence of terminal steady state motion of rigid bodies of arbitrary shape in a Second order fluid with arbitrary ϵ. Though the technique of splitting of the equations into the Stokes and Transport equations is a familiar one it has not been dealt with very much in the literature to consider rotational motions of a sedimenting body, due to the term $\omega \times x$, which blows up as $|x| \to \infty$. Furthermore, previous existence arguments are restricted to bodies of certain restricted shapes such as spheres or prolate and oblate spheroids, whereas our argument holds true for bodies of any arbitrary shape.

The argument outlined in Chapter 9 completely solves the problem of terminal orientation of particles at small Re and We. Previous work in this area has been purely experimental or at most numerical and restricted to either the Newtonian liquid or to two dimensional calculations in the case of viscoelastic liquids. Our contribution to the problem has been extensive mathematically where several different fluid models have been dealt with, each highlighting an essential feature of liquids. Our numerical computations to calculate the torques imposed on a prolate spheroid due to the liquid is performed in three dimensions and for Newtonian and viscoelastic cases. This allow us to examine the stability of the equilibrium states and predict the correct terminal orientation which are observed in experiments.

Though we have made significant contributions to this problem, we cannot claim to have had the last word on the subject. What needs to be done is very clear and so is the outcome. However, some essential calculations still need to be done. In the experimental front, we need to investigate the effect of walls on the orientation behavior. All experiments, previous and our own proceed under the assumption that walls do not effect the terminal orientation angles. Though our observations do not indicate any significant changes in orientation in particle orientation as they drift to the wall, a more systematic set experiments must be de-

signed to confirm this claim. Another important set of experiments that must be conducted is to investigate the difference in transition of the orientation angle, with time, for particles with rounded and flat ends. We notice a marked difference in the way the two particles fall. Furthermore, our observations indicate the tilt angles for the flat ended particles only. Perhaps edge effects play some role in the process.

As far as mathematical work is concerned, the primary open question is the confirmation of the tilt angle. We provide a heuristic argument in Section 9.6 to show the existence of the tilt angle. The argument rests on the condition that $\mathcal{G}_{NN}(e, k, \theta) \neq 0$. Calculation of this quantity can help establish (a) the existence of the tilt angle, (b) variation of the tilt angle with the polymeric concentration of the fluid (i.e. with k) and (c) stability of the equilibrium angles. A nonlinear stability argument must also be pursued. Our current argument for stability is a rather simple one motivated by physical arguments on the direction of the torque. Nonlinear analysis will place our results on firmer grounds. A final, though the most essential task that remains is the proof of existence of steady state solutions of a rigid body sedimenting in a viscoelastic shear-thinning liquid.

Several of the problems mentioned above perhaps constitute a doctoral thesis in themselves. However, these are essential to closing the book on the subject of steady state orientation of particles in liquids. The method for showing several of the open questions is clear and is outlined in the relevant chapters of this thesis.

APPENDIX

APPENDIX

STOKES FLOW PAST PROLATE SPHEROID

In cartesian coordinates, the fields $h^{(1)}$, $h^{(2)}$, $H^{(3)} = H$, $P^{(1)} = P_1$ and $P^{(2)} = P_2$ are given by[15]

$$\begin{aligned} h^{(1)} &= -U_1 e_1 + 2\alpha_1 e_1 B_{10} + \alpha_1 r e_r (\frac{1}{R_2} - \frac{1}{R_1}) \\ &- \alpha_1 r^2 e_1 B_{30} + 2\beta_1 \text{grad } B_{11} \end{aligned}$$

$$\begin{aligned} h^{(2)} &= -U_2 e_2 + \alpha_2 e_2 B_{10} + \alpha_2 x_2 e_1 (\frac{1}{R_2} - \frac{1}{R_1}) \\ &+ \alpha_2 r x_2 e_r B_{30} - \beta_2 \text{grad } (x_2 [\frac{x_1 - e}{r^2} R_1 - \frac{x_1 + e}{r^2} R_2 + B_{10}]) \end{aligned}$$

$$\begin{aligned} H &= (\frac{4e^3 y(\alpha_3 - \alpha_3')(e^2 + 5x_1^2)}{5R^5} + \frac{(\gamma_3' - \gamma_3) 4e^3 x_2}{R^3}). \\ &- \frac{16e^5 y}{5R^7} [\beta_3 (\frac{5e^2}{7} + (4x_1^2 - x_2^2 - x_3^2)) - \beta_3' (4x_1^2 - x_2^2 - x_3^2)]) e_1 \\ &+ (\frac{4e^3 x_1 x_2^2 (\alpha_3 - \alpha_3')}{R^5} + \frac{16e^5 (x_1^2 + x_3^2 - 4x_2^2)(\beta_3 - \beta_3')}{5R^7} + \frac{4e^3 x_1 (\gamma_3 - \gamma_3')}{3R^3}) e_2 \\ &+ (\frac{4e^3 x_1 x_2 x_3 (\alpha_3 - \alpha_3')}{R^5} - \frac{16c^5 x_1 x_2 x_3 (\beta_3 - \beta_3')}{R^7}) e_3 \end{aligned}$$

where $e_r = (x_2 e_2 + x_3 e_3)/r$ and

$$
\begin{aligned}
r &= \sqrt{x_2^2 + x_3^2},\ R = \sqrt{x_1^2 + r^2} \\
R_1 &= \sqrt{(x_1+e)^2 + r^2},\ R_2 = \sqrt{(x_1-e)^2 + r^2} \\
B_{10} &= \ln \frac{R_2 - x_1 + e}{R_1 - x_1 - e},\ B_{11} = R_2 - R_1 + B_{10} \\
B_{30} &= \frac{1}{r^2}(\frac{x_1+e}{R_2} - \frac{x_1-e}{R_1}),\ B_{31} = (\frac{1}{R_2} - \frac{1}{R_1}) + x_1 B_{30} \\
\alpha_1 &= e^2[-2e + (1+e^2)\ln\frac{1+e}{1-e}]^{-1}, \\
\alpha_2 &= 2e^2[2e + (3e^2-1)\ln\frac{1+e}{1-e}]^{-1} \\
\beta_1 &= \frac{(1-e^2)\alpha_1}{2e^2}, \\
\beta_2 &= \frac{(1-e^2)\alpha_2}{2e^2} \\
\alpha_3 &= \frac{4e^2}{(1-e^2)}, \\
\beta_3 &= 2e^2\gamma_3[-2e + \ln\frac{1+e}{1-e}][2e(2e^2-3) + 3(1-e^2)\ln\frac{1+e}{1-e}]^{-1} \\
\gamma_3 &= (1-e^2)[-2e + (1+e^2)\ln\frac{1+e}{1-e}]^{-1} \\
\alpha_3' &= \frac{4e^2}{(1-e^2)} \\
\beta_3' &= e^2\gamma_3'[-2e + (1-e^2)\ln\frac{1+e}{1-e}][2e(2e^2-3) + 3(1-e^2)\ln\frac{1+e}{1-e}]^{-1} \\
\gamma_3' &= \frac{\gamma_3}{e^2-1}
\end{aligned}
$$

It is next observed that our future calculations can be considerably simpler in prolate-spheroidal coordinates (ζ,μ,θ) with the transformation from cartesian coordinates given by[36]

$$
\begin{aligned}
x_1 &= e\mu\zeta, \\
x_2 &= e\sqrt{\mu^2-1}\sqrt{1-\zeta^2}\cos\theta, \\
x_3 &= e\sqrt{\mu^2-1}\sqrt{1-\zeta^2}\sin\theta,
\end{aligned}
$$

and the scale factors

$$\begin{aligned} q_\mu &= \frac{\sqrt{\mu^2-1}}{e\sqrt{\mu^2-\zeta^2}}, \\ q_\zeta &= \frac{\sqrt{1-\zeta^2}}{e\sqrt{\mu^2-\zeta^2}}, \\ q_\theta &= \frac{1}{e\sqrt{\mu^2-1}\sqrt{1-\zeta^2}}. \end{aligned}$$

The components of $h^{(i)}$, $i = 1, 2$, and H in these new coordinates are given by

$$\begin{aligned} h_\mu^{(1)} &= \zeta u_1 \\ h_\zeta^{(1)} &= u_2 \\ h_\theta^{(1)} &= 0 \\ h_\mu^{(2)} &= \zeta v_1 \cos\theta \\ h_\zeta^{(2)} &= v_2 \cos\theta \\ h_\theta^{(2)} &= v_3 \sin\theta \\ H_\mu &= \zeta H_1 \cos\theta \\ H_\zeta &= H_2 \cos\theta \\ H_\theta &= H_3 \zeta \sin\theta \end{aligned}$$

with

$$
\begin{aligned}
u_1 &= \frac{-(-1+4\beta_1\mu+\mu^2-2(\alpha_1+\beta_1)(\mu^2-1)ln\frac{\mu+1}{\mu-1}}{\sqrt{\mu^2-1}\sqrt{\mu^2-\zeta^2}} \\
u_2 &= \frac{\sqrt{1-\zeta^2}}{\sqrt{\mu^2-\zeta^2}}(-2\alpha_1-4\beta_1-\mu+2(\alpha_1+\beta_1)\mu ln\frac{\mu+1}{\mu-1}) \\
v_1 &= \frac{1-2\beta_2\mu+\mu^2-(\alpha_2-\beta_2)(\mu^2-1)ln\frac{\mu+1}{\mu-1}}{\sqrt{\mu^2-1}}\sqrt{\mu^2-\zeta^2} \\
v_2 &= \frac{\sqrt{1-\zeta^2}}{(\mu^2-1)\sqrt{\mu^2-\zeta^2}}(2\beta_2(\mu^2-2)-\mu(\mu^2-1) \\
&+ 2\alpha_2(\mu^2-1)+(\alpha_2-\beta_2)\mu(\mu^2-1)ln\frac{\mu+1}{\mu-1}) \\
v_3 &= \frac{1-2\beta_2\mu^2-(\alpha_2-\beta_2)ln\frac{\mu+1}{\mu-1}}{(\mu^2-1)} \\
H_1 &= \frac{-e\sqrt{1-\zeta^2}}{(\mu^2-1)\sqrt{\mu^2-\zeta^2}}[6(1-\mu^2)(\alpha_3'-\alpha_3+\gamma_3'-\gamma_3)+(48\mu^2-56)(\beta_3'-\beta_3) \\
&+ (\mu^2-1)ln\frac{\mu+1}{\mu-1}\left\{(3\mu^2-3)(\alpha_3-\alpha_3')+(1-3\mu^2)(\gamma_3-\gamma_3')+(12-24\mu^2)(\beta_3'-\beta_3)\right\}] \\
H_2 &= \frac{e}{\sqrt{\mu^2-1}(\mu^2-\zeta^2)^{\frac{3}{2}}}[2\zeta^2(\mu^2-1)\{2(-1+\zeta^2)(\alpha_3-\alpha_3')+2\zeta^2(\gamma_3'-\gamma_3)+2\mu^2(\gamma_3-\gamma_3') \\
&- (\gamma_3-\gamma_3')\mu(\mu^2-\zeta^2)ln\frac{\mu+1}{\mu-1}\}+4(\beta_3-\beta_3')(2\zeta^2-1)\left\{4-6\mu^2+3\mu(\mu^2-1)ln\frac{\mu+1}{\mu-1}\right\} \\
&- \frac{\mu(1-\zeta^2)}{(\mu^2-\zeta^2)}\{2\mu(\alpha_3-\alpha_3')(2+\zeta^2-3\mu^2)+2\mu(\gamma_3'-\gamma_3)(\zeta^2-\mu^2)+(3\alpha_3-3\alpha_3' \\
&+ \gamma_3'-\gamma_3)(\mu^2-\zeta^2)(\mu^2-1)ln\frac{\mu+1}{\mu-1}\}] \\
H_3 &= \frac{2e}{\mu^2-1}[(8-12\mu^2)(\beta_3-\beta_3')+2(\mu^2-1)(\gamma_3-\gamma_3') \\
&+ (6\beta_3-6\beta_3'+\gamma_3'-\gamma_3)\mu(\mu^2-1)ln\frac{\mu+1}{\mu-1}] \\
P_1 &= \frac{-4\alpha_1}{e(\mu^2-\zeta^2)} \\
P_2 &= \frac{-4\alpha_2\mu\sqrt{1-\zeta^2}}{e\sqrt{(\mu^2-1)}(\mu^2-\zeta^2)}
\end{aligned}
$$

BIBLIOGRAPHY

BIBLIOGRAPHY

1. Adams, A.R., 1975, Sobolev Spaces, Academic Press, New York.

2. Ardaillon, E., Les Mines du Laurion dans l'Antiqueite', 1897, Thorin, Paris.

3. Aristotle, 1936, On the Heavens, Translated by W. Guthrie, William Heineman Inc., London.

4. Borglet,A., and Phipps, J., 2002, The Experimental Study of Orientation of a Particle in a Flow Chamber, Technical Report, Dept. of Mechanical Engineering, University of Pittsburgh.

5. Bird, R., B., and Armstrong R., C., 1987, Dynamics of Polymeric Liquids,Volume I, Wiley-Interscience Publications.

6. Bohnenblust, H., F., and Karlin, S., Contributions to the theory of games, Ann. of Math. Studies, Princeton univ. Press, 24, 155-160.

7. Brenner, H., 1964, The Stokes Resistance of an Arbitrary Particle II., Chem. Engng. Sci., 19, 599-624.

8. Brunn, P., 1980, The motion of rigid particles in viscoelastic fluids, Journal of Non-Newtonian Fluid Mechanics, 7, 271-288.

9. Burger, R., and Wendland, W., L., 2001, Sedimentation and suspension flows: Historical perspectives and some recent developments, Journal of Engineering Mathematics, 41, 101-116.

10. Carapau, F.L., 2004, Development of 1D Fluid Models Using the Cosserat Theory: Numerical Simulations and Applications to Haemodynamics, Ph.D. Thesis, Department of Mathematics, IST, Lisboa, Portugal.

11. Chabra, R.P., 1995, Wall effects on the free-settling velocity o fnon-spherical particles in viscous media in cylindrical tubes, Powder Technology, 85,83-90.

12. Chabra, R.P., 1996, Wall effects on the terminal velocity of non-spherical particles in non-Newtonian polymer solutions, Powder Technology, 88, 39-44.

13. Cho, K., Cho, Y.I., and Park, N.A., 1992, Hydrodynamics of Vertically falling Thin Cylinders in non-Newtonian Fluids, J. Non-Newtonan Fluid Mech., 45, 105-145.

14. Chiba, K., Song, K., and Horikawa, A., 1986, Motion of a Slender body in a Quiescent Polymer Solution, Rheol. Acta, 25, 380-388.

15. Chwang, A.T., and Wu, T.Y., 1975, Hydromechanics of Low-Reynolds-Number Flow. Part 2. Singularity Method for Stokes Flows, J. Fluid Mech., 67, 787-815

16. Coscia, V., and Galdi, G., P., 1994, Existence, Uniqueness and Stability of of regular steady flow of a second-grade fluid, Int. Journal of Nonlinear Mechanics, 29, 493-512.

17. Cox, R.G., 1965, The Steady Motion of a Particle of Arbitrary Shape at Small Reynolds Numbers, J. Fluid Mech., 23, 625-643.

18. Dunn, J.E. and Fosdick, R.L., 1974, Thermodynamics and Stability of Non-Linear Fluids, Arc. Rat. Mech., 56, 191.

19. Evans, L.C., 1998, Partial Differential Equations, American Mathematical Society.

20. Folland G.B., 1995, Introduction to Partial Differential Equations, Princeton University Press.

21. Fosdick, R.L. and Rajagopal, K.R., 1979, Anamalous features in the model of a second order fluids, Arch. Rat. Mech., 70, 145-152.

22. Galdi, G.P., Sequeira, A. and Videman, J.H., 1997, Steady Motions of a Second-Grade Fluid in an Exterior Domain, Adv. Math. Sci. Appl., 7, 977-995.

23. Galdi, G.P., 1998, Slow Motion of a Body in a Viscous Incompressible Fluid with Application to Particle Sedimentation, from Developments in Partial Differential Equations, Quaderni di Matematica della II Università di Napoli, Vol 2, V.A. Solonnikov Ed., 2-50.

24. Galdi G.P., 2000, Slow Steady Fall of a Rigid Body in a Second-Order Fluid, J. Non-Newtonian Fluid Mech., 93, 169-177.

25. Galdi, G. P., 1998, An Introduction to the Mathematical Theory of the Navier-Stokes Equations, Vol 1, 2nd Corrected Edition, Springer Verlag.

26. Galdi, G.P., Sequeira, A., and Vaidya A., 2000, Translational Steady Fall of Symmetric Bodies in an Oldroyd-B Liquid at Nonzero Reynolds Number, in preparation.

27. Galdi G. P., Vaidya, A., 2001, Translational Steady fall of Symmetric Bodies in Navier-Stokes Liquid, with Application to Particle Sedimentation, J. Math. Fluid Mech., 3, 183-211.

28. Galdi G.P., Vaidya A., Pokorny, M., Joseph, D.D. and Feng, J., 2002, Translational Steady Fall of Symmetric Bodies in a Second-Order Liquid at Nonzero Reynolds number, Math. Models and Methods in Appl. Sci., Vol.12, 11, 1653-1690.

29. Galdi G.P. and Vaidya A., 2004, A Note on the Orientation of Symmetric Bodies in Power-Law Fluids, submitted for publication.

30. Galdi G.P. and Rajagopal, K., R., 1997, Slow motion of a body in a fluid of second grade, Int. Journal of Engineering Science, 35, 33-67.

31. Galdi, G., P., 2002, On the Motion of a Rigid Body in a Viscous Fluid: A Mathematical Analysis with Applications, Handbook of Mathematical Fluid Mechanics, Elsevier Science, 105 pp, to be published.

32. Galdi, G.P., Padula, M. and Rajagopal, K.R., 1990, On the conditional stability of the rest state of a second grade fluid in unbounded domain, Arch. Rat. Mech. and Anal., 109, 173-182.

33. Gibala,G., and O'Brien,K., 2002, Design and Study of a Fixed Particle in a Horizontal Flow Chamber, Technical Report, Dept. of Mechanical Engineering, University of Pittsburgh.

34. Giesekus, H., Die Simultane Translations and Rotations Bewegung einer Kugel in einer Elastovisken Flussigkeit, 1963, Rheol. Acta, 3, 59-71.

35. Grossman, P.D., and Soane, D.S., 1990, Orientation Effects on the Electrophoretic Mobility of Rod-Shaped Molecules in Free Solution, Anal. Chem., 62, 1592-1596.

36. Happel, V., and Brenner, H., 1965, Low Reynolds Number Hydrodynamics, Prentice Hall.

37. Huang, P.Y., Hu, H.H., and Joseph, D.D., 1998, Direct Simulation of the Sedimentation of Elliptic Particles in Oldroyd-B Fluids, J. Fluid Mech., 362, 297-325.

38. Joseph, D.D., and Liu, Y.J., 1993, Orientation of Long Bodies Falling in a Viscoelastic Fluid, J. Rheol., 37, 961-983.

39. Joseph, D.D., and Feng, J., 1996, A Note on the Forces that Move Particles in a Second-Order Fluid, J. Non-Newtonian Fluid Mech., , 64, 299-302.

40. Joseph, D.D., 1993, Finite Size Effect in Fluidized Suspension Experiments, in Particulate Two-Phase Flow, M.C.Roco, Ed., Butterworth-Heinemann, 300-324.

41. Joseph, D.D., 1996, Flow Induced Microstructure in Newtonian and Viscoelastic Fluids, in Proceedings of the Fifth World Congress of Chemical Engineering, Particle Technology Track, 6, 3-16.

42. Joseph D. D., 2000, Interrogations of Direct Numerical Simulations of Solid-Liquid Flow, Web Site : http://www.aem.umn.edu/people/faculty/joseph/interrogation.html

43. Juha, V., 1997, Mathematical Analysis of Viscoelastic Non-Newtonian Fluids, PH.D. Thesis, Instituto Superior Tecnico, Lisbon.

44. Juarez, L. H., 2001, Numerical Simulation of sedimentation of an elliptic body in an incompressible viscous fluid, C.R. Acad. Sci, Paris, 329, Series IIb, 221-224.

45. Kim, S., 1986, The motion of ellipsoids in a second order fluid, Journal of Non-Newtonian Fluids, 21, 255-269.

46. Kiger, K.T., Pan, C., 2001, Suspension Mechanism of Solid Particulates in a Horizontal Turbulent Channel Flow, Second International Symposium on Turbulent Shear Flow Phenomenon, Sweden.

47. Kirchoff, G., 1869, Uber die Bewegung enines Rotationskorpers in einer flussigkeit, J. Reine Ang. Math. Soc., 71, 237-281.

48. Kraus, M., Wintz, W., Seifert, U. and Lipowsky, R., 1996, Fluid Vescicles in Shear Flow, Phys. Rev. Lett., 77, 3685-8.

49. Kreyzig, E., 1978, Introductory Functional Analysis with Applications, Wiley, New York.

50. Lamb, H., 1932, Hydrodynamics, Cambridge University Press.

51. Leal, L.G., 1975, The Slow Motion of Slender Rod-Like Particles in a Second-Order Fluid, J. Fluid Mech., 69, 305-337.

52. Leal, L.G., 1980, Particle Motion in a Viscous Fluid, Ann. Rev. Fluid Mech., 12, 435-476.

53. Lee, S.C., Yang, D.Y., Ko, J., and You, J.R.,1997, Effect of compressibility on flow field and fiber orientation during the filling stage of injection molding, J Mater. Process. Tech., 70, 83-92.

54. Liu, Y.J., and Joseph, D.D., 1993, Sedimentation of Particles in Polymer Solutions, J. Fluid Mech., 255 565-595.

55. Lusternik, L.I.A. and Sobolev, V.J., 1962, Elements of Functional Analysis, Taylor and Francis.

56. Macosko, C. W., 1994, Rheology, Principles, Measurements and Applications, Wiley-Vch.

57. Morrison, F.A., 2001, Understanding Rheology, Oxford University Press.

58. Newton, I., 1687, Philosophiae Naturalis Principia Mathematica, tanslated by Andrew Motte in 1729, English translation published by Prometheus Books in 1989.

59. Novotny, A., Sequeira, A. and Videman, J.H., 1997, Existence of Three Dimensional Flows of Second-Grade Fluids Past an Obstacle, 30, No.5, 3051-3058.

60. Novotny, A., Sequeira, A., and Videman, J., 1999, Steady Motions of Viscoelastic Fluid in 3-D exterior domains- existence, uniqueness and asymptotic behavior, Archive of Rational Mechaics and Analysis, 149, 49-67.

61. T.W. Pan, R. Glowinski, Galdi G.P., 2002, Direct Simulation of a settling ellipsoid in a Newtonian fluid, Science and Engineering Computations for the 21st Century, Proccedings of the 15th Toyota conference.

62. Pettyjohn, E. A. and Christiansen E. B., 1948, Effect of Particle Shape on Free-Settling Rates of Isometric Particles, Chem. Eng. Prog., 44, 526.

63. Pokorny, M., 1999, Comportement Asymptotique des Solutions de Quelques Equations aux Derivees Partielles Decrivant L'Ecoulement de Fluides dans les Domaines Non-Bornes, Doctoral Thesis, University of Toulon and Var. Charles University.

64. Reddy, B.D., 1991, Introductory Functional Analysis, Springer Texts in Applied Mathematics, Vol. 27.

65. Roco M.C., (Ed.), 1993, Particulate Two-Phase Flow, Butterworth-Heinemann Publ., Series in Chemical Engineering.

66. Rudin, W., 1973, Functional Analysis, Tata-McGRAW-Hill.

67. Sequeira A. and Baia M., 1999, A finite element approximation for the steady solution of a second grade fluid model, Journal of computation and applied mathematics, 111, 281-295.

68. Serre, D., 1987, Chute Libre d'un Solide dans un Fluide Visqueux Incompressible, Existence, Japan Journal Applied Math, 4, 99-110.

69. Shapiro, A.H., 1961, Shape and Flow, The Fluid Synamics of Drag, Anchor Books, Doubleday & Company.

70. Simader, C.G., and Sohr, H., 1997, The Dirichlet Problem for the Laplacian in Bounded and Unbounded Domains, Pitman Research Notes in Mathematics Series, Longman Scientific & Technical, Vol. 360

71. Smirnov, V.I., 1964, A Course of Higher Mathematics, Volume 5: Integration and Functional Analysis, Pergamon Press.

72. Steffe, J.F., 1996, Rheological Methods in Food Process Engineering, Second Edition, Freeman Press.

73. Strang, G., 1976, Linear Algebra and its Applications, Academic Press.

74. Taylor, G.I., Low Reynolds Number Flow, Videotape, 33 min, Encyclopaedia Britanicca Educational Corporation.

75. Thomson, W. and Tait, P.G., 1879, Natural Philosophy, Vols. 1 and 2, Cambridge University Press.

76. Tokaty, G.A., 1971, A History and Philosophy of Fluid Mechanics, Dover Publications Inc.

77. Truesdell, C. and Rajagopal, K.R., 2000, Non-Linear Fluid Dynamics, Birkshauser Verlag.

78. Truesdell, C., 1968, Essays in the History of Mechanics, Springer-Verlag, New York.

79. Vaidya, A., 2004, Slow, Steady, Freefall of Bodies of arbitrary shape in a Second Order Fluid at zero Reynolds number, to appear in Jap. Journal of Ind. and Appl. Math.

80. Vaidya A. and Galdi G.P., 2004, Observations on the Transient Nature of Shape-tilting Bodies Falling in Polymeric Liquids, submitted for publication.

81. Wang, J., Bai, R., Lewandowski, C., Galdi, G.P and Joseph, D.D., 2003, Sedimentation of Cylindrical Particles in a Viscoelastic Liquid: Shape Tilting, Journal of Particuology, to appear.

82. Weinberger, H.F., 1972, Variational Properties of Steady fall in a Stokes Flow, Journal of Fluid Mechanics, 52, 321-344.

83. Weinberger, H.F., 1973, On the Steady Fall of a Body in a Navier-Stokes Fluid, Proc. Symp. Pure Mathematics, 23, 421-440.

84. Wilson, A., J., 1994, The Living Rock, Woodland Publishing Ltd.

85. Zeidler, E., 1991, Applied Functional Analysis, Springer Verlag.

86. Plasma Viscosity and Blood Viscoelasticity, Retrieved April 2004 from www.vilastic.com/tech10.html